DEVELOPMENT OF A DISCRETE DESIGN METHODOLOGY FOR FIBER-REINFORCED SOIL

By: Jorge G. Zornberg, Ph.D., P.E.

Geotechnical Research Report

University of Colorado at Boulder

July 2000

DEVELOPMENT OF A DISCRETE DESIGN
METHODOLOGY FOR FIBER-REINFORCED SOIL
By: Jorge G. Zornberg, Ph.D., P.E.

SUMMARY

A consistent design methodology is proposed for the design of fiber-reinforced soil slopes. When characterization of fiber-reinforced soil is done using traditional composite approaches, a nonconventional laboratory testing program on composite fiber-reinforced soil specimens should be implemented to define the material properties. Instead, if characterization of fiber-reinforced soil is done using the discrete approach proposed herein, only conventional properties are needed. That is, the performance of fiber-reinforced soil can be characterized by independent laboratory testing of soil specimens and of fiber specimens. Avoiding testing of fiber-reinforced soil specimens for specific engineering projects is a major objective of the proposed approach, as this will significantly foster implementation of fiber-reinforcement in soil slope stabilization.

After presenting an overview of previous work on fiber-reinforcement of soil, this report discusses the advantages of a discrete methodology compared to a soil/reinforcement composite approach. Subsequently, the results of an experimental testing program on fiber-reinforced triaxial specimens are presented. A discrete theoretical framework is then presented for the design of fiber-reinforced soil slopes, and experimental results are used to validate the discrete method. The proposed framework is implemented into a design methodology for the stability of fiber-

reinforced slopes. Design examples are finally presented, which illustrate the advantages of the proposed design methodology in the design of fiber-reinforced slopes.

ACKNOWLEDGEMENTS

DEVELOPMENT OF A DISCRETE DESIGN
METHODOLOGY FOR FIBER-REINFORCED SOIL

TABLE OF CONTENTS

vi

1. INTRODUCTION

This report presents a consistent methodology for the design of fiber-reinforced soil slopes that involves use of a discrete approach to characterize the influence of the fibers on stability. A composite approach has been typically used in the design of fiber-reinforced soil slopes. In a composite approach, the fiber-reinforced soil is characterized as a "single homogenized" material, the performance of which is characterized by laboratory testing of composite fiber-reinforced soil specimens. Instead, in the discrete approach proposed herein, fiber-reinforced soil is characterized as a two-component (soil and fibers) material. That is, only independent testing of soil specimens and of fiber specimens is needed to characterize the performance of fiber-reinforced soil. Avoiding the test of soil-reinforced specimens is a major objective of the proposed approach, since the need of testing soil composite specimens for engineering projects has been probably the major drawback in the implementation of fiber-reinforcement in soil stabilization projects. Accordingly, the discrete approach used in this report quantifies the effect of the fibers and of the soil matrix independently to evaluate the stability of a fiber-reinforced soil slope. The proposed methodology for stability analysis of fiber-reinforced soil slopes is generic (i.e. not product-specific). The methodology treats the fibers as discrete reinforcing elements that contribute to stability by mobilizing the tensile strength and/or pullout resistance of the reinforcing fibers. This contribution adds to the stabilizing shear stresses developed by the soil along a shear plane.

A composite approach in which the fiber-reinforced soil mass is treated as a homogeneous composite material is conventionally used in the design of fiber-reinforced soil structures. This composite approach assumes that fibers contribute to stability by increasing the shear strength of the "homogenized" composite reinforced mass. However, as in the case of continuous planar reinforcements (e.g. geogrids, geotextiles), the reinforcing fibers actually work in tension and not in shear. The use of a discrete approach, which accounts for the actual tensile reinforcement mechanism

developed within the fibers, provides a better representation of the beneficial effects of fiber-reinforcement than a composite approach. A discrete approach is better suited for design purposes because it would not require performing tests on composite specimens on a project-specific basis. In addition, it would more accurately represent the behavior of fiber-reinforcement, facilitating more economical design solutions by the engineer and allowing the manufacturer to optimize the characteristics of the fibers.

Complemented with further experimental testing and analytic validation, the generic framework for characterizing the fiber-reinforced soil presented in this report is anticipated to evolve into a product-specific, easy to apply set of design guidelines suitable for use in engineering practice. The use of randomly distributed fibers present great opportunities for cost savings in transportation, commercial, industrial, residential, and landfill development projects. In summary, the development of a consistent design methodology that accounts for the contribution of fiber-reinforcement to stability in a discrete manner will allow engineers to:

(1) define design properties without the need for nonconventional, soil-specific shear strength testing of fiber-reinforced specimens,

(2) optimize the "mix" (e.g. fiber content) of the fiber-reinforced soil, and

(3) develop improved products (fibers) for use in engineering practice.

The discrete approach will facilitate assessment by the engineering community of the potential economic and technical benefits of fiber-reinforcement to a greater extent than possible with current design procedures. It is anticipated that the better quantification and understanding of fiber-reinforcement enabled by use of a discrete approach will also facilitate development of a larger market for fiber-reinforcement products.

The framework presented herein for characterization of the strength of fiber-reinforced soil is preliminary. Ongoing experimental testing and analytic validation is currently being pursued in order to facilitate implementation of this methodology in engineering practice. This document presents an overview of previous work on fiber-reinforcement of soil, discusses the advantages of a discrete methodology compared to a soil/reinforcement composite approach, describes the results of an experimental testing program on fiber-reinforced triaxial specimens, develops a discrete theoretical framework to establish the fiber properties needed to characterize the strength of fiber-reinforced soil, and implements the proposed framework into a design methodology for the stability of fiber-reinforced slopes. Design examples are presented, which illustrate the advantages of the proposed design methodology in the design of fiber-reinforced slopes.

2. OVERVIEW OF FIBER-REINFORCEMENT

2.1 Review of Previous Investigations

Soil reinforcement techniques have enabled engineers to effectively use marginal soils as reliable construction materials for a wide range of geotechnical and geoenvironmental applications. Traditional soil reinforcing techniques typically involve the use of continuous planar inclusions (e.g. geogrids, geotextiles) oriented in a preferred direction to enhance the stability of the soil mass. In the early stages of development of these techniques, designers of these now conventional soil reinforcement systems usually considered the reinforced soil mass as a homogeneous composite material. Even though reinforcement inclusions work in tension, the composite approach assumed that their contribution to stability could be quantified by an increase in shear strength (typically an increase in the cohesive component of the shear strength) in an equivalent homogeneous reinforced soil mass. Subsequently, both geotechnical designers and geosynthetic manufacturers realized about the significant advantages of using a discrete approach to evaluate the contributions of the reinforcement to slope stability would bring to design.

The contribution of continuous planar reinforcement to stability is more accurately accounted in the discrete approach than in the composite approach. In the discrete approach, the effect of continuous reinforcements is quantified by assessing the development of tensile forces in the reinforcement and by accounting for these tensile forces in limit equilibrium analyses. Because the behavior of reinforced soil structures was more accurately characterized by a discrete approach, design solutions could be implemented more cost effectively, manufacturers could optimize geosynthetic reinforcement products, and the use of continuous inclusions for soil reinforcement grew rapidly. By using a discrete approach, the geotechnical designer acquired a better understanding of the actual contribution of the continuous geosynthetic product to the stability of the soil structure. Furthermore, geosynthetic manufacturers could focus on the properties of their products rather than on developing methods for estimating the properties of a composite material over which they had little

control. Currently, soil structures reinforced with continuous inclusions are no longer designed using the composite approach.

Differently than for the case soil structures reinforced using continuous planar reinforcements, soil structures reinforced using randomly distributed fibers are still conventionally designed using composite approaches to characterize the contribution of the fibers to stability. One of the main reasons for use of the composite approach for this purpose is the difficulty of quantifying the properties of individual fibers. However, the use of the empirical composite approach has prevented both proper characterization of the actual contribution of the fibers to stability and optimization of fiber products. In addition, the use of a composite approach requires that the design engineer perform shear strength tests on fiber-reinforced soil specimens, rather than on soil only specimens, to define key properties for the design.

Relevant contributions have been made by several investigators towards the understanding of the behavior of fibers within a soil mass. A soil mass reinforced with discrete, randomly distributed fibers is similar to a traditional reinforced soil system in its engineering properties but mimics admixture stabilization in the method of its preparation (Gray and Al-Refeai, 1986). Advantages of randomly distributed fibers over continuous inclusions include maintaining strength isotropy and the absence of the potential planes of weakness that can develop parallel to continuous planar reinforcement elements such as geotextiles or geogrids (Maher and Gray, 1990; Maher and Woods, 1990). Potential advantages of fiber-reinforced solutions over the use of other slope stabilization technologies have been identified, for example, for the case of slope repairs in transportation infrastructure projects (e.g. Gregory and Chill, 1998) and for the use of recycled and waste products such as shredded tires in soil reinforcement (Foose et al., 1996). Fiber-reinforcement techniques for soils also include the use of "Texol", which consists of monofilament fibers injected randomly into sand (Leflaive, 1985) and the use of randomly distributed polymeric mesh elements (McGown et al., 1985; Morel and Gourc, 1997). The use of fiber-reinforced clay backfill to mitigate the development of tension cracks was evaluated by several investigators (e.g. Al Wahab

and El-Kedrah, 1995; Maher and Ho, 1994). However, the use of fiber-reinforced to reinforce clay backfills deserves special attention, similar to the case of slope stabilization of poorly draining fills using continuous planar reinforcements (Zornberg and Mitchell, 1994; Mitchell and Zornberg, 1995).

Several composite models have been proposed in the literature to explain the behavior of randomly distributed fibers within a soil mass. The proposed models have been based on a mechanistic approach (Maher and Gray, 1990), on an energy dissipation approach (Michalowski and Zhao, 1996), and on a statistics-based approach (Ranjar et al., 1996). Common findings from the various studies include:

- randomly distributed fibers provide strength isotropy in a soil composite, in contrast to the potential planes of weakness that can develop parallel to continuous planar reinforcements;

- fiber inclusion significantly increases the "equivalent" shear strength within a reinforced soil mass for both cohesionless and cohesive soils; and

- the "equivalent" strength increase is a function of fiber content, fiber length (or aspect ratio), fiber stiffness, and soil-fiber interface friction.

The mechanistic models proposed by Gray and Ohashi (1983) and Maher and Gray (1990) quantify the "equivalent shear strength" of the fiber-reinforced composite as a function of the thickness of the shear band that develops during failure. However, shear band thickness is a parameter that is difficult to assess. Shewbridge and Sitar (1990) provide additional insight into the shear band characteristics of the shear band that develops for different types of reinforcement. The required information to characterize shear band development for these models is, however, difficult to quantify.

Under dynamic loading conditions, the use of fibers in sands has been found to provide increased resistance to liquefaction and a higher dynamic shear modulus under both low and high amplitude vibrations (Maher and Woods, 1990). For unpaved road applications, a comprehensive field study was undertaken by the U.S. Army Corps of Engineers and Synthetic Industries to evaluate the benefits of the addition of discrete fibrillated polypropylene fibers in highly plastic clay soils (Gorgan and Johnson, 1994). This project demonstrated the feasibility of the application of fibers to stabilize clay subgrades supporting high traffic loads. However, full-scale projects have not yet been undertaken for evaluating the use of fiber-reinforcement in slope stabilization projects.

Appendix B presents a comprehensive list of references on investigations involving fiber-reinforcement.

2.2 Potential Slope Stabilization Applications of Fiber-Reinforcement

In applications involving slope stabilization, either fiber-reinforcement or continuous planar reinforcement can be used to increase the factor of safety (i.e. stabilize the slope). Cost, availability, and standards of practice are among the more significant factors that the engineer usually considers when selecting the stabilization method for a project. In some slope stabilization applications, though, use of fiber-reinforcements provides clear advantages over the use of continuous planar reinforcements. One such application is the reinforcement of thin soil veneers. In relatively thin soil veneers, small amounts of cohesion (i.e., shear strength at low confining pressure) have a significant impact on stability. An increase in the shear strength at low confining pressure (i.e. cohesion) can be achieved to a limited extent simply by increasing the compactive effort during placement of the veneer soils. However, an increase in cohesion is often insufficient and deemed unreliable to achieve the strength required for static and/or seismic stability. The use of continuous horizontal reinforcements to stabilize a soil veneer requires anchoring of the reinforcement into competent material below the veneer, while the use of continuous

planar reinforcements parallel to the slope requires anchoring the reinforcement at top of the slope crest and is limited by the interface shear strength of the soil. Fiber-reinforcement may provide an economically and technically feasible alternative solution for veneer stability, as the tension developed by the fibers within the soil-fiber composite can often provide the additional strength at low confining pressures required for veneer stability.

Some of the more promising potential applications for the use of fiber-reinforcement to enhance veneer stability are in the area of landfill engineering. One example is the potential use of fiber-reinforcement in the design of evapotranspirative cover systems constructed on steep landfill slopes (Zornberg and Caldwell, 1998). In this application, fiber-reinforcement would provide not only increased stability for the soil cover veneer, but it would also mitigate the potential for crack development and provide erosion control. By requiring lower compaction requirements than for unreinforced soil of equivalent shear strength, fiber-reinforcement also facilitates vegetation development. The additional benefits provided by the use of fiber-reinforcement in relation to continuous planar reinforcement regarding tension crack and erosion control are particularly relevant for the case of cohesive soils used in waste containment cover systems. The development of a consistent design methodology based upon a discrete approach to model the influence of fiber-reinforcement will facilitate the acceptance of fiber-reinforced soil products in innovative solutions in geotechnical practice.

Another slope stabilization application in which the use of fiber-reinforcement offers benefits when compared to the use of continuous planar reinforcements is in the localized repair of failed slopes. In this case, geometric constrains posed by the irregular shape of the soil "patches" to be constructed make the use of fiber-reinforcement an appealing alternative in relation to conventional continuous planar reinforcements from a constructibility standpoint.

Finally, in areas prone to seismic activity, the use of fiber-reinforcement within the soil mass can significantly increase the yield acceleration of a slope, i.e. increase the threshold acceleration at which permanent seismic displacements develop

for a design earthquake. Higher yield acceleration reduces the permanent displacements in seismic events. The use of fiber-reinforcement to induce an "effective apparent cohesion" (i.e. shear strength at low confining pressure) would be of significant benefit in the design of embankments (particularly of hydraulic fills) in seismic areas and deserves serious further investigation. As pointed out by Dr. J.P. Giroud in his keynote lecture to the Third International Conference on Geotextiles (Giroud, 1986), the use of micro-reinforcement could fulfill an old dream of the geotechnical engineer: a cohesive material with high hydraulic conductivity. One application in which the use of fiber-reinforcement is particularly intriguing is its application for mitigation of liquefaction potential of granular soils. Fiber-reinforcement of hydraulic fill for the purpose of decreasing liquefaction potential may offer significant economic benefits compared to other stabilization measures if it can be shown to be technically feasible.

A design methodology for fiber-reinforced soil structures using a discrete approach would be more consistent with the actual soil improvement mechanism than the composite material design approach currently employed in engineering practice. Consequently, the development of a discrete design methodology can lead not only to a more accurate design but also to the development of more adequate field specifications, standards of practice, and quality control guidelines.

2.3 Evaluation of Design Criteria for Slope Stability Applications

Design criteria for the use of fibers as reinforcement elements should be based upon established standards of geotechnical and geosynthetics practice. However, supplemental criteria need to be established in order to consider specific aspects of this technology. Preliminary recommendations for these design criteria, subject to revision based upon observation of the performance of full-scale structures or physical models, include:

- *Static Stability Criteria.* The proposed design criterion for the static stability of permanent slopes is generally a factor of safety of 1.5. At this time, it is recommended that the target value of 1.5 also be used for fiber-reinforced soil slopes. Lower factors of safety (e.g. 1.30) are recommended in current FHWA guidelines for structures reinforced using continuous elements (Elias and Christopher, 1997) and could be considered in the future based on the observed performance of fiber-reinforced soil structures.

- *Seismic Stability Criteria.* A performance criterion based upon permanent seismic deformation is recommended for seismic design of fiber-reinforced soil structures. Consistent with current standards of practice, calculated permanent displacements estimated using a Newmark-type analysis should not exceed 36 in. (900 mm) for the case of general embankments and 12 in. (300 mm) for covers of waste containment systems. These recommendations are based on the use of residual shear strength values for the fiber-reinforced soil mass.

- *Method of Analysis.* Guidelines for the use of total or effective stress methods of analyses should follow current guidelines for the use of continuous planar reinforcements. Particularly, an effective stress analysis shall be used for the analysis of long-term conditions. Total stress analysis shall be used for seismic stability evaluations. The method of analysis to be used for cohesive soil slopes shall follow recommendations proposed by Christopher et al. (1998) for the case of reinforced soil structures that do not offer in-plane drainage capabilities.

- *Fiber Tensile Strength Reduction Factors.* Guidelines established by the FHWA (Elias, 1997) regarding reduction factors for creep and durability should be considered as preliminary guidelines to establish the allowable tensile strength from the measured ultimate tensile strength of individual

fibers. It seems logical that construction damage reduction factors should not be considered (i.e. should be equal to unity) for small fibers, although testing and observation should confirm this recommendation.

- *Mixing Reduction Factor*. Empirical coefficients may need to be established to account for the efficiency of the methods used to mix fibers with soil during construction. Mixing reduction factors to account for non-uniform distribution of fibers throughout the soil mass will need to be evaluated experimentally and are expected to depend on the fiber content, soil type, and mixing method. That is, for a certain mixing method, the reduction factor is expected to increase with increasing fiber contents.

- *Construction Quality Assurance.* Construction Quality Assurance testing may initially include strength testing of specimens mixed and compacted in the laboratory to the target field density as well as testing of intact samples recovered following field compaction. Once sufficient experience is accumulated to eliminate construction damage as a source of concern it may be possible to eliminate or significantly reduce and rely solely on control of fiber content placed in the field and field density measurements.

2.4 Advantages of a Discrete Approach in the Design of Fiber-reinforced Slopes

A major objective of the discrete framework for design of fiber-reinforced soil slopes is to allow the engineer to perform a fiber-reinforced slope design without having to implement a nonconventional, soil-specific shear strength testing program on fiber-reinforced specimens. Using the discrete framework developed herein, it is anticipated that stability analyses could be accomplished by using:

(1) data provided to the design engineer by the geosynthetic manufacturer regarding the properties of the fiber products; and

(2) data collected by the design engineer regarding the shear strength of the candidate backfill soil.

The major difference between the approach proposed herein and the conventional composite approach is that the data described in item (2) above is the conventional shear strength parameters for (unreinforced) soil. Extensive experience exists on values of these parameters used for design of geotechnical projects. Depending on the criticality of the project, the engineer may opt for not performing laboratory tests and estimating the required soil shear strength data using local experience or correlations with soil index properties. The data described in item (1) can be selected by the designer based on manufacturer's data and can be written into the project specifications. In fact, a major hurdle that the engineer has to overcome at the present time when designing using a composite approach is that the material specifications refer to the fiber-reinforced composite material. However, if native soils are used, the contractor has no control over the properties of the soil matrix and thus little control over the properties of the composite material. By using a discrete approach, the material specifications will, instead, be established for the geosynthetic products (geosynthetic fibers) for which construction quality control and construction quality assurance procedures are already well established in geosynthetics practice.

In addition to the benefits from the designer's standpoint regarding the availability of data required for design, the use of a discrete approach also aims at facilitating a better understanding of the behavior and modes of failure of fiber-reinforced soil structures. This enhanced understanding may lead to the optimization (e.g. optimized length, aspect ratio, surface characteristics) of the fiber products used for soil slope stabilization.

3. EXPERIMENTAL TESTING PROGRAM

3.1 <u>General</u>

The use of fiber-reinforcement was identified as a potential alternative for stabilization of steep (1.5H:1V) veneer cover slopes at the Operating Industries Inc. (OII) Superfund Landfill. The landfill is located approximately 10 miles (16 km) east of downtown Los Angeles, in an area of high seismicity, and is undergoing final closure under the US Environmental Protection Agency (USEPA) Superfund program. An evapotranspirative cover system consisting of 6.0 ft (1.8 m) of engineered soil has been approved by USEPA as the final cover. In addition to increasing the static and seismic stability of the soil cover veneer, the use of fiber-reinforcement in a steep soil veneer cover system like those at OII provides additional unquantified benefits.   These benefits include increased resistance to crack development, enhanced erosion control, use of a comparatively low soil density that facilitates vegetation development, and better response to differential settlements.

The testing program on fiber-reinforced soil specimens for the OII project was coordinated by Synthetic Industries as part of an initiative to evaluate the feasibility of a fiber-reinforced alternative. The objective of the testing was to compare the mechanical and hydraulic properties of the fiber-reinforced soils to those of unreinforced soils. The soils used as part of this preliminary testing program were provided by New Cure Inc. (NCI) and sent to the geotechnical laboratory at Fugro McClelland (Southwest) Inc. Dr. Jorge G. Zornberg in coordination with Mr. David Chill defined the scope of the testing program. The shear strength and hydraulic conductivity tests were performed under supervision of Mr. Gary H. Gregory.

The soils tested as part of this experimental program were collected from a stockpile of borrow soil material at the landfill site. The borrow source is an excavation at the Belmont School in the Los Angeles area. The index properties of the borrow soils are: Liquid Limit (LL) of 49%, a Plastic Limit (PL) of 24%, and a

Plasticity Index (PI) of 25%. The percentage of material passing the #200 sieve is 82.6%. The soil classifies as a CL material using the Unified Soil Classification System.

The fiber products were provided by Synthetic Industries. Two fiber types were used in this investigation:

- Fibrillated polypropylene fibers (2600 deniers) with a nominal length of 1 in. (25 mm).

- Fibrillated polypropylene fibers (360 deniers) with a nominal length of 2 in. (50 mm).

The following (gravimetric) fiber contents were selected for this investigation:

- no fibers (unreinforced control specimens)

- 0.2% by weight (weight of fibers/weight of dry soil)

- 0.4% by weight (weight of fibers/weight of dry soil)

The testing program included triaxial compression shear strength testing to evaluate the "equivalent" shear strength of fiber-reinforced specimens and saturated hydraulic conductivity tests to evaluate the impact of the fibers on the hydraulic performance of cover soils.

The compaction characteristics of the unreinforced soil were evaluated by performing ASTM D698 test (Standard Proctor compaction test). The maximum dry unit weight for the unreinforced soil was determined as 96.8 pcf (15.5 kN/m^3) and the optimum moisture content was 22.5 %. Remolded specimens for triaxial and hydraulic conductivity testing were prepared at a target dry unit weight of 90% of the maximum dry unit weight and at the optimum moisture content.

Also, an experimental testing program was implemented to evaluate the tensile strength of the individual fibers used in the triaxial compression and hydraulic conductivity tests. The laboratory tests were performed at the Synthetic Industries Material Testing Laboratory in Chattanooga, Tennessee, under supervision of Mr. Bobby Kennedy of Synthetic Industries.

3.2 Shear Strength Testing Program

The triaxial compression testing program consisted of backpressure saturated ICU triaxial tests with measurement of pore water pressure. The tests were performed in general accordance with ASTM D 4767. A total of five shear strength envelopes were defined in this manner as part of this experimental program. Each shear strength envelope was defined using the results from specimens tested at confining pressures of 3.5, 7.0, and 14.0 psi (24, 48, and 96 kPa). Figure 1 shows the shear strength envelope obtained using the control (unreinforced) specimens. The control (unreinforced) series yielded a shear strength defined by an effective cohesion of 1.73 psi (11.9 kPa) and an effective friction angle of 31.2 degrees. Figures 2 to 5 show the shear strength envelopes obtained using the fiber-reinforced specimens. The shear strength envelopes were obtained from linear regression of the maximum shear stress points (K_f line) at the three confining pressures plotted in a *p-q* diagram (Lambe and Whitman, 1979). Table 1 summarizes the results of the shear strength testing program for each of the series of tests. These results show a clear increase in shear strength with increasing fiber content. Furthermore, for the same fiber content by weight, the 2 in. (50 mm) fibers yield higher "equivalent" shear strength than the 1 in. (25 mm) fibers.

Figure 6 compares the K_f line obtained for the control specimens to the K_f line for the 1 in. (25 mm) fiber-reinforced specimens (effect of increasing fiber content). Figure 7 compares the strength test results for the control specimen to those from the 2 in. (50 mm) fiber-reinforced specimen. Figure 8 compares the strength envelope for the control to the strength envelope for the 0.2% fiber content specimens. Figure 9 compares the strength test results for the control to the strength test results for the 0.4% fiber content specimens. These figures clearly show the increase in "equivalent" shear strength with increasing fiber content and with increasing fiber length.

Shear strength test data is presented in Appendix C.

3.3 Hydraulic Conductivity Testing Program

The saturated hydraulic conductivity of control specimens and fiber-reinforced specimens was evaluated as part of the experimental program. The hydraulic conductivity tests were performed in general accordance with ASTM D 5084. Considering that the fiber-reinforcement application under evaluation was a landfill cover system, the potential impact of the fibers on the hydraulic conductivity of the soil was of major relevance. Hence, hydraulic conductivity measurements on fiber-reinforced specimens were implemented as part of the experimental testing program. Table 2 reports the hydraulic conductivity test results. Figure 10 shows saturated hydraulic conductivity as a function of the gravimetric fiber content obtained for the control and fiber-reinforced specimens. As shown in the figure, the hydraulic conductivity shows no clear trend with increasing fiber content. The range of hydraulic conductivity results shown in this figure may be attributable to experimental scatter.

The lack of trend in the saturated hydraulic conductivity results observed in this investigation provides encouraging evidence regarding the potential use of fiber-reinforced soils in the design of landfill cover systems. At least for the range of fiber content considered in this investigation, it appears that the hydraulic performance of the fiber-reinforced soil does not differ from that of unreinforced soil and can be evaluated from hydraulic conductivity tests on unreinforced specimens. Hydraulic conductivity test results are also presented in Appendix C.

3.4 Fiber Tensile Strength Testing Program

One of the parameters used for discrete characterization of the fiber-reinforced soil is the tensile strength of individual fibers. Consequently, a preliminary tensile strength testing program was implemented as part of the scope of this report. The tensile strength indicated in the general manufacturers specifications for the fiber

products used in this investigation is 40,000 psi (275,800 kPa), as determined by ASTM D 2256-97 (Section D.1 of Appendix D).

The scope of the testing program performed on the fibers as part of this work included a sensitivity evaluation of the impact on the tensile strength of the loading rate and the gauge length. A series of baseline tests were performed in general accordance with ASTM D 2256-97, Standard Test Method for Tensile Properties of Yarns by the Single-Strand Method (Section D.2 of Appendix D). In addition, tests were performed using a loading rate of 1 in. (25 mm)/min. instead of the standard loading rate of 12 in. (50 mm)/min. and using a gauge length of 3 in. (75 mm) instead of the standard gauge length of 10 in. A total of eight series of tensile strength tests were performed (2 fiber types, 2 loading rates, 2 gauge lengths). A total of three tests were performed in each series of tests in order to obtain representative results.

The tensile test results are reported in Section D.3 of Appendix D. Table 3 presents a summary of the test results. The values reported in the table are the average of the three tests performed for each series. The results indicate that, for the two fibers tested as part of this testing program, the tensile strength is not very sensitive to the loading rate or gauge length. The measured tensile strength of the fibers was approximately 60,000 psi (413,700 kPa), which is above the specified value of 40,000 psi (275,800 kPa).

4. DISCRETE FRAMEWORK FOR FIBER-REINFORCEMENT

4.1 Tensile Contribution of Fiber-reinforcement

4.1.1 General

The basis of the discrete framework proposed herein is to quantify the contribution to stability provided by fibers in a fiber-reinforced soil mass by a fiber-induced distributed tension, t. This fiber-induced distributed tension can then be incorporated as a discrete component in limit equilibrium analyses, as it is the case for stability analyses performed using uniaxial planar reinforcement inclusions. The tension t to be used in the analysis represents the tensile force per unit area carried by randomly distributed fibers. As shown later in this section, the magnitude of the fiber-induced distributed tension can be defined as a function of properties of the individual fibers (i.e. their tensile strength and interface shear strength). The purpose of this section is then to develop the framework for evaluating the tensile contribution of the fibers to the stability of a fiber-reinforced soil mass. Developing this framework involves defining the relationships between the fiber-induced distributed tension, t, and properties of the individual fibers.

The direction of the fiber-induced distributed tension, t, should be identified or assumed in the discrete model. Figure 11 shows a schematic representation of a soil mass reinforced using randomly distributed fibers, which are along a potential failure plane before mobilization of tensile stresses in the fibers. The following assumptions could be possibly adopted regarding the orientation of the fibers once they mobilize tensile stresses:

1.   The fiber-induced distributed tension t can be assumed to act, for design purposes, along the failure surface (Figure 12). By making this assumption, the discrete fiber-induced tensile contribution t can be

directly "added" to the shear strength contribution of the soil in a limit equilibrium analysis.

2. The fiber-induced distributed tension t can be assumed to act, for design purposes, in a horizontal direction (Figure 13), consistent with the design of reinforced soil structures using continuous planar reinforcements.

3. The fiber-induced distributed tension t can be assumed to act in a direction which is somewhere in between the initial fiber orientation (which is random) and the orientation of the failure plane.

The alternative assumptions listed above could be evaluated experimentally, using parametric evaluations, or by comparison between experimental and analytical results. Final conclusions regarding the orientation of the fiber-induced distributed tension t to be used for design are not presented in this report. However, since Assumption (1) simplifies the analysis, this assumption was adopted for the analyses presented in this report. Experimental test results reported by Gray and Ohashi (1983) provide supporting evidence for selection of Assumption (1). Their experimental results suggest that, if the fibers are randomly oriented, the "equivalent" shear strength increase is independent of the orientation at which the failure plane intercepts the many randomly oriented fibers. Figure 14 compares the results of direct shear tests performed using fiber-reinforced dry sand specimens in which the fibers are oriented either perpendicularly or randomly in relation to the shear plane. As can be observed in the figure, the shear strength envelopes are similar. Also, it has been reported that, in granular backfill, the assumed orientation of the reinforcements does not affect significantly the calculated factor of safety (Wright and Duncan, 1991; Zornberg et al., 1998b). It may then be inferred that, for design purposes, the calculated factors of safety will not be very sensitive to the selected orientation of the tensile forces developed by the fibers (i.e. to the selection of one of the three alternatives listed above). Nonetheless, although Assumption (1) is adopted for the remainder of this report, further evaluations

are necessary in future stages of development of the discrete methodology to confirm or refine this assumption.

4.1.2 Definitions

This section presents a series of definitions needed in development of the analytical framework proposed in this report.

The volumetric fiber content, χ, is defined as:

$$\chi = \frac{V_f}{V} \tag{1}$$

where V_f is the volume of fibers and V is the control volume of fiber-reinforced soil.

The gravimetric fiber content, χ_w, is defined as:

$$\chi_w = \frac{W_f}{W_s} \tag{2}$$

where W_f is the weight of fibers and W_s is the dry weight of soil. The dry weight of soil is used in the definition above instead of the dry weight of fiber-reinforced soil in order to facilitate use of this concept in engineering practice. Note that the definition of (gravimetric) fiber content in Equation (2) is analogous to the classic definition of the (gravimetric) moisture content of soils.

The total dry unit weight of the fiber-reinforced soil composite, γ, is defined as:

$$\gamma = \frac{W_f + W_s}{V} \tag{3}$$

From Equations (1), (2), and (3), the gravimetric fiber content can be defined from the volumetric fiber content as follows (see Section E.1 in Appendix E):

$$\chi_w = \frac{\chi \cdot G_f \cdot \gamma_w}{\gamma - \chi \cdot G_f \cdot \gamma_w} \tag{4}$$

where G_f is specific gravity of the fibers (dimensionless) and γ_w is the unit weight of water.

Similarly, the volumetric fiber content can be obtained from the gravimetric fiber content as follows (see Section E.2 in Appendix E):

$$\chi = \frac{\chi_w \cdot \gamma}{(1 + \chi_w) \cdot G_f \cdot \gamma_w} \tag{5}$$

4.1.3 Fiber-Induced Distributed Tension in Fiber Breakage Failure Mode

This section defines the magnitude of the fiber-induced distributed tension at breakage, t_t, which is the fiber-induced distributed when failure is governed by fiber breakage (i.e. when the ultimate tensile strength of individual fibers is achieved).

The ultimate tensile strength of the individual fiber, $\sigma_{f,ult}$, can be defined by tensile testing of individual fiber specimens in the laboratory. The ultimate tensile strength of individual fibers can be characterized by the ultimate tensile load carried by all individual fibers crossing a control section A divided by the cross-sectional area A_f of all the fibers in the control section (Figure 15). The soil itself is assumed to have zero tensile strength. Therefore, provided that failure is governed by the tensile strength of fibers, the tensile force carried by the individual fibers in control section A can be defined as follows:

$$Ultimate\ Tensile\ Force = t_t \cdot A = \sigma_{f,ult} \cdot A_f \tag{6}$$

The definition of the ultimate tensile force indicated above implies that all fibers in the control section A act in the same direction at the moment of failure. The tensile force carried by the fibers can then be defined either in terms of the fiber-induced distributed tension per unit area A or in terms of the individual fiber tensile strength per unit area A_f. Considering that, from Equation (1), $\chi = V_f/V = A_f/A$, then using (1) and (6):

$$t_t = \sigma_{f,ult} \cdot \chi \qquad (7)$$

4.1.4 Fiber-Induced Distributed Tension in Fiber Pullout Failure Mode

This section defines the magnitude of the fiber-induced distributed tension at pullout, t_p, which is the fiber-induced distributed when failure is governed by the pullout (rather than breakage) of individual fibers. The interface shear resistance of individual fibers, f_f, can be defined by pullout testing of individual fiber specimens in the laboratory. The interface shear resistance of individual fibers can be defined as:

$$f_f = a + \tan\delta \cdot \sigma_n \qquad (8)$$

where a is the adhesive component of the interface shear strength between soil and the polymeric fibers, $\tan\delta$ is the frictional component, and σ_n is the normal stress.

The concept of an interaction coefficient, commonly used in the soil reinforcement literature for continuous planar reinforcement, is adopted herein to relate the components of the interface shear strength to the shear strength of the soil matrix. The interface shear strength of individual fibers can then be expressed in terms of the backfill soil shear strength as follows:

$$f_f = c_{i,c} \cdot c + c_{i,\phi} \cdot \tan\phi \cdot \sigma_n \qquad (9)$$

where $c_{i,c}$ and $c_{i,\phi}$ are the interaction coefficients for the cohesive and frictional components of the interface shear strength (i.e. c and $\tan\phi$), respectively. The interaction coefficients are defined as:

$$c_{i,c} = \frac{a}{c} \tag{10}$$

$$c_{i,\phi} = \frac{\tan\delta}{\tan\phi} \tag{11}$$

The embedment length of a fiber, l_e, is the length of the shorter portion of the fiber on either side of the failure surface (Figure 16). For the purposes of this analysis, the equivalent diameter d_f of a single fiber is defined as:

$$d_f = \left(\frac{4\,A_{f,i}}{\pi}\right)^{1/2} \tag{12}$$

where $A_{f,i}$ is the cross-sectional area of an individual fiber.

The pullout resistance shall be estimated for the shortest side of the two portions of a fiber intercepted by the failure plane. Statistically, the average embedment length of the fibers $l_{e,ave}$ is (e.g. Maher and Gray, 1990):

$$l_{e,ave} = \frac{l_f}{4} \tag{13}$$

where l_f is the fiber length.

Instead of computing the pullout resistance developed along the actual embedment length, l_e, of the different fibers intercepted by the failure plane, the pullout resistance can also be quantified by computing the pullout resistance along the average embedment length, $l_{e,ave}$, of all individual fibers crossing a control surface A (Figure 17). Provided that failure is governed by pullout of the individual fibers, the

tensile force carried at failure by the individual fibers intersecting control section A can be defined, in the case of a *cohesionless soil*, as follows:

$$Ultimate\ Tensile\ Force = t_p \cdot A = \pi \cdot d_f \cdot l_{e,ave} \cdot \sigma_n \cdot c_{i,\phi} \cdot \tan\phi \cdot n \qquad (14)$$

where n is the number of fibers intersecting the control section A.

The number of fibers in the control section A can be defined using (12) as a function of the cross sectional area of all the individual fibers $A_{f,i}$ as follows:

$$n = \frac{A_f}{A_{f,i}} = \frac{A_f}{\dfrac{\pi \cdot (d_f)^2}{4}} \qquad (15)$$

The aspect ratio η of individual fibers is defined as:

$$\eta = \frac{l_f}{d_f} \qquad (16)$$

Using (13), (14), (15), and (16), the distributed tension when failure is governed by the pullout of individual fibers, t_p can be estimated as (cohesionless case):

$$t_p = \eta \cdot \chi \cdot c_{i,\phi} \cdot \tan\phi \cdot \sigma_n \qquad (17)$$

It should be noted that t_p is not only a function of the fiber interaction properties but also of the confining pressure.

An adhesion component, *a*, of the pullout resistance can also be accounted for in the expression for interface shear strength of the fiber. In this case, the tensile force at failure carried by the individual fibers in the control section A can be defined as follows:

$$Ultimate\ Tensile\ Force = t_p \cdot A = \pi \cdot d_f \cdot l_{e,ave}(c \cdot c_{i,c} + \sigma_n \cdot c_{,i,\phi} \cdot \tan\phi) \cdot n \qquad (18)$$

Using (13), (15), (16), and (18), the distributed tension when failure is governed by the pullout of individual fibers, t_p can be estimated as (cohesive case):

$$t_p \;=\; \eta \cdot \chi \cdot c_{i,c} \cdot c + \eta \cdot \chi \cdot c_{i,\phi} \cdot \tan\phi \cdot \sigma_n \tag{19}$$

That is, in the case of a fiber with an adhesive component to the interface shear strength, the fiber-induced distributed tension t_p includes tensile component at zero confining pressure. As in the case of cohesionless soils, t_p is not only a function of the fiber interaction properties but also of the confining pressure.

4.1.5 Fiber-Induced Distributed Tension

The fiber-induced distributed tension t to be used in a discrete approach to account for the tensile contribution of the fibers in a limit equilibrium analysis is defined as:

$$t = \min\!\left(t_t, t_p\right) \tag{20}$$

Or, equivalently:

$$\frac{t}{\chi} = \min\!\left(\frac{t_t}{\chi}, \frac{t_p}{\chi}\right) \tag{21}$$

In case of a granular soil, using Equations (7), (17), and (21), the normalized fiber-induced distributed tension t/χ can be defined as:

$$\frac{t}{\chi} = \min\!\left(\sigma_{f,ult}, \left(\eta_f \cdot c_{i,\phi} \cdot \tan\phi \cdot \sigma_n\right)\right) \tag{22}$$

Figure 18 shows the bilinear representation of the normalized fiber-induced distributed tension as a function of the confining pressure σ_n , which results form the analysis developed herein for the case of a cohesionless soil.

In case of a cohesive soil, the normalized fiber-induced distributed tension can be defined using Equations (7), (19), and (21), as follows:

$$\frac{t}{\chi} = \min\left(\sigma_{f,ult}, \left(\eta \cdot \chi \cdot c_{i,c} \cdot c + \eta \cdot \chi \cdot c_{i,\phi} \cdot \tan\phi \cdot \sigma_n\right)\right) \tag{23}$$

Figure 19 shows the bilinear representation of the normalized fiber-induced distributed tension as a function of the confining pressure that corresponds to a cohesive soil.

The critical confining pressure $\sigma_{n,crit}$ that defines the change in the failure mode governing the behavior of the fiber-reinforced soil mass is the confining pressure at which failure would occur, simultaneously, by fiber breakage and by fiber pullout. That is:

$$at\ \sigma_{n,crit} \Rightarrow \frac{t_t}{\chi} = \frac{t_p}{\chi} \tag{24}$$

For the case of cohesionless soils, using (7) and (17):

$$\sigma_{n,crit} = \frac{\sigma_{f,ult}}{\eta \cdot c_{i,\phi} \cdot \tan\phi} \tag{25}$$

For the case of cohesive soils, using (7) and (19):

$$\sigma_{n,crit} = \frac{\sigma_{f,ult} - \eta \cdot c_{i,c} \cdot c}{\eta \cdot c_{i,\phi} \cdot \tan\phi} \tag{26}$$

Equations (25) and (26) define the value of the critical confining pressure as a function of the fiber geometry (i.e. η), the fiber tensile strength (i.e. $\sigma_{f,ult}$), the soil shear strength (i.e. c and ϕ) and the individual fiber-soil interaction properties (i.e. $c_{i,\phi}$ and $c_{i,c\phi}$). It should be noted that the critical confining pressure is not a function of the fiber content. As in the case of soil structures reinforced with continuous planar

reinforcements, it seems appropriate to define the fiber interaction properties using interaction coefficients. Using this approach, conservative assumptions may be made for design in the absence of project-specific test results to define the interaction coefficients. Reported data on interaction coefficients between soil and continuous planar reinforcements has indicated that the interaction coefficients can be established with a reasonable degree of confidence without site-specific interface shear testing in noncritical applications. It should be noted that the critical confining pressure and the fiber-induced distributed tension t can be obtained without performing nonconventional shear strength tests (e.g. triaxial tests) on fiber-reinforced specimens.

Maher and Gray (1990) and other investigators have also identified the existence of a critical confining stress, at which level there is a change in the "equivalent" shear strength behavior of a fiber-reinforced composite. Even though these previous investigations have defined the magnitude of the critical confining pressure experimentally, an analytic formulation for its determination was still to be defined. Experimental results reported by previous investigators (e.g. Maher and Gray, 1990) indicated that:

- The "equivalent" shear strength envelope obtained from triaxial tests shows either a curved or bilinear shape with a transition at a certain critical confining stress.

- An increase in fiber aspect ratio results in a lower critical confining pressure and a higher "equivalent" shear strength.

- An increase in fiber content shows no apparent change in the critical confining pressure.

- The "equivalent" shear strength increases approximately linearly with increasing amounts of fiber and then approaches an asymptotic upper limit governed mainly by confining stress and fiber aspect ratio.

- Well-graded sands with a high coefficient of uniformity (i.e. sands with a comparatively higher shear strength) result in a lower critical confining pressure and a higher "equivalent" shear strength.

The above experimental observations on the critical confining pressure can all be explained by Equation (26) obtained using the analytical framework proposed herein.

Key elements in the expressions for t and $\sigma_{n,crit}$ developed in this section are the tensile strength and the interface shear strength of individual fibers. Testing methodologies for defining the individual fiber properties have not been developed yet, but existing testing standards provide a good initial basis for these tests. If these properties were provided by the geosynthetic manufacturer for specific fiber products, the designer would no longer need to perform shear strength tests on fiber-reinforced specimens. Fiber properties have been reported in the literature (e.g. Alwahab and Al-Ourna; 1995, Al-Refeai, 1991). However, additional effort should be made to appropriately define the mechanical properties of individual fibers. Section D.3 of Appendix D presents the results of tensile tests performed for two fiber products used in the testing program described in Section 3.

4.2 "Equivalent" Shear Strength of a Reinforced Fiber Composite

Triaxial tests have been usually performed to define an "equivalent" shear strength of fiber-reinforced composite specimens (e.g. Maher and Gray, 1990; Al-Refeai, 1991; Gregory and Chill, 1998). This section establishes relationships between the "equivalent shear strength" of fiber-reinforced specimens, the fiber-induced distributed tension t (defined in Section 4.1), and the soil shear strength properties. These relationships are useful not only for design but also for validation purposes of the proposed discrete framework. That is, triaxial test results on fiber-reinforced

specimens can be used to validate the relationships developed in Section 4.1. An important assumption made regarding the development of the relationships in Section 4.1 is the orientation used for design purposes for the fiber-induced distributed tension t. Figure 20 shows two directions (out of the three alternatives discussed in Section 4.1.1) which could be assumed for the fiber-induced distributed tension t for interpretation of triaxial tests: (1) fiber-induced distributed tension parallel to the shear plane; and (2) horizontal fiber-induced distributed tension.

The discrete framework proposed in this report for evaluation of contribution of fiber-reinforcement to stability is for Assumption (1) in Section 4.1.1 . That is, the fiber-induced distributed tension t is assumed parallel to the shear plane. In this case, the magnitude of the normal stress acting on the shear plane is not affected by the fiber-induced distributed tension t. The equivalent shear strength of the fiber-reinforced soil, S_{eq} , can be defined as:

$$S_{eq} \ = \ S + \alpha \cdot t \tag{27}$$

where S is the shear strength of the soil (unreinforced) and α is an empirical coefficient that accounts for the effect of the direction of t on S_{eq} .

If the assumption regarding the orientation of the fiber-induced distributed tension t is correct (Figure 20a), the empirical coefficient α shall equal 1.0 . It should be noted that, if the fiber-induced distributed tension t is not parallel to the failure surface (e.g. Figure 20b), the direct contribution of the fiber-reinforcement to the "equivalent shear strength" would be smaller than in the parallel case. This is because the component of t in the direction of the shear plane is smaller than in Case (1) (and, consequently, α shall be less than 1.0). However, the component of the fiber-induced distributed tension perpendicular to the shear plane will induce a local increase of the normal stress (i.e. $\sigma_{n,b} > \sigma_{n,a}$), which will result in an increased soil shear strength (i.e. $S_b > S_a$). These two compensating effects regarding the assumed orientation of the fiber-induced distributed tension t may result in similar shear strength values for $S_{eq,a}$ and $S_{eq,b}$. Additional evaluation shall provide insight into the adequacy of the different

assumptions regarding the orientation of the fiber-induced distributed tension t and the value of the coefficient α in Equation (27), if different than 1.0 .

Figure 21 shows a schematic representation of the equivalent shear strength S_{eq} for the case of a cohesionless soil. In this case, for $\sigma_n < \sigma_{n,crit}$, and using Equations (17) and (27) (see derivation in Section E.3 of Appendix E):

$$S_{eq} = \tan\phi \left(1 + \alpha \cdot \eta \cdot \chi \cdot c_{i,\phi}\right) \sigma_n \tag{28}$$

Similarly, for the case of a granular soil and $\sigma_n > \sigma_{n,crit}$, using Equations (7) and (27) (see derivation in Section E.4 of Appendix E):

$$S_{eq} = \alpha \cdot \chi \cdot \sigma_{f,ult} + \tan\phi \cdot \sigma_n \tag{29}$$

Figure 22 shows a schematic representation of the equivalent shear strength S_{eq} for the generic case of a cohesive soil.

As observed in Figures 21 and 22, the analytically obtained equivalent shear strength envelopes are bilinear. The linear expressions defining the two portions of the bilinear envelope can be defined as $S_{eq,1}$ and $S_{eq,2}$ for the cases in which the normal stress is, respectively, below or above $\sigma_{n,crit}$.

For a generic cohesive-frictional soil, $S_{eq,1}$ (i.e. case $\sigma_n < \sigma_{n,crit}$) can be defined using Equations (19) and (27) as follows (see derivation in Appendix E.5):

$$S_{eq,1} = c_{eq,1} + \left(\tan\phi\right)_{eq,1} \cdot \sigma_n \tag{30}$$

where:

$$c_{eq,1} = \left(1 + \alpha \cdot \eta \cdot \chi \cdot c_{i,c}\right) \cdot c \tag{31}$$

$$\left(\tan\phi\right)_{eq,1} = \left(1 + \alpha \cdot \eta \cdot \chi \cdot c_{i,\phi}\right) \cdot \tan\phi \tag{32}$$

Similarly, for a generic cohesive-frictional soil, the linear envelope $S_{eq,2}$ (i.e. case $\sigma_n > \sigma_{n,crit}$) can be defined using Equations (7) and (27) (see derivation in Section E.6 of Appendix E):

$$S_{eq,2} \ = \ c_{eq,2} + \left(\tan\phi\right)_{eq,2} \cdot \sigma_n \tag{33}$$

where:

$$c_{eq,2} \ = \ c + \alpha \cdot \chi \cdot \sigma_{f,ult} \tag{34}$$

$$\left(\tan\phi\right)_{eq,2} \ = \ \tan\phi \tag{35}$$

As previously mentioned, the magnitude of the equivalent shear strength is defined as a function of the (unreinforced) soil shear strength properties and the properties of the individual fibers. That is, no testing of the soil fiber composite would be needed to define the equivalent properties. Specifically, the coefficients $c_{eq,1}$, $(\tan\phi)_{eq,1}$, $c_{eq,2}$, and $(\tan\phi)_{eq,2}$ are a function of the adhesion interaction coefficient, frictional interaction coefficient, and tensile strength of the individual fiber-reinforcements. Figure 23 illustrates the generic "equivalent strength" envelope for a fiber-reinforced soil mass.

4.3 Examples of Analytic Determination of Fiber-reinforcement Properties

4.3.1 Example 1: Determination of Properties for 1 in. (25 mm) Fibers

Objective: Establish the equivalent shear strength of a soil to be reinforced using 1 in. (25 mm) long Geofibers (Geofibers 2610B). Consider fiber contents (gravimetric) of 0.2 and 0.4%. The soil shear strength at the dry target unit weight of 87 pcf (13.9 kN/m^3) has an effective cohesion of 1.7 psi (11.7 kPa) and an effective friction angle of 31 degrees.

Consider the following fiber properties (provided by Synthetic Industries for Geofibers 2610B, see Section D.1 in Appendix D):

- Fiber thickness: 0.0017 in.

- Fiber width: 0.289 in.

- Fiber length: 1.0 in.

- Fiber specific gravity: 0.91

- Fiber ultimate tensile strength: 40,000 psi (275,800 kPa) (based on ASTM D 2256)

- Fiber linear density: 2610 deniers (note: a denier is one grams/9,000 meters)

The following values are assumed for the purposes of this example:

- $c_{i,c} = 0.8$

- $c_{i,\phi} = 0.8$

- $\alpha = 1.0$

Steps (a) through (e) lead to the determination of the "equivalent" shear strength to be used by the designer in his/her stability analysis, assuming that the fiber-induced distributed tension is parallel to the failure plane.

a) Determination of the volumetric fiber content, χ:

For the case of a gravimetric fiber content of 0.002, and using Equation (5):

$$\chi = \frac{\chi_w \cdot \gamma}{(1 + \chi_w) \cdot G_f \cdot \gamma_w} = \frac{0.002 \cdot 87\,pcf}{(1 + 0.002) \cdot 0.91 \cdot 62.4\,pcf} = 0.002 \cdot 1.529 = 0.0031$$

For the case of a gravimetric fiber content of 0.004, and using Equation (5):

$$\chi = \frac{\chi_w \cdot \gamma}{(1 + \chi_w) \cdot G_f \cdot \gamma_w} = \frac{0.004 \cdot 87\,pcf}{(1 + 0.004) \cdot 0.91 \cdot 62.4\,pcf} = 0.004 \cdot 1.526 = 0.0061$$

b) Determination of the equivalent diameter, d_f :

b.1) Determination of the cross-sectional area of individual fibers $A_{f,i}$ (using reported fibers geometry):

$A_{f,i}$ = 0.00171 in. x 0.289 in. = 0.0004942 in^2

Note that this area corresponds to the entire fiber and ignores splitting of the fibrillated yarns during mixing.

b.2) Determination of the cross-sectional area of individual fibers $A_{f,i}$ (using reported linear density of the fibers):

This second calculation of the cross-sectional area is presented as a check to the value obtained in (b.1). The weight and volume of a single fiber, which is 1 in. (25 mm) long and has a denier of 2610 g/9000 m, is:

Weight of single fiber = 2610 g/9000m x 0.0254 m = 0.007366g

Volume of single fiber = 0.007366g/ (0.91 x 1 g/cm^3) =

$$= 0.0080945 \text{ cm}^3 = 0.0004939 \text{ in}^3$$

Cross-sectional area of single fiber = $A_{f,i}$ = 0.0004939 in^3 / 1 in.

$$= 0.0004939 \text{ in}^2$$

This value is consistent with the area obtained previously from the width and thickness measurements. A cross-sectional area $A_{f,i}$ = 0.000494 in^2 is adopted for a single fiber in this example.

b.3) Determination of d_f:

Using Equation (12):

$$d_f = \left(\frac{4\,A_{f,i}}{\pi} \right)^{1/2} = \left(\frac{4 \cdot 0.000494}{\pi} \right)^{1/2} = 0.02508 \; in$$

The determination of the equivalent diameter is an issue to be further investigated for the case of noncylindrical fibers. In this case, fibrillation of the yarns may need to be taken into consideration. The determination of the equivalent diameter by Equation (12), however, is considered for the purposes of this example.

c) Determination of the fiber aspect ratio, η:

The aspect ratio is determined using Equation (16):

$$\eta = \frac{1.0 in}{0.02508 in} \cong 40$$

d) Determination of $\sigma_{n,crit}$:

Using Equation (26):

$$\sigma_{n,crit} = \frac{\sigma_{f,ult} - \eta \cdot c_{i,c} \cdot c}{\eta \cdot c_{i,\phi} \cdot \tan\phi} = \frac{40,000\,psi - 40 \cdot 0.8 \cdot 1.7\,psi}{40 \cdot 0.8 \cdot \tan 31\circ} = 2077\,psi$$

The critical confining pressure is too high for practical applications [for a soil unit weight of 87 pcf (13.9 kN/m^3), the critical confining pressure corresponds to a depth of more than 3,000 ft (914 m)]. Consequently, only the first portion of the bilinear equivalent shear strength envelope of the fiber-reinforced composite is of interest for this example.

e) Determination of S_{eq} :

The equivalent shear strength for the range of confining pressures of interest (i.e. the first portion of the bilinear envelope) is obtained using Equation (30) as:

$$S_{eq,1} = c_{eq,1} + (\tan\phi)_{eq,1} \cdot \sigma_n$$

For a gravimetric fiber content of 0.002, the cohesive component of the equivalent shear strength is estimated using Equation (31) as:

$$c_{eq,1} = (1 + \alpha \cdot \eta \cdot \chi \cdot c_{i,c}) \cdot c = (1 + 1.0 \cdot 40 \cdot 0.0031 \cdot 0.8) \cdot 1.7\,psi$$
$$c_{eq,1} = 1.0992 \cdot 1.7\,psi = 1.87\,psi$$

Also, for a gravimetric fiber content of 0.002, the frictional component of the equivalent shear strength is defined using Equation (32) as:

$$(\tan\phi)_{eq,1} = (1 + \alpha \cdot \eta \cdot \chi \cdot c_{i,\phi}) \cdot \tan\phi = (1 + 1.0 \cdot 40 \cdot 0.0031 \cdot 0.8) \cdot \tan 31°$$
$$(\tan\phi)_{eq,1} = 1.0992 \cdot \tan 31° = 0.67008$$
$$\phi_{eq,1} = 33.4°$$

For a gravimetric fiber content of 0.004, the cohesive component of the equivalent shear strength is defined using Equation (31) as:

$$c_{eq,1} = \left(1 + \alpha \cdot \eta \cdot \chi \cdot c_{i,c}\right) \cdot c = \left(1 + 1.0 \cdot 40 \cdot 0.0061 \cdot 0.8\right) \cdot 1.7\,psi$$

$$c_{eq,1} = 1.1952 \cdot 1.7\,psi = 2.03\,psi$$

Also, for a gravimetric fiber content of 0.004, the frictional component of the equivalent shear strength is defined using Equation (32) as:

$$\left(\tan\phi\right)_{eq,1} = \left(1 + \alpha \cdot \eta \cdot \chi \cdot c_{i,\phi}\right) \cdot \tan\phi = \left(1 + 1.0 \cdot 40 \cdot 0.0061 \cdot 0.8\right) \cdot \tan 31°$$

$$\left(\tan\phi\right)_{eq,1} = 1.1952 \cdot \tan 31° = 0.7181$$

$$\phi_{eq,1} = 35.7°$$

4.3.2 Example 2: Determination of Properties for 2 in. (50 mm) Fibers

Objective: Establish the equivalent shear strength of a soil to be reinforced using 2 in. (50 mm) long Geofibers (Geofibers 360). Consider fiber contents (by weight) of 0.2 and 0.4%. The soil shear strength at the dry target unit weight of 87 pcf (13.9 kN/m^3) has an effective cohesion of 1.7 psi (11.7 kPa) and an effective friction angle of 31 degrees.

Consider the following fiber properties:

- Fiber length: 2.0 in. (50 mm)

- Fiber specific gravity: 0.91

- Fiber ultimate tensile strength: 40,000 psi (275,800 kPa) (based on ASTM D 2256)

The following values are assumed for the purposes of this example:

- $c_{i,c} = 0.8$

- $c_{i,\phi} = 0.8$

- $\alpha = 1.0$

- $d_f = 0.02508$ in (assumed the same as in Example 1)

The "equivalent" shear strength to be used by the designer using the 2 in. (50 mm) long fibers in this example is determined next.

a) Determination of the volumetric fiber content, χ:

The determination of the volumetric fiber contents is as in Example 1. The volumetric fiber contents that correspond to the gravimetric fiber contents of 0.002 and 0.004 are, respectively, 0.0031 and 0.0061.

b) Determination of the equivalent diameter, d_f :

The 1 in. (25 mm) and 2 in. (50 mm) fibers have a different width. However, because of the fibrillation, it is expected that the equivalent diameter that will contribute to pullout resistance of these two fibers is similar. Consequently, for the purpose of this example, it is assumed that the equivalent diameter for the 2 in. (50 mm) fibers is the same as the one for the 1 in. (50 mm) fibers. As mentioned previously, determination of the equivalent diameter for fibrillated yarns should be further evaluated experimentally.

c) Determination of the fiber aspect ratio, η:

Using Equation (16):

$$\eta \; = \; \frac{2.0\,in}{0.02508\,in} \cong 80$$

d) Determination of $\sigma_{n,crit}$:

Using Equation (26):

$$\sigma_{n,crit} \; = \; \frac{\sigma_{f,ult} - \eta \cdot c_{i,c} \cdot c}{\eta \cdot c_{i,\phi} \cdot \tan \phi} \; = \; \frac{40{,}000\,psi - 80 \cdot 0.8 \cdot 1.7\,psi}{80 \cdot 0.8 \cdot \tan 31^\circ} = 1037\,psi$$

As in the previous example, the critical confining pressure is too high to be of significance for most practical applications [for a soil unit weight of 87 pcf (13.9 kN/m³), the critical confining pressure corresponds to a depth of more than 1,700 ft (518 m)]. Consequently, only the first portion of the bilinear equivalent shear strength envelope of the fiber-reinforced composite is of interest for this example.

e) Determination of S_{eq} :

The equivalent shear strength for the range of confining pressures of interest (i.e. the first portion of the bilinear envelope) is obtained from Equation (30) as:

$$S_{eq,1} \; = \; c_{eq,1} + \left(\tan \phi \right)_{eq,1} \cdot \sigma_n$$

For a gravimetric fiber content of 0.002, the cohesive component of the equivalent shear strength is estimated using Equation (31) as:

$$c_{eq,1} = \left(1 + \alpha \cdot \eta \cdot \chi \cdot c_{i,c} \right) \cdot c = \left(1 + 1.0 \cdot 80 \cdot 0.0031 \cdot 0.8 \right) \cdot 1.7\,psi$$
$$c_{eq,1} = 1.1984 \cdot 1.7\,psi = 2.04\,psi$$

Also, for a gravimetric fiber content of 0.002, the frictional component of the equivalent shear strength is defined using Equation (32) as:

$$(\tan\phi)_{eq,1} = (1 + \alpha \cdot \eta \cdot \chi \cdot c_{i,\phi}) \cdot \tan\phi = (1 + 1.0 \cdot 80 \cdot 0.0031 \cdot 0.8) \cdot \tan 31°$$
$$(\tan\phi)_{eq,1} = 1.1984 \cdot \tan 31° = 0.72007$$
$$\phi_{eq,1} = 35.8°$$

For a gravimetric fiber content of 0.004, the cohesive component of the equivalent shear strength is defined using Equation (31) as:

$$c_{eq,1} = (1 + \alpha \cdot \eta \cdot \chi \cdot c_{i,c}) \cdot c = (1 + 1.0 \cdot 80 \cdot 0.0061 \cdot 0.8) \cdot 1.7\,psi$$
$$c_{eq,1} = 1.3904 \cdot 1.7\,psi = 2.36\,psi$$

Also, for a gravimetric fiber content of 0.004, the frictional component of the equivalent shear strength is defined using Equation (32) as:

$$(\tan\phi)_{eq,1} = (1 + \alpha \cdot \eta \cdot \chi \cdot c_{i,\phi}) \cdot \tan\phi = (1 + 1.0 \cdot 80 \cdot 0.0061 \cdot 0.8) \cdot \tan 31°$$
$$(\tan\phi)_{eq,1} = 1.3904 \cdot \tan 31° = 0.8354$$
$$\phi_{eq,1} = 39.9°$$

4.4 Preliminary Validation of the Discrete Analytical Framework

The examples presented in Section 4.3 correspond to the soil and the two fiber types used in the preliminary experimental testing program described in Section 3. Figures 24 and 25 present the results of the experimental testing program described in Section 3 for the series of tests performed using 1 in. (25 mm) long fibers (Geofibers 2610b) at gravimetric fiber contents of 0.2 and 0.4%. The shear strength results shown in the figures for the fiber-reinforced specimens are well represented by the shear strength envelope obtained analytically in the example in Section 4.3.1.

Figures 26 and 27 present the results of the experimental testing program described in Section 3 for the series of tests performed using 2 in. (50 mm) long fibers (Geofibers 360) at gravimetric fiber contents of 0.2 and 0.4%. The shear strength results shown in the figures for the fiber-reinforced specimens are well represented by the shear strength envelope obtained analytically in the example in Section 4.3.2.

The comparisons shown in Figures 24 through and 27 between analytic and experimental results should be considered preliminary. This is because interface shear strength and tensile strength testing of individual fibers should be further evaluated before final conclusions can be drawn of the validity of the formulation presented herein. Nevertheless, the good match obtained for the preliminary tests performed so far provides encouraging evidence regarding the suitability of the analytical framework developed in this report.

It should be emphasized that the analytic equivalent shear strength envelope was obtained using properties of the fibers and of the soil independently. Consequently, once the relationships proposed herein are validated, the designer would no longer need to depend on project-specific shear strength testing of fiber-reinforced specimens for compiling the design.

4.5 Additional Validation of the Discrete Framework for Fiber-Reinforcement

Section 4.4 provided experimental evidence that validates the proposed discrete framework for fiber-reinforcement for the case of soils tested as part of the OII experimental testing program. In addition, results from triaxial compression tests using fiber-reinforced soil specimens that correspond to four other soils were used to validate the proposed discrete framework. Details of the experimental test results and of the comparison between experimental and predicted shear strength values are presented in Appendix G, "Experimental Validation of the Discrete Framework." These additional

results provide significant additional evidence on the suitability of the proposed discrete approach for the design of fiber-reinforced soil.

4.6 Sensitivity Evaluation

4.6.1 Sensitivity of the Equivalent Shear Strength

The equivalent shear strength of the fiber-reinforced soil in the example presented in Section 4.4 for the case of 1 in. (25 mm) fibers with a gravimetric fiber content of 0.4% is used as the baseline case for the sensitivity evaluation presented in this section. Figure 28 shows the sensitivity of the equivalent shear strength to the selected aspect ratio of the fiber-reinforcement. The thicker line represents the baseline case. In the case of soil structures where the range of confining pressures of interest is well below the critical normal stress, the equivalent shear strength of the composite material is sensitive to the aspect ratio of the fibers. The higher the aspect ratio of the fibers, the higher the equivalent shear strength of the composite. It is anticipated that, for comparatively high aspect ratios (i.e. comparatively long fibers), the validity of the relationships developed herein will be compromised by the difficulty in achieving good mixing of the fibers. The aspect ratio at which the validity of these relationships is compromised should be evaluated experimentally.

Figure 29 shows the sensitivity of the equivalent shear strength to the selected fiber content (gravimetric). The equivalent shear strength of the fiber-reinforced soil in the previous example for the case of 1 in. (25 mm) fibers with a gravimetric fiber content of 0.4% is also considered as the baseline case herein. When the range of confining pressures of interest is well below the critical normal stress, the equivalent shear strength of the composite is very sensitive to the aspect ratio of the fibers. The higher the fiber content, the higher the shear strength of the composite. Also in this case, it is anticipated that the validity of the relationships developed herein will be compromised for comparatively high fiber contents by the difficulty in achieving

good mixing of the fibers. The fiber content at which the validity of these relationships is compromised should be evaluated experimentally.

4.6.2 Implications on Optimization of Fiber Products

Based on the framework developed in this report, insight can be gained regarding the optimization of fiber-reinforcement products for slope stabilization projects. An optimized product shall provide an adequate balance between the fibers' mobilized tensile strength and the fibers' mobilized pullout resistance. Ideally, an optimum fiber product is one in which the critical confining stress corresponds to the range of typical working confining stresses. If the range of working stresses in a fiber-reinforced mass is considerably lower than the critical stress, the fibers will fail by pullout. Consequently, their cross-sectional area is larger than needed because the ultimate tensile strength of the fibers is far from being achieved. In this case, the aspect ratio of the fibers could be increased to optimize the fiber product. Conversely, if the range of working stresses in a fiber-reinforced soil mass is considerably larger than the critical stress, the fibers will fail by achieving their ultimate tensile strength. Consequently, their length is larger than needed as the pullout resistance of the fibers is not reached. In this case, the aspect ratio of the fibers could be decreased to optimize the fiber product. In addition to optimizing the aspect ratio of the fibers, other considerations for product optimization are evaluating different surface textures (which will affect the interface shear strength) and different fiber material types (which will affect the ultimate tensile strength of individual fibers).

5. DESIGN METHODOLOGY

5.1 <u>General</u>

The focus of this section is the development of a limit equilibrium approach for analysis of fiber-reinforced slopes. The proposed approach is generic, but it paves the way for the development of product-specific approaches. It is intended that such product-specific design approaches will facilitate widespread use of fiber-reinforcement in geotechnical practice. In order to develop a product-specific consistent design methodology, the following additional evaluations should be pursued:

1. characterization of the tensile strength of individual fibers;

2. characterization of the interface shear strength of the individual fibers (e.g. evaluation of the pullout resistance of individual fibers);

3. quantification of the distribution and orientation of the fibers within a fiber-reinforced soil mass, and/or sensitivity evaluation of the calculated factors of safety to the assumed orientations.

The use of the discrete framework for fiber-reinforcement is illustrated in this section for both one-dimensional (i.e. infinite slope) and two dimensional slope stability analyses.

5.2   Approaches in Design of Fiber-reinforced Soil Slopes

The limit equilibrium method (Fellenius, 1936; Terzaghi, 1956) still remains the most widely used approach in geotechnical engineering to analyze slope stability problems. This method assumes a kinetically admissible failure surface and a statically admissible stress distribution along that surface. Figure 30 illustrates the use of the conventional method of slices to calculate the factor of safety for a circular potential failure surface in a limit equilibrium analysis. The shear strength required to satisfy equilibrium is equal to the ultimate shear strength S that may develop along the potential failure surface divided by the factor of safety, FS.

In the case of soil slopes reinforced using randomly distributed fiber-reinforcement, stability analysis may also be performed using the conventional limit equilibrium approach. As previously discussed, the contribution of the fibers to stability is typically accounted for in a limit equilibrium analysis by considering the fiber-reinforced soil as a composite material (the composite approach). Figure 31 illustrates the use of the conventional method of slices to calculate the factor of safety for a circular potential failure surface in a fiber-reinforced soil mass. Using this approach, the fiber-reinforced soil mass is considered to behave as a composite material having an ultimate shear strength of $S + \Delta S$, where ΔS represents the contribution of the fibers to the strength of the soil (stability of the slope). The ultimate shear strength of the composite is obtained from laboratory testing on fiber-reinforced soil specimens.

Although the composite approach is conceptually simple to use, it does not quantitatively account for the actual behavior of the fiber-reinforcements (i.e. the fibers work in tension and not in shear) and requires unconventional testing to evaluate the shear strength increase ΔS. Not many soil laboratories are equipped to perform triaxial tests of fiber-reinforced specimens. Furthermore, such triaxial testing typically includes specimens prepared with site-specific soils and different percentages (by weight) of fiber-reinforcement, which can be quite costly and time consuming. Therefore, the use of fiber-reinforcement as a stabilization measure may be cost-prohibitive for small to medium-sized projects because of the cost of performing the necessary specialized tests.

In the case of soil slopes reinforced using continuous inclusions (e.g. geotextiles, geogrids), design and analysis are also typically performed using limit equilibrium methods. In addition to the shape of the failure surface, other information needed for the stability analysis of soil reinforced using continuous inclusions include the inclination (e.g. horizontal, tangential), and the distribution (e.g. triangular, constant with depth) of the reinforcement tensile forces along the selected failure surface. Figure 32 illustrates the use of the conventional limit equilibrium method of slices to calculate the factor of safety for a circular potential failure surface when continuous planar reinforcement elements are used to enhance stability (i.e. to increase the factor of safety). Although the ultimate shear strength S that may develop along the potential failure surface of the reinforced slope is the same as in the unreinforced case (Figure 30), tensile forces (T_j) which develop in the discrete reinforcement elements contribute to increase the factor of safety. The definition of the factor of safety in the case of a reinforced soil slope designed using a discrete approach (Figure 32) is still the same as in the case of unreinforced slopes. That is:

$$FS \;=\; \frac{Available\ soil\ shear\ strength}{Soil\ shear\ stress\ required\ for\ equilibrium} \qquad (36)$$

The use of limit equilibrium stability analyses as a design tool for reinforced slopes and the use of the discrete approach to characterize the behavior of soil structures reinforced by continuous planar inclusions has been successfully validated by centrifuge model tests (Zornberg et al., 1998a, 1998b). The failure surfaces most widely used in limit equilibrium analysis of reinforced soil slopes include the planar wedge (e.g. Schlosser and Vidal, 1969), the bilinear wedge surface (e.g. Jewell, 1991), the logarithmic spiral (e.g. Leshchinsky and Boedeker, 1989), and the circular surface (e.g. Wright and Duncan, 1991). Several of these analysis methods have been used to develop design charts to help determine reinforcement requirements for simple slopes.

5.3 Use of the Discrete Framework in Limit Equilibrium

The design methodology for fiber-reinforced soil slopes described in this section uses the discrete framework developed in Section 4 to quantify the contribution of the fiber's tensile forces to stability. Figure 33 illustrates the use of the discrete approach with the conventional method of slices for a circular potential failure surface for the case in which fiber-reinforcement is used to enhance the factor of safety. A horizontal orientation of the fiber-induced distributed tension is used in the figure for illustration purposes only. As discussed in Section 4.1.1, the orientation of the fibers during shearing is an important assumption that must be made for the purposes of the analysis. Contrary to the composite approach illustrated in Figure 31, the contribution of the fibers to stability is quantified by a fiber-induced distributed tensile stress, t, along the potential failure surface. The ultimate shear strength S that may develop in the soil along the potential failure surface is the same as in the unreinforced case (Figure 30), but the distributed tensile stress t that develops along the potential failure surface due to the presence of fibers increases the factor of safety compared to the unreinforced case.

Figure 34 illustrates the case in which the fiber-induced distributed tension is assumed to act parallel to the potential failure plane, which is consistent with the assumption made in Section 4. This assumption implies that, independent of the initial fiber orientation, the fibers will "kink" during shearing when intercepted by the failure plane and will contribute to the stability of the slope by developing tensile forces parallel to the failure surface. The use of this assumption in combination with the discrete design approach is appealing because it is easily implemented in conventional limit equilibrium computer codes. For this assumption, the magnitude of the fiber-induced distributed tension t is calculated as described in Section 4 and this distributed tension acts in the same direction as the mobilized soil shear strength. Consequently, the strength contribution of the fibers can be incorporated in the input file of a limit equilibrium analysis as an "equivalent" increased shear strength. By assuming an orientation parallel to the failure plane for the tensile forces, the normal stresses along the potential failure surface are the same as those calculated for an unreinforced soil mass. Even though a fiber-reinforced slope analyzed assuming fiber forces parallel to the failure surface incorporates the fiber-induced tensile forces as an increased "equivalent" shear strength (i.e. as in the composite approach), it should be noted that the

magnitude of the tensile forces (or the increased "equivalent" strength) is obtained using the discrete framework described in Section 4.

The assumption made in the remainder of this section regarding the orientation of the fiber-induced distributed tension is that the fiber-induced distributed tension acts *parallel to the potential failure surface*. That is, independent of the initial fiber orientation, the fibers "kink" when intercepted with the failure plane and contribute to stability with a force parallel to the failure surface. As mentioned previously in Section 4, the main reason for considering this assumption is because it renders a simpler approach from an analysis standpoint. Also as discussed previously, available information indicates that the results of the analysis may be relatively insensitive to this assumption. The sensitivity of the results to the assumed orientation is not evaluated as part of the scope of this report. Such a sensitivity analysis should, however, be evaluated before final implementation of the methodology proposed herein.

5.4 <u>One-Dimensional Analysis</u>

This section illustrates implementation of the discrete framework developed in Section 4 to the case of a "veneer slope". In this case, the failure plane is parallel to the slope and, as mentioned previously, the analysis assumes that the fiber-induced distributed tension acts also parallel to the slope.

5.4.1 Unreinforced Veneer Slope

The stability of an infinite (unreinforced) soil slope veneer is described in this section. Figure 35 shows a schematic view of a soil veneer. From the figure, it can be inferred that:

$$W \sin \beta = S \qquad\qquad (37)$$

$$W \cos \beta = N \tag{38}$$

where W is the weight of the control volume, β is the slope inclination, S is the shear force developed at the base of the control volume, and N is the normal force at the base of the control volume.

The stability of an infinite soil veneer is established by calculating the factor of safety using the rigorous definition established in Equation (36). Considering a Mohr Coulomb shear soil shear strength envelope and the forces indicated in Figure 35, the factor of safety FS for the infinite slope can be calculated from Equation (36) as follows:

$$FS = \frac{c + (N / L) \tan \phi}{S / L} \tag{39}$$

Using Equations (37), (38), and (39):

$$FS = \frac{c.L + W \cos \beta \tan \phi}{W \sin \beta} \tag{40}$$

The weight of the control volume can be established as:

$$W = \gamma \, L \, T \tag{41}$$

where γ is the soil unit weight, L is the length of the control volume along the slope, and T is the thickness of the veneer.

From Equations (40) and (41):

$$FS = \frac{c.L + \gamma \, L \, T \cos \beta \tan \phi}{\gamma \, L \, T \sin \beta} \tag{42}$$

Or, equivalently:

$$FS = \frac{c}{\gamma\, T \sin \beta} + \frac{\tan \phi}{\tan \beta} \tag{43}$$

Equation (43) is the classic relationship for the factor of safety of an infinite (unreinforced) veneer infinite slope. Using Equation (43), the required cohesion c_{req} that a generic infinite slope should have in order to achieve the target factor of safety FS is:

$$c_{req} = \left(FS - \frac{\tan \phi}{\tan \beta} \right) \gamma\, T \sin \beta \tag{44}$$

The relationship above is only valid for $\tan\phi/\tan\beta < FS$.

5.4.2 Fiber-Reinforced Veneer Slope

Figure 36 shows a schematic view of a fiber-reinforced infinite soil veneer. The orientation of the fiber-induced distributed tension t is assumed parallel to the failure surface. The stability of the soil veneer is established by calculating the factor of safety by the rigorous definition provided in Equation (36), as follows:

$$FS = \frac{c + (N\,/\,L) \tan \phi}{S\,/\,L - \alpha \cdot t} \tag{45}$$

Even though the coefficient α is equal to unity if the assumption regarding orientation parallel to the failure surface is used, it is included in Equation (45) for completeness and in order to account for a mixing factor which may be defined experimentally.

Using Equations (37), (38), and (45):

$$FS = \frac{c.L + W \cos \beta \tan \phi}{W \sin \beta - \alpha \cdot t \cdot L} \tag{46}$$

From Equations (41) and (46):

$$FS = \frac{c + \gamma\, T \cos\beta \tan\phi}{\gamma\, T \sin\beta - \alpha \cdot t} \tag{47}$$

The fiber-induced distributed tension t_{req} required in a generic infinite slope with a given soil shear strength in order to achieve the target factor of safety FS can be obtained using Equation (47) as follows (see Section E.7 in Appendix E):

$$t_{req} = \frac{\gamma\, T \sin\beta}{\alpha \cdot FS}\left(FS - \frac{c}{\gamma\, T \sin\beta} - \frac{\tan\phi}{\tan\beta}\right) \tag{48}$$

Or, equivalently, by considering the Factor of Safety for an unreinforced slope, FS_{unr}, as the FS defined by Equation (43):

$$t_{req} = \frac{\gamma\, T \sin\beta}{\alpha \cdot FS}\left(FS - FS_{unr}\right) \tag{49}$$

As discussed in Section 4, the behavior of the fiber-reinforced soil mass depends on whether the failure mode is governed by fibers pullout or by fibers breakage. The governing mode behavior of the fiber-reinforced soil mass depends on the magnitude of the critical normal stress, $\sigma_{n,crit}$, which should be compared to the magnitude of the normal stress σ_n at the base of the veneer. The critical normal stress is defined using Equation (26). The normal stress at the base of the veneer is defined by Equations (39) and (40), as follows:

$$\sigma_n = N/L = \gamma \cdot T \cdot \cos\beta \tag{50}$$

If $\sigma_n < \sigma_{n,crit}$, the dominant mode of failure is the fibers pullout. In this case, the magnitude of t_{req} calculated by Equation (50) can to be used to define the fiber-reinforcement requirements using Equation (19). A convenient expression can be obtained to define the fiber content, $\chi_{req,1}$, required to satisfy a given FS criterion.

Section E.8 in Appendix E shows that the required fiber content for the case of $\sigma_n <$ $\sigma_{n,crit}$, is defined by:

$$\chi_{req,1} = \frac{FS - \left(\dfrac{c}{\gamma\, T \sin\beta} + \dfrac{\tan\phi}{\tan\beta}\right)}{\alpha \cdot FS \cdot \eta \left(c_{i,c}\, \dfrac{c}{\gamma\, T \sin\beta} + c_{i,\phi}\, \dfrac{\tan\phi}{\tan\beta}\right)} \tag{51}$$

Similarly, if $\sigma_n > \sigma_{n,crit}$, the dominant mode of failure is fibers breakage. In this case, the magnitude of t_{req} calculated by Equation (50) can to be used to define the fiber-reinforcement requirements using (7). A convenient expression can be obtained to define the fiber content, $\chi_{req,2}$, required to satisfy a given FS criterion. Section E.9 in Appendix E shows that the required fiber content for the case of $\sigma_n > \sigma_{n,crit}$, is defined by:

$$\chi_{req,2} = \frac{\gamma\, T \sin\beta}{\alpha \cdot FS \cdot \sigma_{f,ult}} \left(FS - \frac{c}{\gamma\, T \sin\beta} - \frac{\tan\phi}{\tan\beta}\right) \tag{52}$$

It should be noted that the expressions obtained in this section are *not* the same as would be obtained by implementing the equations for the equivalent shear strength S_{eq} (Section 4.2) into Equation (36). This is because in the derivation presented in this section, the fiber-induced distributed tension increases the factor of safety calculated using Equation (36) by decreasing the *Soil shear stress required for equilibrium* [denominator of Equation (36)]. If S_{eq} is used, the fiber-induced distributed tension would increase the factor of safety calculated using Equation (36) by increasing the *Available soil shear strength* [numerator of Equation (36)]. The use of the fiber tension contribution in the numerator or in the denominator of Equation (36) would lead to different expressions for the factor of safety. However, the fiber-induced distributed tension required to achieve a factor of safety equal to unity (i.e. the soil is at failure) is the same, independent of the way the fiber-induced distributed tension is implemented for calculation of the Factor of Safety. Note that the

"equivalent" shear strength calculated in 5.2 from triaxial tests is independent of the definition of factor of safety (i.e. specimens are at FS=1).

5.4.3 Example 3: Fiber-Reinforced Veneer Slope

As part of the final closure of a municipal solid waste landfill, a 10 ft (3 m) thick soil veneer should be constructed on top of a 1.5H:1V slope of competent waste material. The soil at these steep slopes can be comfortably compacted to a dry unit weight of 105 pcf (16.8 kN/m^3). The shear strength of the soil at this dry unit weight is characterized by an effective cohesion of 100 psf (4.8 kPa) and an effective friction angle of 30 degrees. The design criteria for the project require a static factor of safety FS = 1.50.

Objective: (a) Assuming that additional compactive effort will increase only the cohesive component of the soil shear strength, estimate the required soil cohesion which should be achieved (by additional compaction) in order to satisfy the stability criterion. (b) Using the 1 in. (25 mm) long fiber products described in Example 1 (Section 4.3.1), estimate the fiber content required to satisfy the stability criterion [consider the soil compacted to a dry unit weight of 105 pcf (16.8 kN/m^3)]. (c) Evaluate the cohesion in an unreinforced soil veneer required to achieve a target factor of safety of 1.5 for a varying range of cover thicknesses and a varying range of slope inclinations. (d) Evaluate the fiber content required in a reinforced soil veneer in order to achieve a target factor of safety of 1.5 for a varying range of cover thicknesses and a varying range of slope inclinations. Consider the 1 in. (25 mm) fiber described in Example 1 (Sections 5.3.1) and the 2 in. (50 mm) fiber described in Example 2 (Section 4.3.2).

The inclination of the slope in this example is:

$$\beta = \tan^{-1}(1/1.5) = 33.7°$$

(a) The cohesion required in order to achieve a factor of safety of 1.50 is obtained using Equation (44), as follows:

$$c_{req} = \left(FS - \frac{\tan\phi}{\tan\beta}\right)\gamma\,T\sin\beta = \left(1.5 - \frac{\tan 30°}{\tan 33.7°}\right)105\,pcf \cdot 10\,ft \cdot \sin 33.7° = 370\,psf$$

The additional cohesion needed for stability is considerable (approximately a 150% increase of the measured value). While it may be possible to achieve this cohesion through additional compactive effort, this may be difficult to achieve on steep slopes.

(b) In order to define the required fiber content, the critical confining pressure must be defined using Equation (26) and the fiber information provided in Example 1 (Section 4.3.1), as follows:

$$\sigma_{n,crit} = \frac{\sigma_{f,ult} - \eta \cdot c_{i,c} \cdot c}{\eta \cdot c_{i,\phi} \cdot \tan\phi} = \frac{40,000\,psi \cdot 144\,psf\,/\,psi - 40 \cdot 0.8 \cdot 100\,psf}{40 \cdot 0.8 \cdot \tan 30°} = 311,600\,psf$$

The critical confining pressure should be compared to the normal pressure at the base of the veneer. The normal pressure can be defined using Equation (50), as follows:

$$\sigma_n = \gamma \cdot T \cdot \cos\beta = 105\,pcf \cdot 10\,ft \cdot \cos 33.7° = 874\,psf$$

As the normal stress is well below the critical confining pressure, the fiber-reinforced mass is dominated by a pullout mode of failure. Consequently, the required (volumetric) fiber content $\chi_{req,1}$ can be estimated using Equation (51) as follows:

$$\chi_{req,1} = \frac{FS - \left(\frac{c}{\gamma \ T\sin\beta} + \frac{\tan\phi}{\tan\beta}\right)}{\alpha \cdot FS \cdot \eta \left(c_{i,c} \ \frac{c}{\gamma \ T\sin\beta} + c_{i,\phi} \ \frac{\tan\phi}{\tan\beta}\right)} =$$

$$\chi_{req,1} = \frac{1.5 - \left(\frac{100\,psf}{105\,pcf\cdot10\,ft\cdot\sin33.7\circ} + \frac{\tan30\circ}{\tan33.7\circ}\right)}{1.0\cdot1.5\cdot40\left(0.8\,\frac{100\,psf}{105\,pcf\cdot10\,ft\cdot\sin33.7\circ} + 0.8\,\frac{\tan30\circ}{\tan33.7\circ}\right)} =$$

$$\chi_{req,1} = \frac{1.5 - (0.1716 + 0.8657)}{1.0\cdot1.5\cdot40\,(0.8\cdot0.1716 + 0.8\cdot0.8657)} = 0.0093 = 0.93\%$$

The required gravimetric fiber content $\chi_{w,req,1}$ can be obtained using Equation (4) as follows:

$$\chi_w = \frac{\chi\cdot G_f\cdot\gamma_w}{\gamma - \chi\cdot G_f\cdot\gamma_w} = \frac{0.0093\cdot0.91\cdot62.4\,pcf}{105\,pcf - 0.0093\cdot0.91\cdot62.4\,pcf} = 0.0050 = 0.5\%$$

(c) The cohesion required in order to achieve a factor of safety of 1.50 is obtained using Equation (44) for increasing values of veneer thickness and slope inclinations. Figure 37 shows the results, obtained using a baseline friction angle of 30° for veneer thicknesses ranging from 5 to 14 ft (1.5 to 4.2 m), and for slope inclinations ranging from 1.4H:1V to 2.2H:1V.

For the purposes of this example, it is assumed that the friction angle remains constant with increasing compactive effort and that the soil cohesion is a function of the compactive effort imparted to the soil. As can be observed in the figure, a high cohesion is required for comparatively thick and steep soil veneers.

(d) The gravimetric fiber content required in order to achieve a factor of safety of 1.50 is obtained using Equations (51) and (4) for increasing values of veneer thickness and slope inclinations.

Figure 38 shows the results obtained when the fiber-reinforcement product used are the 1 in. (25 mm) fibers described in Example 1 (Section 4.3.1) . The results are for an effective soil friction angle of 30°, an effective soil cohesion of 100 psf, veneer thicknesses ranging from 5 to 14 ft (1.5 to 4.2 m), and slope inclinations ranging from 1.4H:1V to 2.2H:1V. The figure shows that, for the parameters considered in this example, the gravimetric fiber content values required to satisfy the stability criterion is well within the range of typical fiber contents used in practice (less than 1%). In addition, it can be observed that the required gravimetric fiber content tends to an asymptotic value for high veneer thicknesses. In fact, from inspection of Equation (51), the required fiber content is independent of the veneer thickness if the soil veneer has zero cohesion (or it is assumed to be zero).

Figure 39 shows the results obtained when the fiber-reinforcement product used are the 2 in. (50 mm) fibers described in Example 2 (Section 4.3.2). The results are for a soil friction angle of 30°, a soil cohesion of 100 psf, veneer thicknesses ranging from 5 to 14 ft (1.5 to 4.2 m), and slope inclinations ranging from 1.4H:1V to 2.2H:1V. As can be inferred from inspection of Equation (51), the use of fibers with an aspect ratio equal to twice the aspect ratio considered in the previous alternative, will result in a required fiber content equal to half the fiber content obtained previously. The gravimetric fiber content values required to satisfy the stability criterion in this case is also well within the range of typical fiber contents used in practice (less than 1%).

Figures 38 and 39 are good examples of product-specific design charts that Synthetic Industries could provide to the geotechnical community for preliminary design purposes.

5.5 Two-Dimensional Analysis

5.5.1 General

This section illustrates the use of the discrete framework for evaluating the strength of reinforced soil developed in Section 4 in a typical two-dimensional limit equilibrium slope stability analysis. The analyses presented in this section assume that the failure plane is circular and that the fiber-induced distributed tension acts parallel to the circular failure plane.

By assuming that fiber tension acts parallel to the failure plane, the tensile contribution of the fibers can be incorporated into the input file of any conventional limit equilibrium computer program as an equivalent shear strength. This "equivalent" shear strength is described in Section 4.2. Note that, even though the limit equilibrium analysis to be performed using the proposed approach uses an "equivalent" shear strength, the magnitude of the increased shear strength is obtained using a discrete framework. As previously discussed regarding calculation of the rigorous stability factor of safety, the fiber-induced distributed tension should, rigorously, be implemented as a decrease in the shear stress instead of as an increase in the available "equivalent" shear strength. Even though the approach considered herein is recognized as nonrigorous, it is considered adequate for design purposes. It should be noted that, in a slope at failure, the factors of safety calculated using both the rigorous and the nonrigorous approaches yield the same factor of safety of unity. The scope of this report does not include a parametric evaluation of the sensitivity of the results to the assumed orientation of the fiber-induced distributed tension. Such an evaluation should be performed before implementation of the current approach in engineering practice.

5.5.2 Example 4: Fiber-Reinforced Two-Dimensional Slope

A 30 ft (10 m) high, 1H:1V embankment is being designed as part of a road widening project. The soil at this location can be comfortably compacted to a dry unit weight of 105 pcf (16.8 kN/m^3). The shear strength of the soil at this dry unit weight is characterized by an effective cohesion of 100 psf and an effective friction angle of 30 degrees. Consider a 20 ft (6 m) wide surcharge of 500 psf (24 kPa) at the crest of the slope. The design criteria require a static factor of safety FS = 1.50.

Objective: (a) Estimate the factor of safety of the embankment without fiber-reinforcement. Also, assuming a width of the fiber-reinforced zone of 25 ft (7.6 m), estimate the (gravimetric) fiber content required to satisfy the static stability criterion. Consider the use of the 2 in. (50 mm) fibers described in Example 2 (Section 4.3.2). (b) Assuming a gravimetric fiber content of 0.6%, estimate the width of the fiber-reinforced zone required to satisfy the static stability criterion. Consider the use of the 2 in. (50 mm) fiber described in Example 2 (Section 4.3.2). Figure 40 shows a schematic representation of the design example under evaluation.

The stability analyses were performed using the Spencer's method of limit equilibrium as implemented in the code Utexas3 (Wright, 1990). The analyses were performed considering circular failure surfaces. Input files are in Appendix F.

(a) The limit equilibrium analysis of the unreinforced slope yielded a factor of safety is 1.055. Figure 41 shows the location of the critical failure surface for this case.

The equivalent shear strength that corresponds to gravimetric fiber contents ranging from 0.1% to 1% (in increments of 0.1%) was determined using the expressions developed in Section 4.2. As discussed when evaluating the properties of the 2 in. (50 mm) fiber in Example 2 (Section 4.3.2), the governing failure mode is fiber pullout and not fiber breakage. Consequently, the equivalent shear strength

defined by $\phi_{eq,1}$ and $c_{eq,1}$ should be used in design. Table 5-1 shows the calculations made to determine the values of $\phi_{eq,1}$ (Column [13]) and $c_{eq,1}$ (Column [14]) for the fiber contents under evaluation.

The input files used in the limit equilibrium analyses performed for this evaluation are presented in Appendix F (file fiber2da.dat). The factors of safety calculated for the analyses performed with increasing fiber contents are shown in Table 5-1 (Column [15]). The factors of safety are also shown in Figure 42. From the results of this investigation, it can be observed that the gravimetric fiber content needed to satisfy the stability criterion is $\chi_w = 0.4\%$. Figure 43 shows the location of the critical failure surface obtained for this case.

The amount of fibers needed for this alternative can be estimated as follows. Considering a volumetric fiber content of 0.007 (see Table 5-1 for $\chi_w = 0.4\%$), the weight of fibers per unit length of slope is:

$$V_f = \chi \cdot V = 0.007 \cdot 30 \, ft \cdot 25 \, ft = 5.25 \, ft^3 \, / \, ft$$
$$W_f = G_f \cdot \gamma_w \cdot V = 0.91 \cdot 62.4 \, pcf \cdot 5.25 \, ft^3 \, / \, ft = 298 \, lb \, / \, ft$$

(b) For a gravimetric fiber content of 0.6%, the previous analysis indicated that a reinforced zone of a width of 25 ft (7.6 m) yielded a factor of safety of 1.80, which exceeds the stability criterion. Consequently, for a fiber content of 0.6%, a more economic design could be obtained by decreasing the width of the fiber-reinforced zone. Analyses were performed to evaluate the factor of safety considering a reinforced zone with a width ranging from zero to 25 ft (7.6 m) [in increments of 5 ft (1.5m)]. The analyses were performed using $\phi_{eq,1} = 44.6°$ and $c_{eq,1} = 170.6$ psf, as indicated in Table 5-1 for a gravimetric fiber content of 0.6%.

The input files used in the limit equilibrium analyses performed for this evaluation are also presented in Appendix F (file fiber2db.dat). The factors of safety

calculated for the analyses performed with increasing fiber contents are shown in Table 5-2. The calculated factors of safety are also shown in Figure 44. From the results of this investigation, it can be observed that the width of the zone reinforced with fibers at a gravimetric fiber $\chi_w = 0.6\%$ is less than 20 ft (6 m) [approximately 17.5 ft (5 m)]. Figure 45 shows the location of the critical failure surface for the case of a width of 20 ft (6 m) for the fiber-reinforced zone.

The amount of fibers needed for this alternative can be estimated for this alternative. Considering a volumetric fiber content of 0.011 (see Table 5-1 for $\chi_w = 0.6\%$), the weight of fibers per unit length of slope is:

$$V_f = \chi \cdot V = 0.011 \cdot 30\,ft \cdot 17.5\,ft = 5.78\ ft^3\,/\,ft$$
$$W_f = G_f \cdot \gamma_w \cdot V = 0.91 \cdot 62.4\ pcf \cdot 5.78\ ft^3\,/\,ft = 328\ lb\,/\,ft$$

Considering material costs only, Alternative (a) is slightly better than Alternative (b) (30 lb. less of fibers per linear foot of slope). However, Alternative (a) requires mixing of a larger volume of fiber-reinforced soil than Alternative (b) (225 ft³/ft more). Thus, the optimal solution depends upon the cost trade-off between using more fiber versus mixing a greater volume of soil. Given fiber unit costs and mixing unit costs, this type of evaluation is easily implemented and provides a rational approach for optimization of fiber-reinforced soil slope projects.

6. CONCLUSIONS

The use of fiber-reinforcement in soil presents opportunities for innovative, cost-effective designs for stabilization of slopes, landfill final covers, and other geotechnical projects. The design of fiber-reinforced slopes is currently performed by considering the reinforced mass as a homogeneous composite material. However, the use of a discrete design approach better represents the actual tensile contribution of the fibers to stability.

This report develops a consistent design methodology for fiber-reinforced soil using a discrete approach. The methodology proposed for stability analysis of fiber-reinforced soil slopes is generic and treats the fibers as discrete reinforcing elements which contribute to stability by developing tensile stresses. The report also presents an overview of fiber-reinforcement, discusses the advantages of a discrete methodology compared to a soil/reinforcement composite approach, describes the results of a preliminary experimental testing program on fiber-reinforced triaxial specimens, develops a theoretical framework to establish the fiber properties needed for a stability analysis of a fiber-reinforced slope using a discrete approach, and implements the proposed framework into a design methodology. Design examples, and recommendations for further evaluation are also presented.

The main conclusions derived from this report are:

- A discrete framework for fiber-reinforced soil can be developed such that the reinforced mass is characterized by the mechanical properties of individual fibers and of the soil matrix instead of the mechanical properties of the fiber-reinforced composite material.

- A critical confining pressure at which there is a change in the fiber-reinforced soil behavior from fiber pullout to fiber breakage can be defined using the individual fiber and soil matrix properties. The critical confining pressure is a function of the fiber content, the

ultimate tensile strength of the fibers, the soil shear strength, and the fiber aspect ratio. Consistent with experimental results reported in the literature, the critical confining pressure is independent of the fiber content.

- According to the discrete framework, the fiber-induced distributed tension is a function of the fiber content, the fiber aspect ratio, and the interface shear strength of individual fibers if the governing mode of failure is by fiber pullout.

- According to the discrete framework, the fiber-induced distributed tension is a function of the fiber content and the ultimate tensile strength of individual fibers if the governing mode of failure is by fiber breakage.

- The analytical framework allows determination, as a function of the individual fiber and soil matrix properties, of the "equivalent" shear strength obtained from triaxial testing of fiber-reinforced specimens.

- The results from a preliminary experimental program consisting on triaxial compression tests on fiber-reinforced specimens showed very good agreement between the test results and the theoretical predictions.

- The results from a preliminary hydraulic conductivity testing program showed no effect of the fibers on saturated hydraulic conductivity.

- Experimental results from triaxial compression tests using fiber-reinforced soil specimens that range from sand to clayey soils show good agreement with the shear strength improvement predicted using the proposed discrete approach.

- The discrete framework can be implemented into an infinite slope limit equilibrium framework. Convenient expressions can be obtained to estimate directly the required fiber content to achieve a target factor of safety.

- The discrete framework can be easily implemented into conventional two dimensional limit equilibrium analyses, and facilitates evaluation of different design scenarios. The analysis can be performed using existing limit equilibrium computer codes.

The proposed design methodology for fiber-reinforced soil structures using a discrete approach is consistent with current design guidelines for the use of continuous planar reinforcements and with the actual soil improvement mechanisms. Consequently, the proposed discrete design methodology can lead not only to a more accurate design but also to the development of more adequate field specifications, standards of practice, and quality control guidelines.

REFERENCES

Christopher, B.R., Zornberg, J.G., and Mitchell, J.K. (1998). "Design Guidance for Reinforced Soil Structures with Marginal Soil Backfills." Proceedings of the *6th International Conference on Geosynthetics*, Atlanta, Georgia, March 1998, Vol. 2, pp. 797-804.

Elias, V. (1997). "Corrosion/Degradation of Soil Reinforcements for Mechanically Stabilized Earth Walls and Reinforced Soil Slopes," Federal Highway Administration Report FHWA-SA-96-72, Washington D.C.

Elias, V. and Christopher, B.R. (1997). "Mechanically Stabilized Earth Walls and Reinforced Soil Slopes, Design and Construction Guidelines" Federal Highway Administration Report FHWA-SA-96-71, Washington D.C.

Fellenius, W. (1936). "Calculation of the Stability of Earth Dams." Proceedings of the *2nd Congress on Large Dams*, Washington, D. C., Vol. 4, pp. 445-462.

Foose, G.J., Benson, C.H., and Bosscher, P.J. (1996), "Sand Reinforced With Shredded Waste Tires," *J. Geotech. Engrg.,* ASCE, Vol. 122, No. 9, pp. 760-767.

Giroud, J.P. (1986). "Geotextiles to Geosynthetics: A Revolution in Geotechnical Engineering," Proc. Third International Conference on Geotextiles, Vienna, Austria, pp.1-18.

Goran, W.P. and Johnson, W.G. (1994). "Stabilization of high plasticity clay and silty sand by inclusion of discrete fibrillated polypropylene fibers for use in pavement subgrades." *CPAR Report GL-94-2*, Geotechnical Laboratory, U.S. Army Corps of Engineers, Vicksburg, MS.

Gray, D.H. and Al-Refeai, T. (1986), "Behavior of Fabric versus Fiber-reinforced Sand," *J. Geotech. Engrg.,* ASCE, Vol. 112, No. 8, pp. 804-820.

Gray, D.H. and Ohashi, H. (1983), "Mechanics of Fiber-reinforcement in Sand," *J. Geotech. Engrg.,* ASCE, Vol. 109, No. 3, pp. 335-353.

Jewell, R. A. (1991). "Application of revised design charts for steep reinforced slopes." *Geotextiles and Geomembranes* 10, 203-233.

Leshchinsky, D. and R. H. Boedeker. (1989). "Geosynthetic reinforced soil structures." *Journal of Geotechnical Engineering, ASCE* 115(10), 1459-1478.

Leflaive, E. (1985), "Soils reinforced with continuous yarns: the Texol," *Proc., Eleventh Int. Conf. on Soil Mech. and Found. Engrg.*, San Francisco, Vol.3, pp.1787-1790.

Maher, M.H. and Gray, D.H. (1990), "Static Response of Sand Reinforced With Randomly Distributed Fibers," *J. Geotech. Engrg.,* ASCE, Vol. 116, No. 11, pp. 1661-1677.

Maher, M. H. and Ho, Y. C. (1994), "Mechanical Properties of Kaolinite/Fiber Soil Composite," *J. Geotech. Engrg.,* ASCE, Vol. 120, No. 8, pp. 1381-1393.

Maher, M.H. and Woods, R.D. (1990), "Dynamic Response of Sand Reinforced With Randomly Distributed Fibers," *J. Geotech. Engrg.,* ASCE, Vol. 116, No. 7, pp. 1116-1131.

McGown, A., Andrawes, K.Z, Hytiris, N., and Mercel, F.B. (1985), "Soil strengthening using randomly distributed mesh elements," *Proc., Eleventh Int. Conf. on Soil Mech. and Found. Engrg.*, San Francisco, Vol.3, pp.1735-1738.

Michalowski, R.L. and Zhao, A. (1996), "Failure of Fiber-Reinforced Granular Soils," *J. Geotech. Engrg.,* ASCE, Vol. 122, No. 3, pp. 226-234.

Mitchell, J.K. and Zornberg, J.G. (1995). "Reinforced Soil Structures with Poorly Draining Backfills. Part II: Case Histories and Applications". *Geosynthetics International* journal, Vol. 2, no. 1, pp. 265-307.

Morel, J.C. and Gourc, J.P., 1997, "Mechanical Behavior of Sand Reinforced with Mesh Elements," *Geosynthetics International*, Vol.4, No.5, pp. 481-508.

Ranjan, G., Vassan, R.M. and Charan, H.D. (1996), "Probabilistic Analysis of Randomly Distributed Fiber-Reinforced Soil," *J. Geotech. Engrg.,* ASCE, Vol. 120, No. 6, pp. 419-426.

Schlosser, F. and Vidal, H. (1969). "La terre armee." *Bull. Liason du Laboratorie Central des Ponts et Chaussees*, Vol.41, 101-144.

Shewbridge, S.E. and Sitar, N. (1990). "Deformation Based Model for Reinforced Sand," *J. Geotechnical Engineering,* ASCE, vol. 116, no. 7, pp. 1153-1170.

Terzaghi, K. (1956). *Theoretical Soil Mechanics*. John Wiley and Sons, Inc., New York, N.Y.

Wright, S.G. (1990). *UTEXAS3 A Computer Program for Slope Stability Calculations*, Austin, Texas.

Wright, S. G. and Duncan, J. M. (1991). "Limit equilibrium stability analyses for reinforced slopes." *Transportation Research Record* 1330, 40-46.

Zornberg, J.G., and Caldwell, J.A. (1998). "Design of Monocovers for Landfills in Arid Locations." *Third International Conference on Environmental Geotechnics*, organized by the International Society of Soil Mechanics and Foundation Engineering, to be held in Lisbon, Portugal, in September 1998.

Zornberg, J.G., Sitar, N., and Mitchell, J.K. (1998a). "Performance of Geosynthetic Reinforced Slopes at Failure." *Journal of Geotechnical and Geoenvironmental Engineering*, *ASCE*, August 1998.

Zornberg, J.G., Sitar, N., and Mitchell, J.K. (1998b). "Limit Equilibrium as a Basis for Design of Geosynthetic Reinforced Slopes." *Journal of Geotechnical and Geoenvironmental Engineering*, *ASCE*, August 1998.

Zornberg, J.G. and Mitchell, J.K. (1994). "Reinforced Soil Structures with Poorly Draining Backfills. Part I: Reinforcement Interactions and Functions". *Geosynthetics International* journal, Vol. 1, No. 2, pp. 103-148.

DEVELOPMENT OF A DISCRETE DESIGN
METHODOLOGY FOR FIBER-REINFORCED SOIL

Jorge G. Zornberg, Ph.D., P.E.

TABLES

Table 1. Summary of Shear Strength Results

Fiber Type (length)	Gravimetric Fiber Content (%)	c' (psi)	φ' (degrees)
no fibers	-	1.73	31.2
2600 denier (1 in.)	0.2	2.26	28.16
2600 denier (1 in.)	0.4	2.48	31.82
360 denier (2 in.)	0.2	2.23	34.59
360 denier (2 in.)	0.4	3.17	35.09

Table 2. Summary of Hydraulic Conductivity Results

Fiber Type (length)	Gravimetric Fiber Content (%)	Hydraulic Conductivity (cm/sec)
no fibers	-	6.05×10^{-7}
2600 denier (1 in.)	0.2	1.15×10^{-6}
2600 denier (1 in.)	0.4	2.00×10^{-7}
360 denier (2 in.)	0.2	9.59×10^{-7}
360 denier (2 in.)	0.4	1.03×10^{-6}

Table 3. Summary of Fiber Tensile Strength Test Results

Fiber Type (length)	Speed (in./min)	Gauge length (in)	Stress at peak (psi)	Max elong. (%)
2600 denier (1 in.)	12	3	62490	16.23
2600 denier (1 in.)	1	3	53780	16.35
2600 denier (1 in.)	12	10	53010	9.974
2600 denier (1 in.)	1	10	53320	11.62
360 denier (2 in.)	12	3	67920	19.24
360 denier (2 in.)	1	3	64620	22.47
360 denier (2 in.)	12	10	66970	15.27
360 denier (2 in.)	1	10	61820	17.87

Note: the reported results correspond to the average of three tests.

DEVELOPMENT OF A DISCRETE DESIGN METHODOLOGY FOR FIBER-REINFORCED SOIL

Jorge G. Zornberg, Ph.D., P.E.

FIGURES
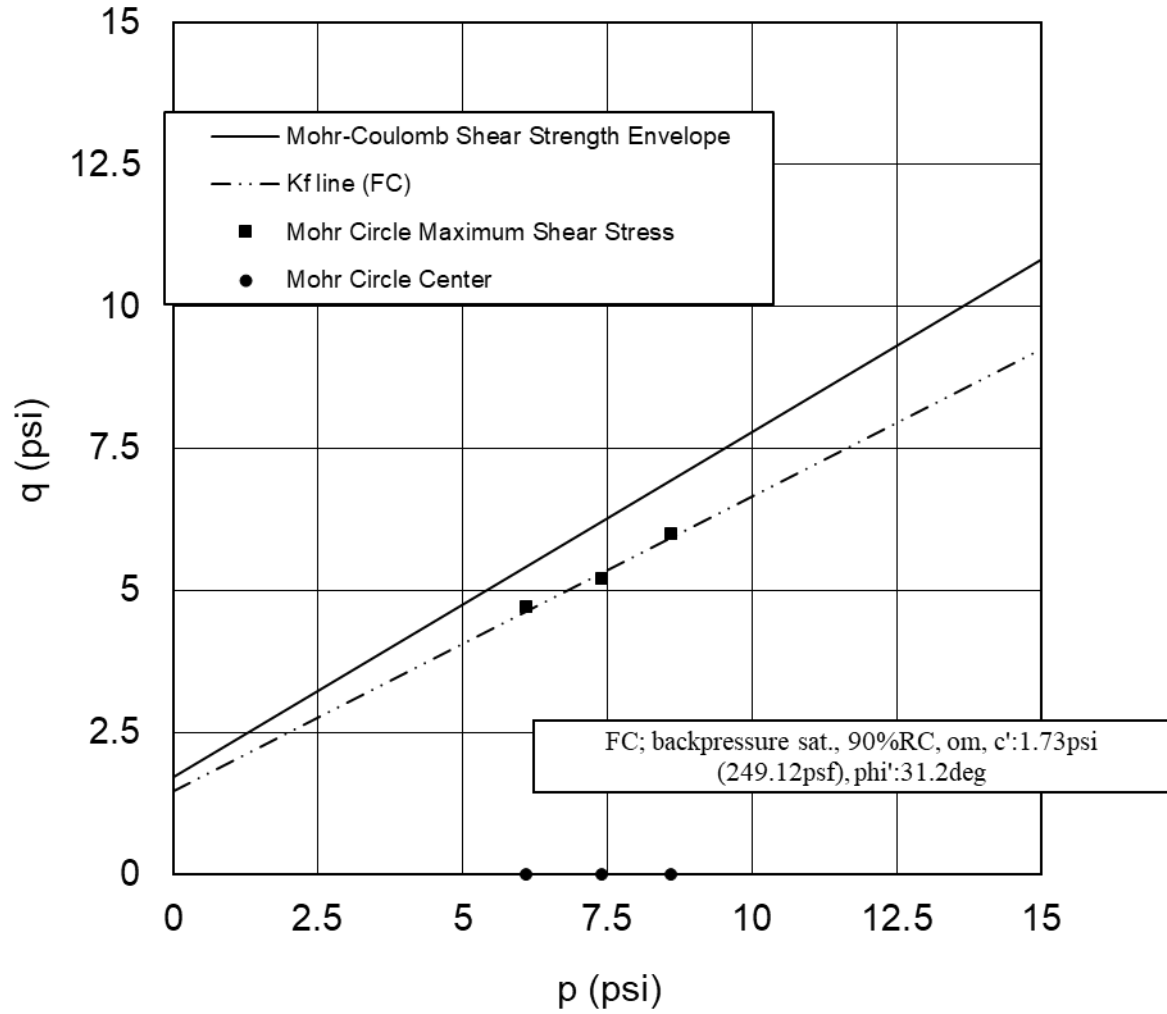
Figure 1: Shear strength envelope for unreinforced specimens
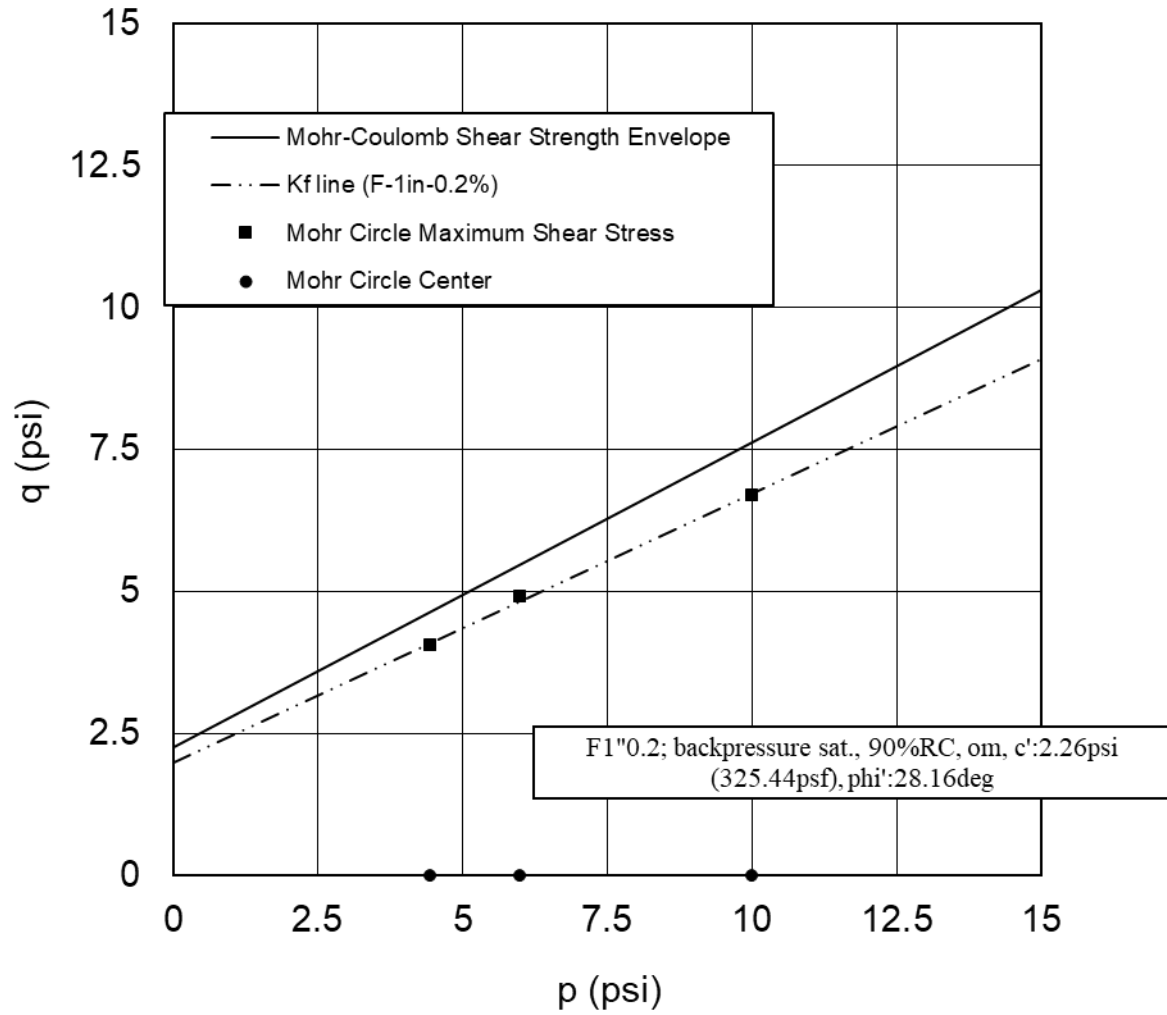
Figure 2: Shear strength envelope for fiber-reinforced specimens (1" fibers, 0.2% fiber content)
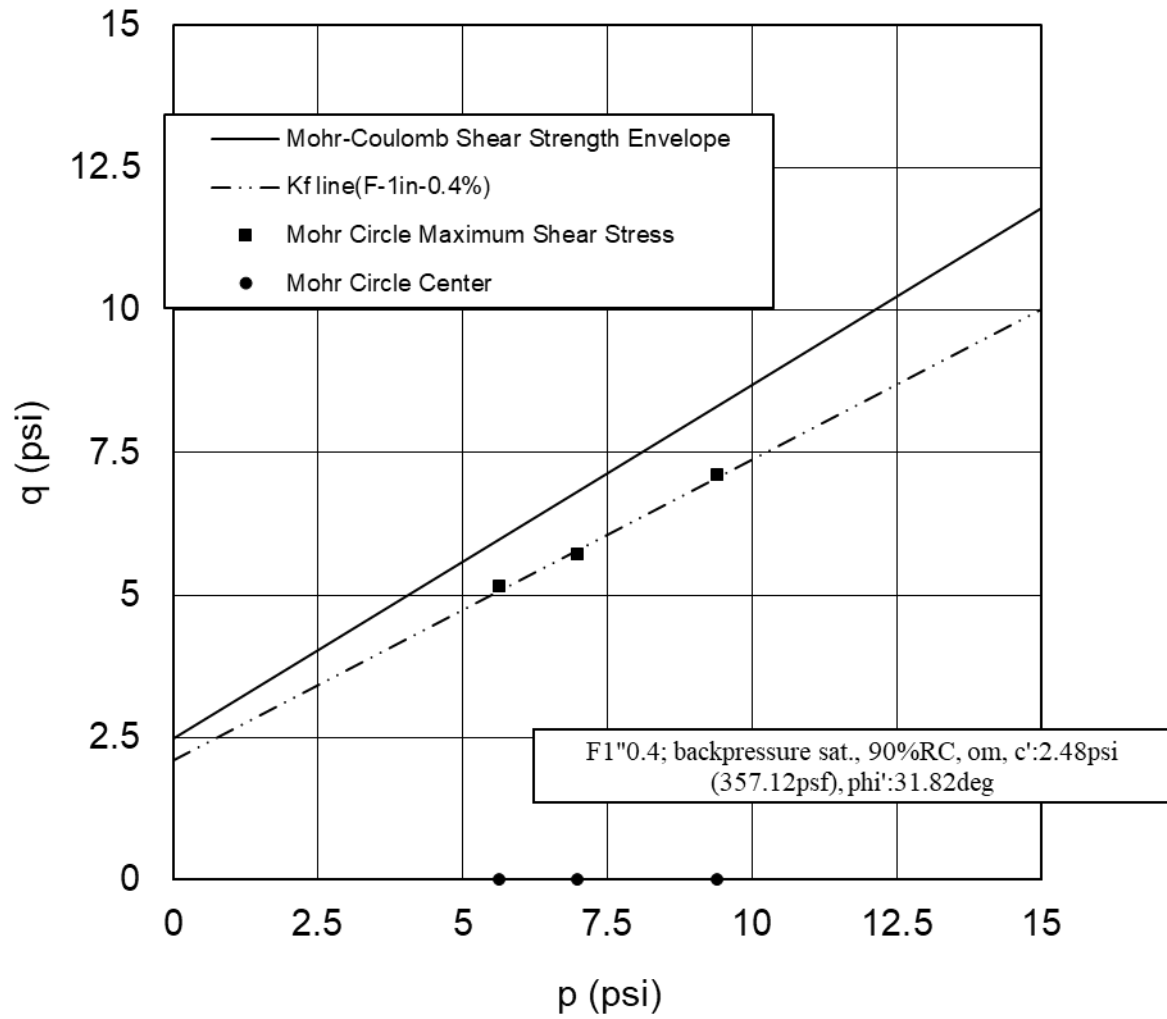
Figure 3: Shear strength envelope for fiber-reinforced specimens (1" fibers, 0.4% fiber content)
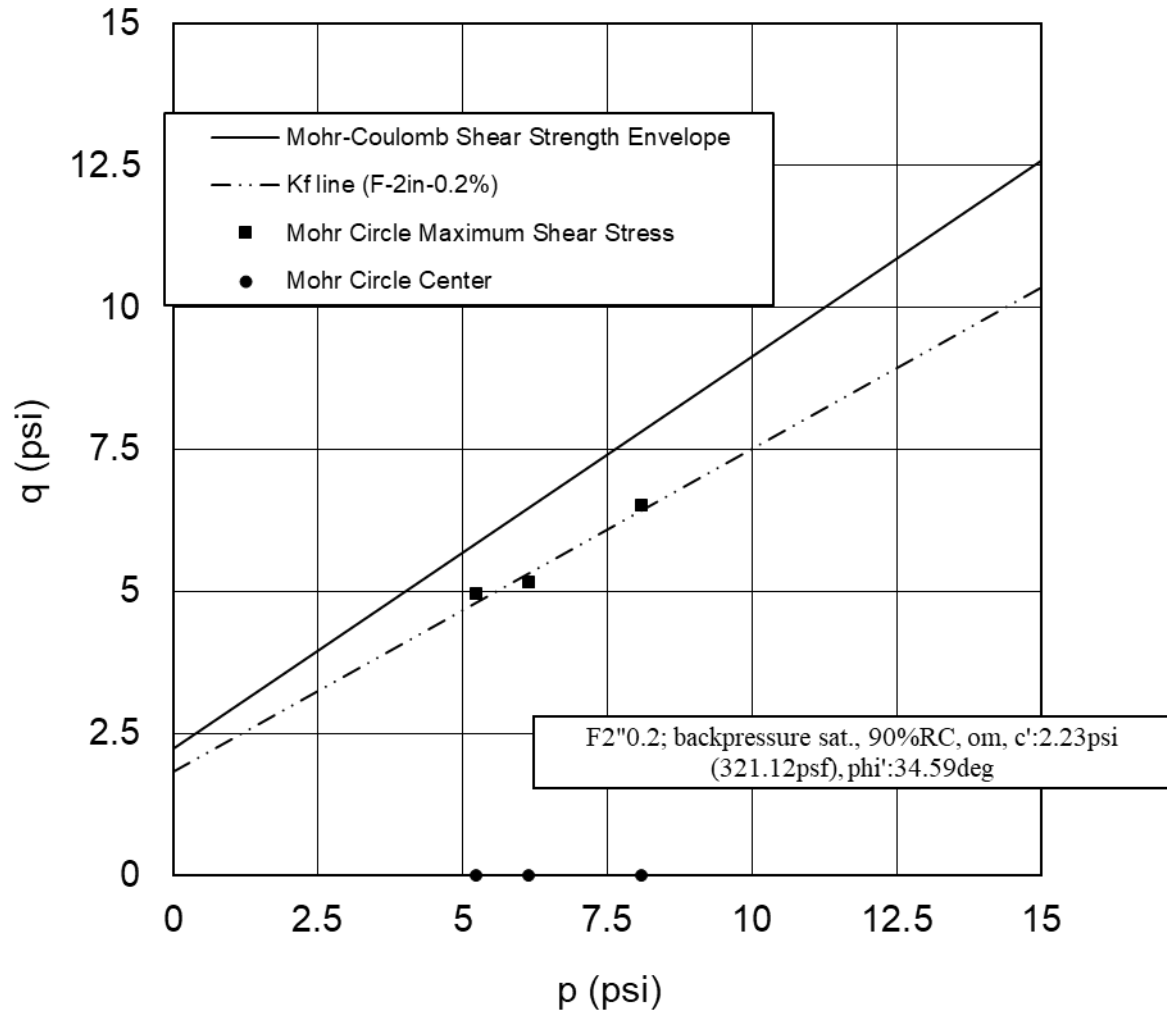
Figure 4: Shear strength envelope for fiber-reinforced specimens (2" fibers, 0.2% fiber content)
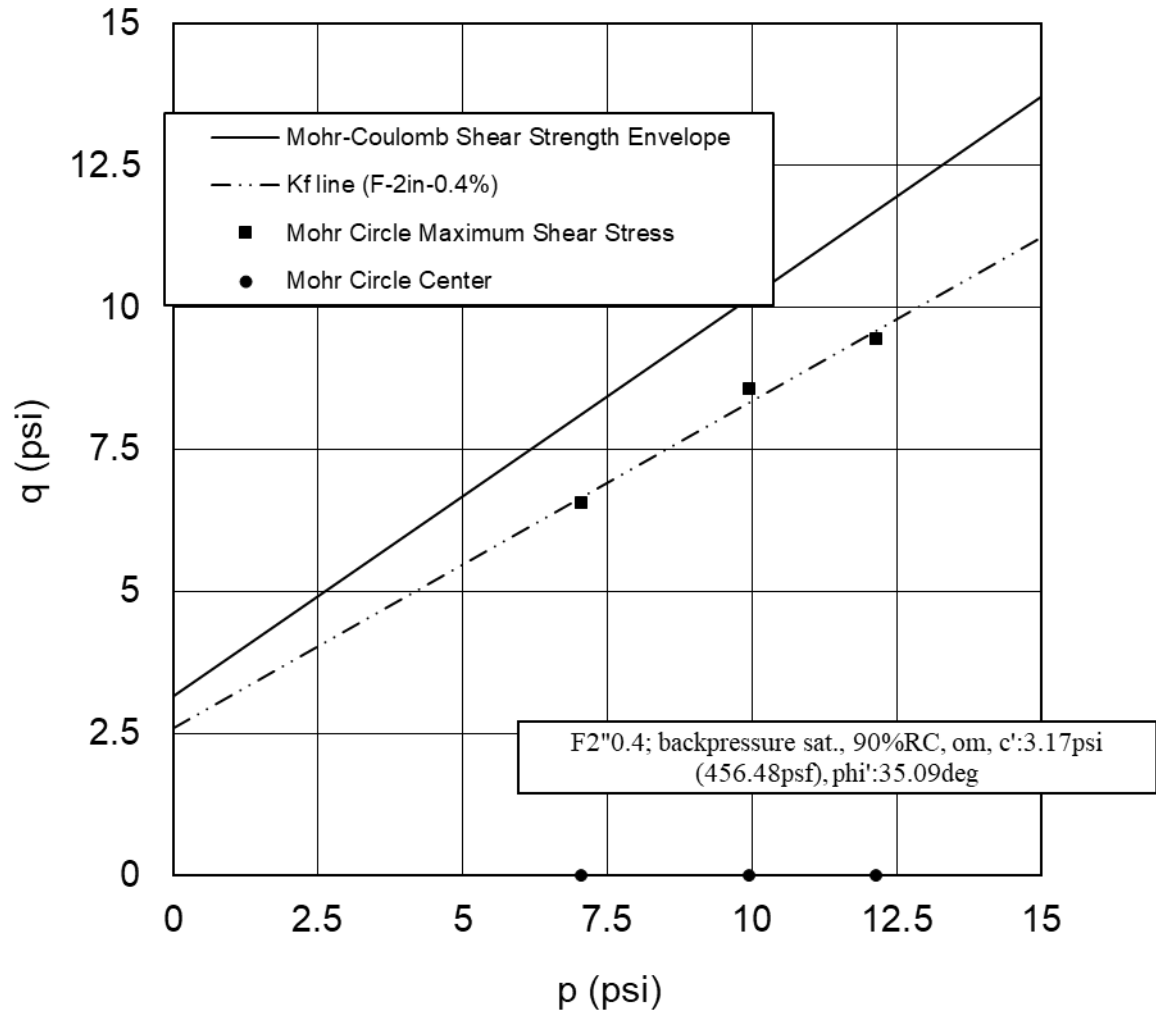
Figure 5: Shear strength envelope for fiber-reinforced specimens (2" fibers, 0.4% fiber content)
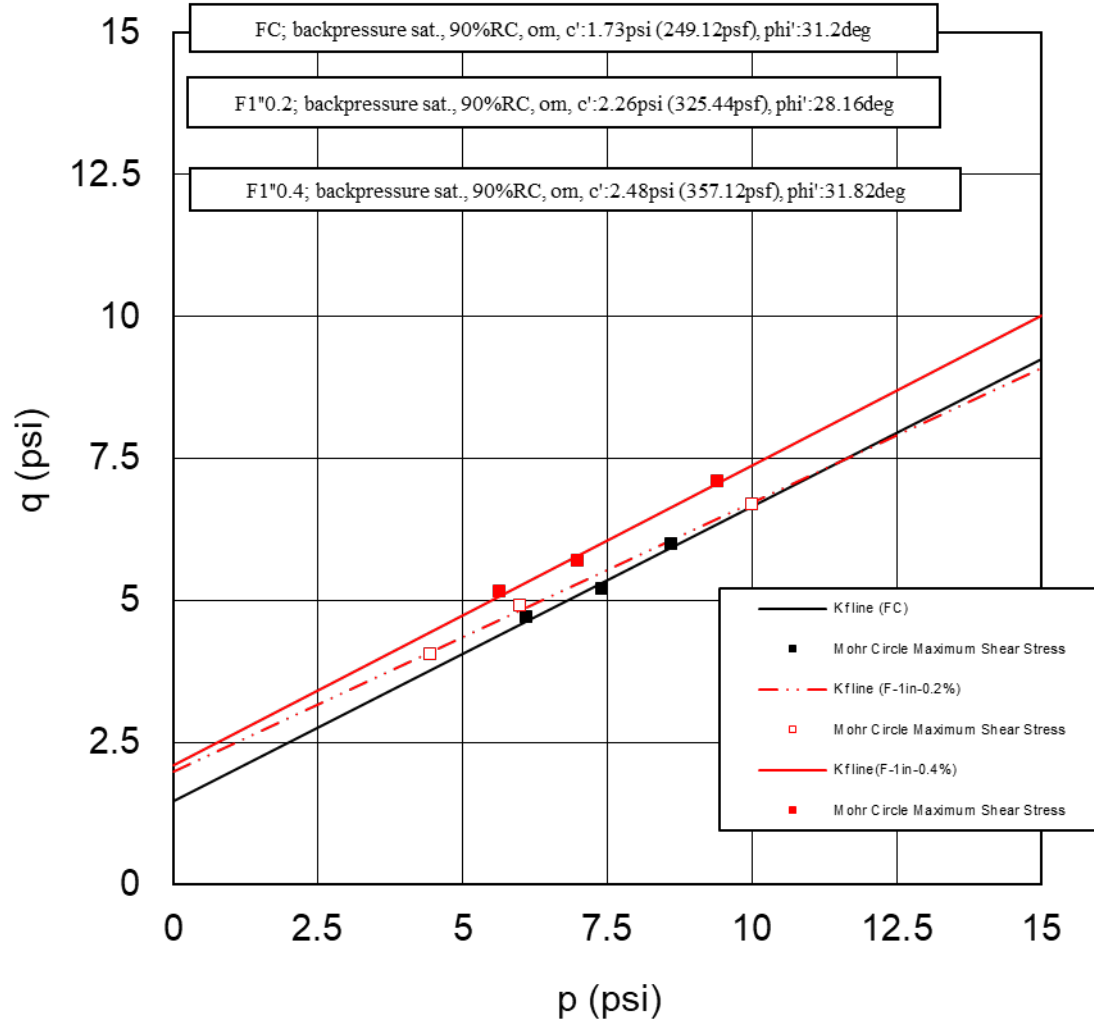
Figure 6: Effect of increasing fiber content (1" fibers)
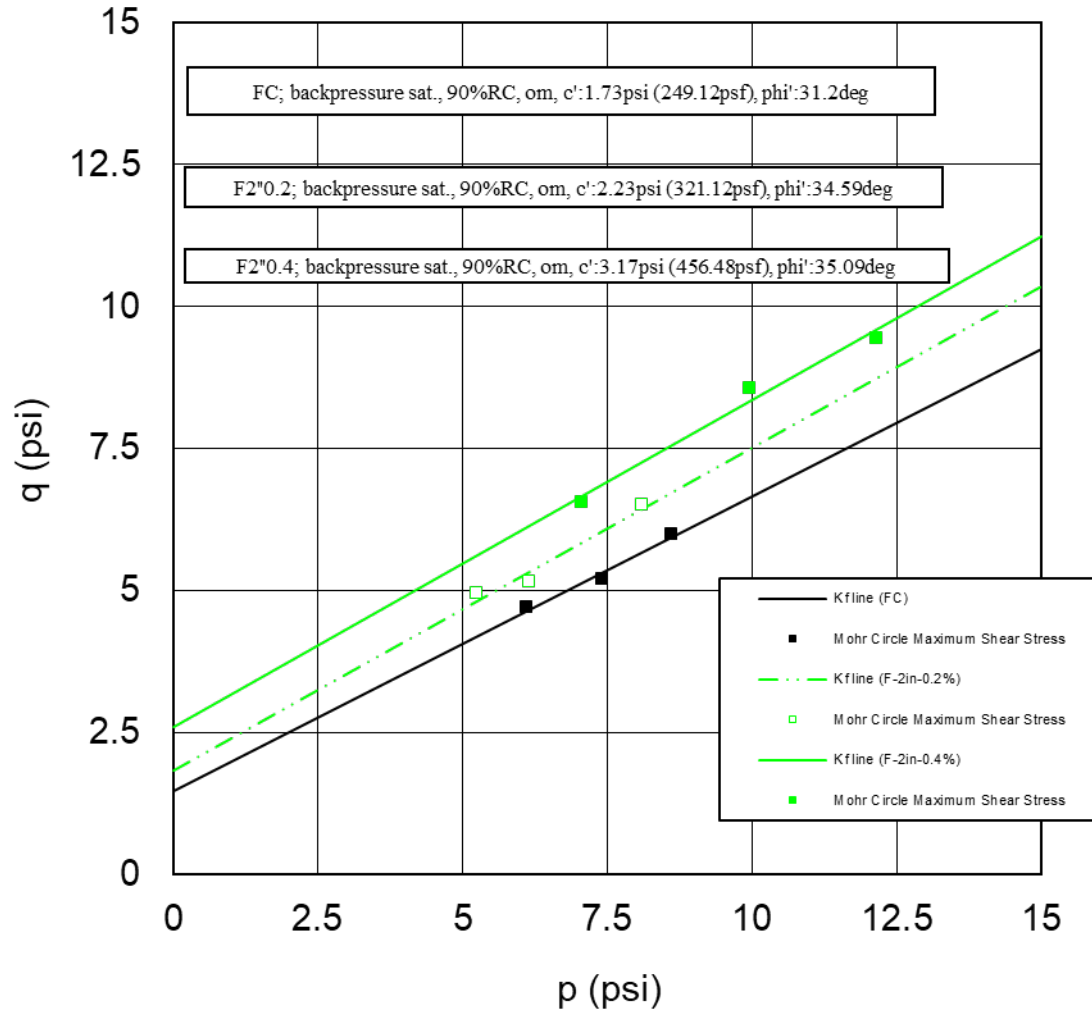
Figure 7: Effect of increasing fiber content (2" fibers)
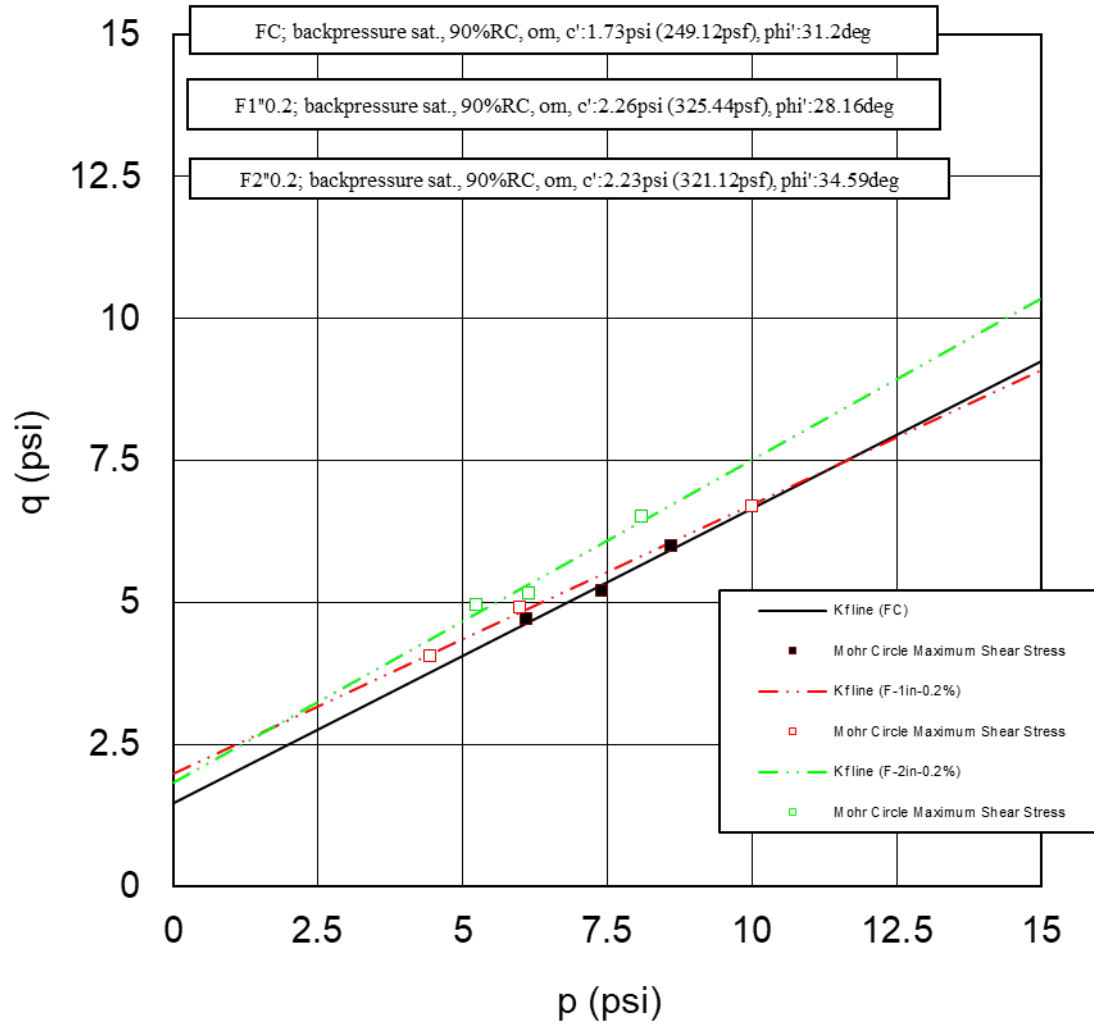
Figure 8: Effect of increasing fiber length (0.2% fiber content)
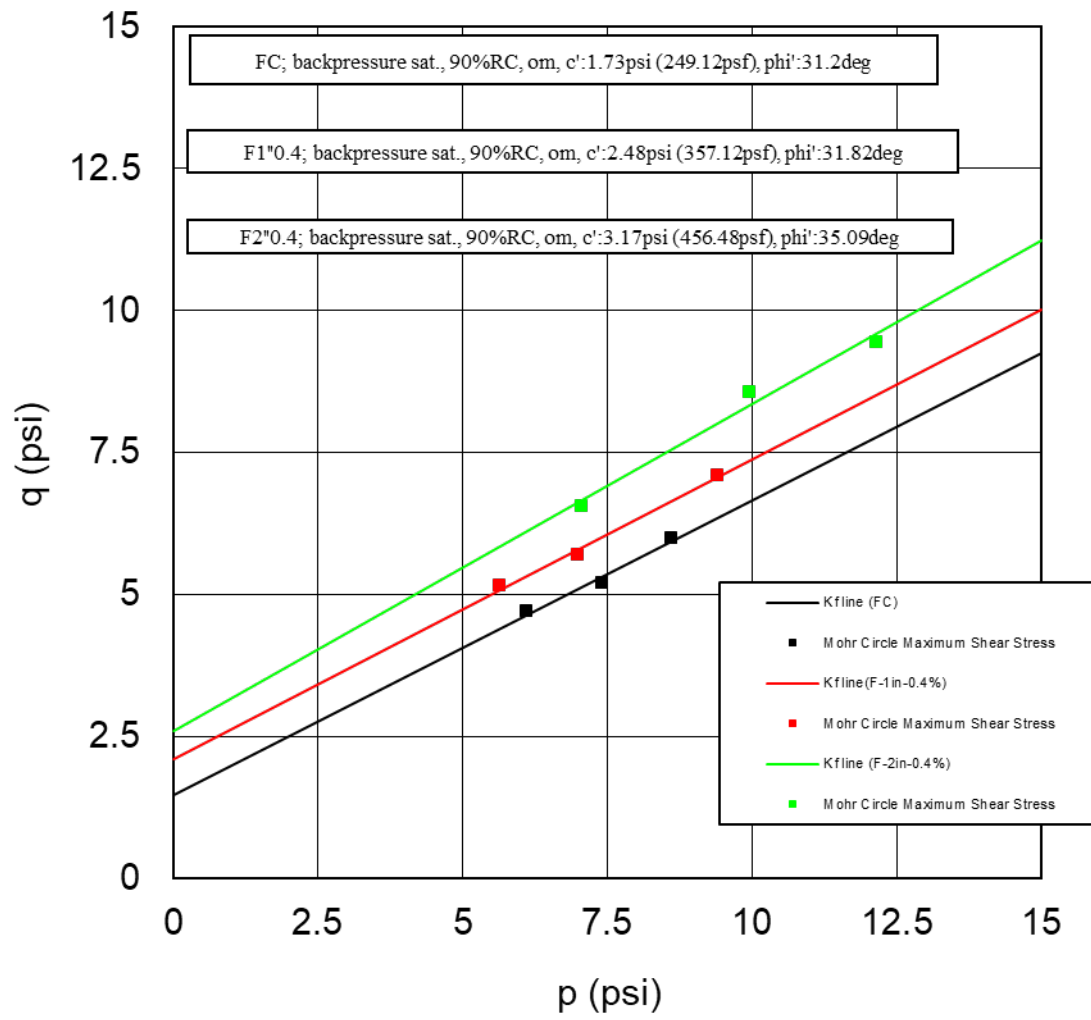
Figure 9: Effect of increasing fiber length (0.4% fiber content)
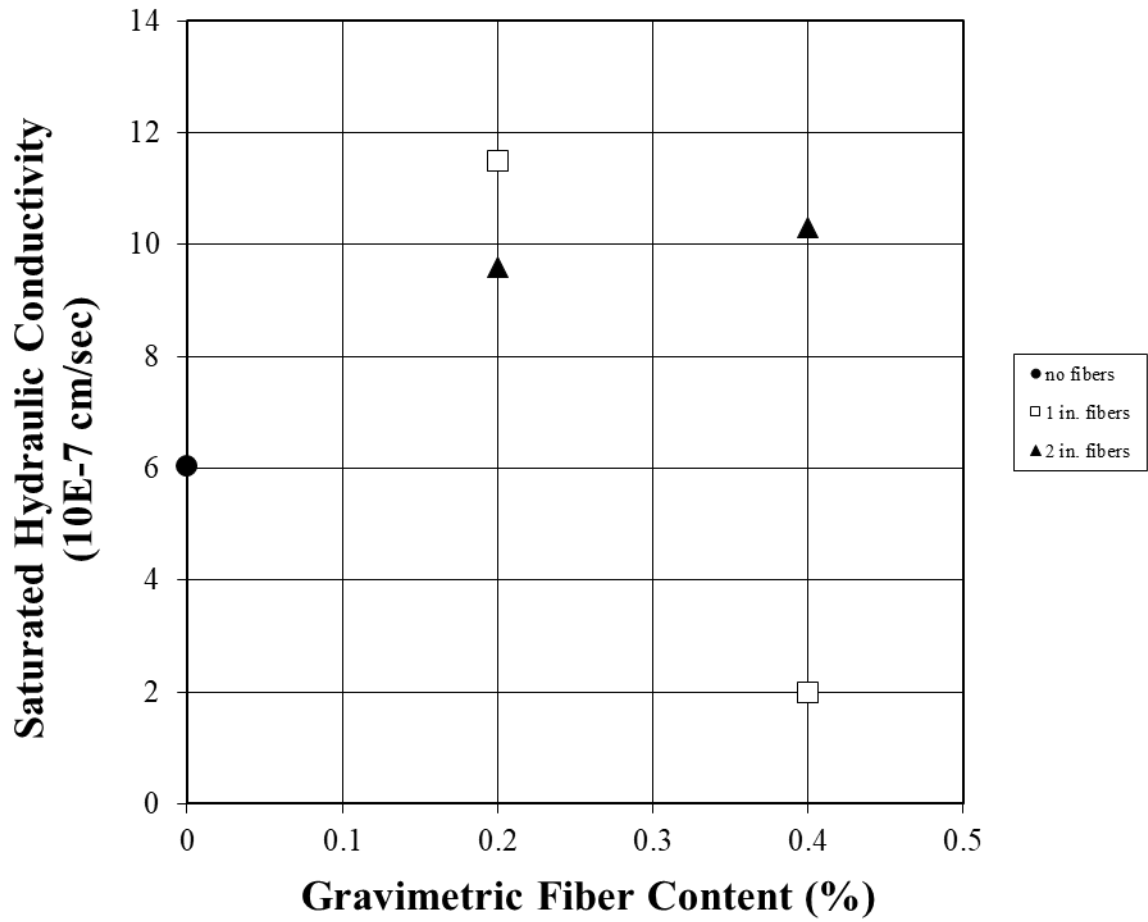
Figure 10: Effect of fiber content on saturated hydraulic conductivity
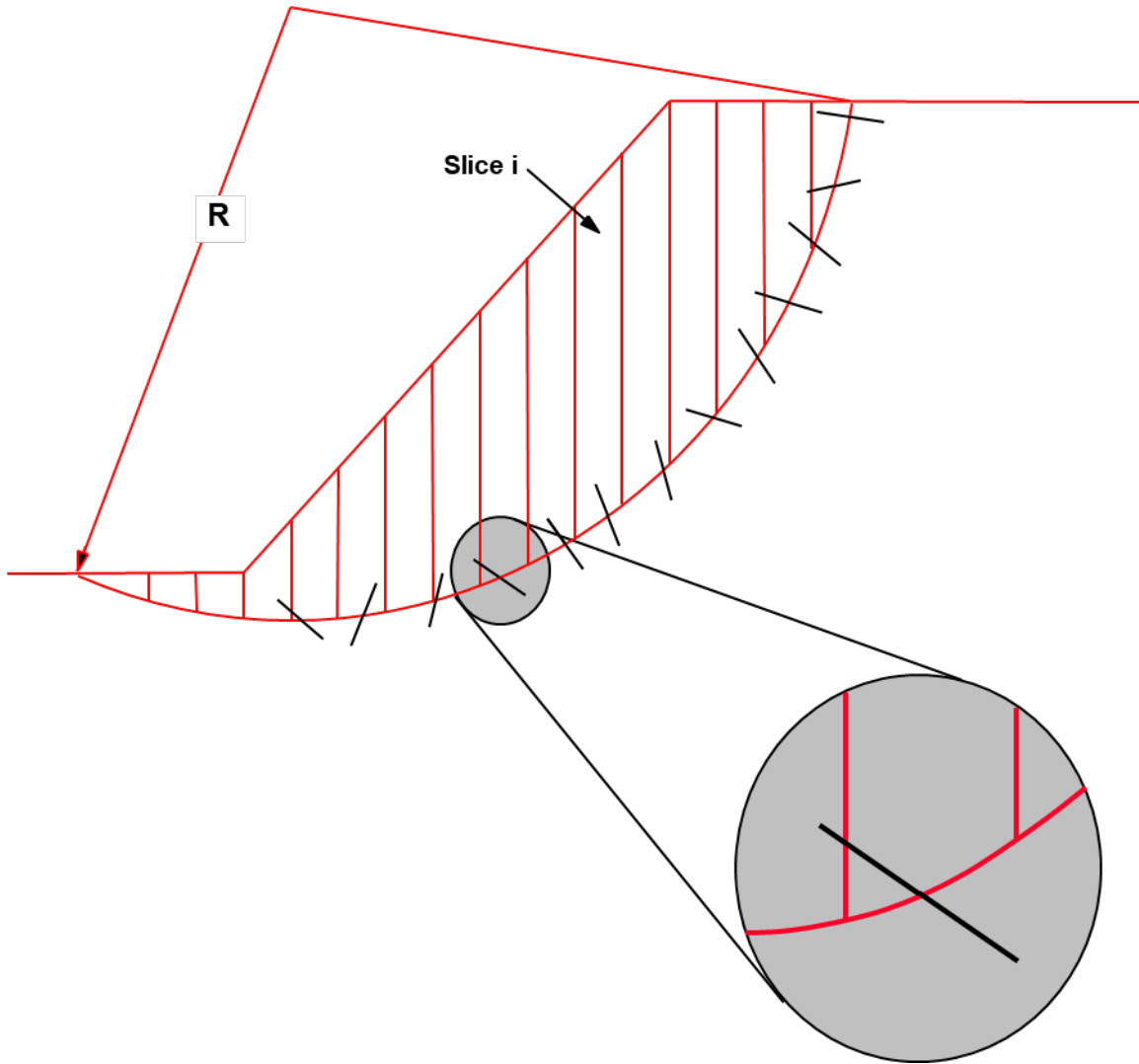
Figure 11: Soil mass reinforced using randomly distributed fibers
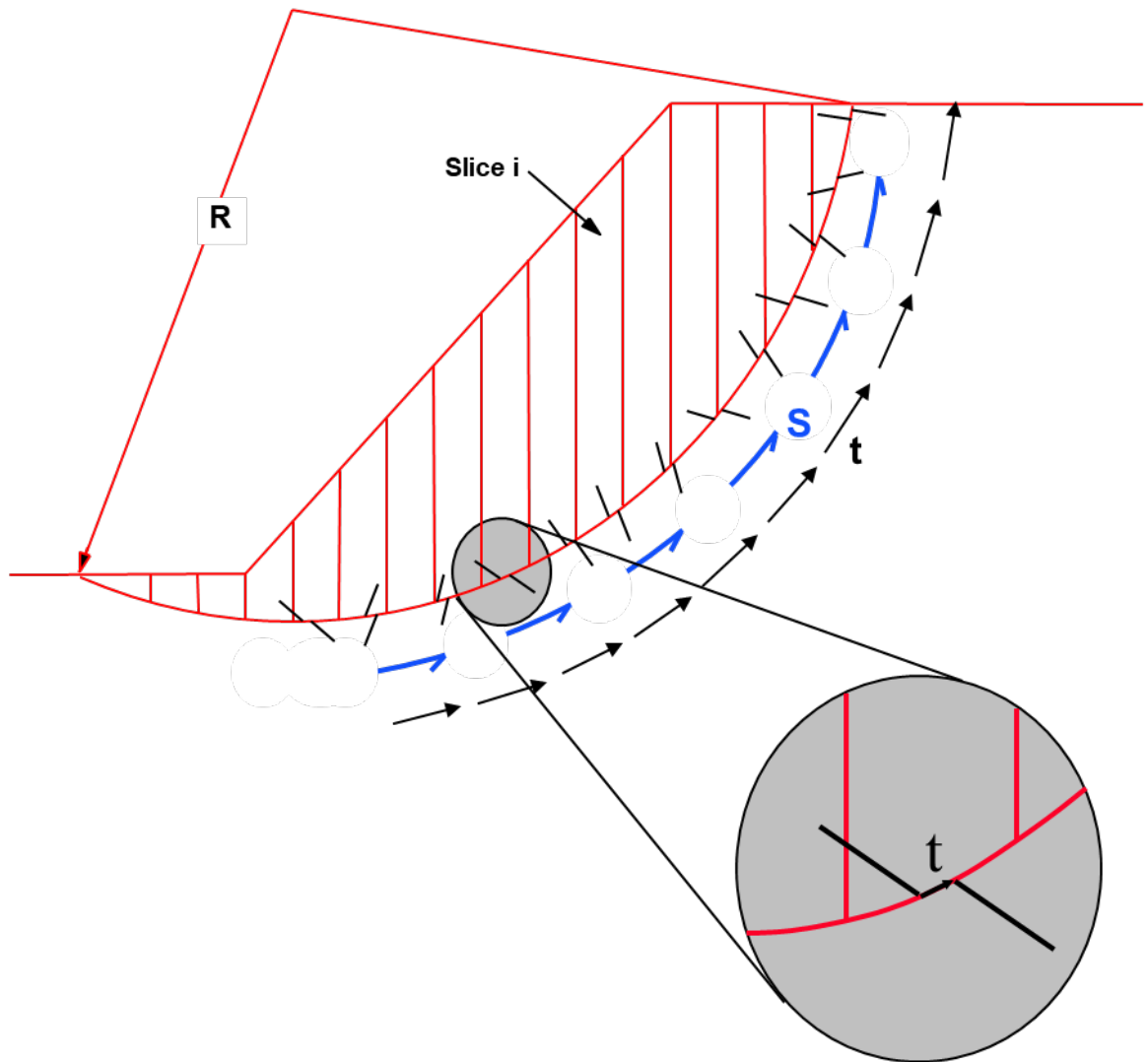
Figure 12: Fiber-induced distributed tension parallel to failure surface
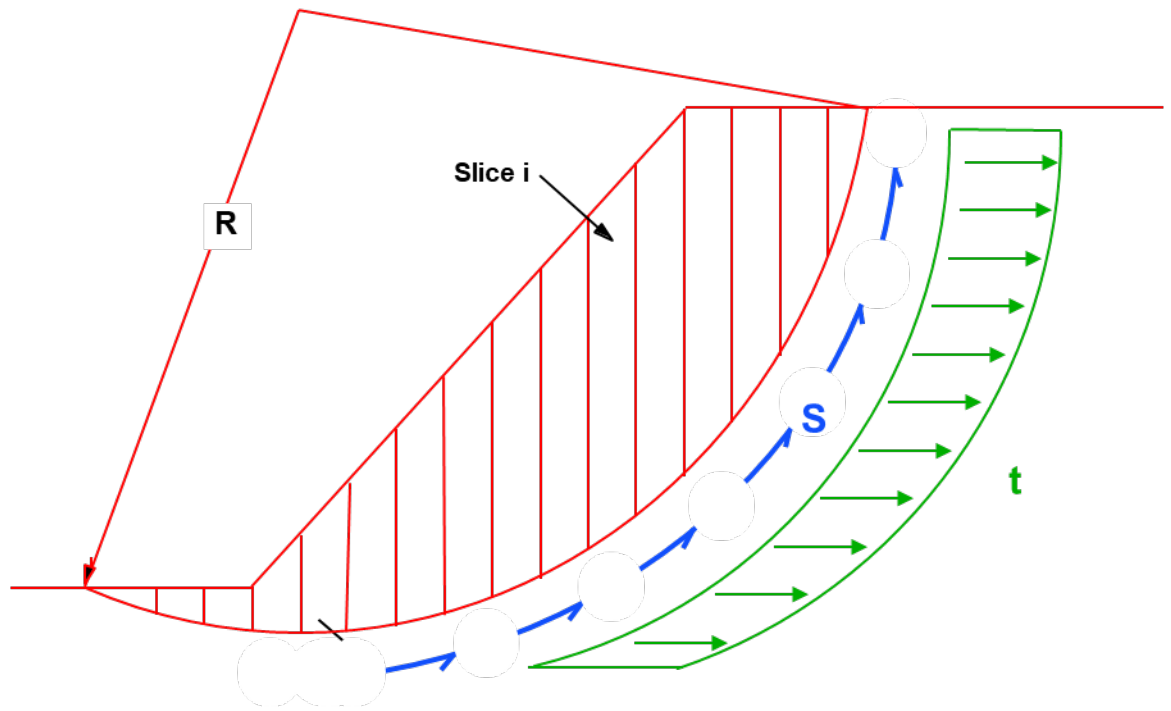
Figure 13: Horizontal fiber-induced distributed tension
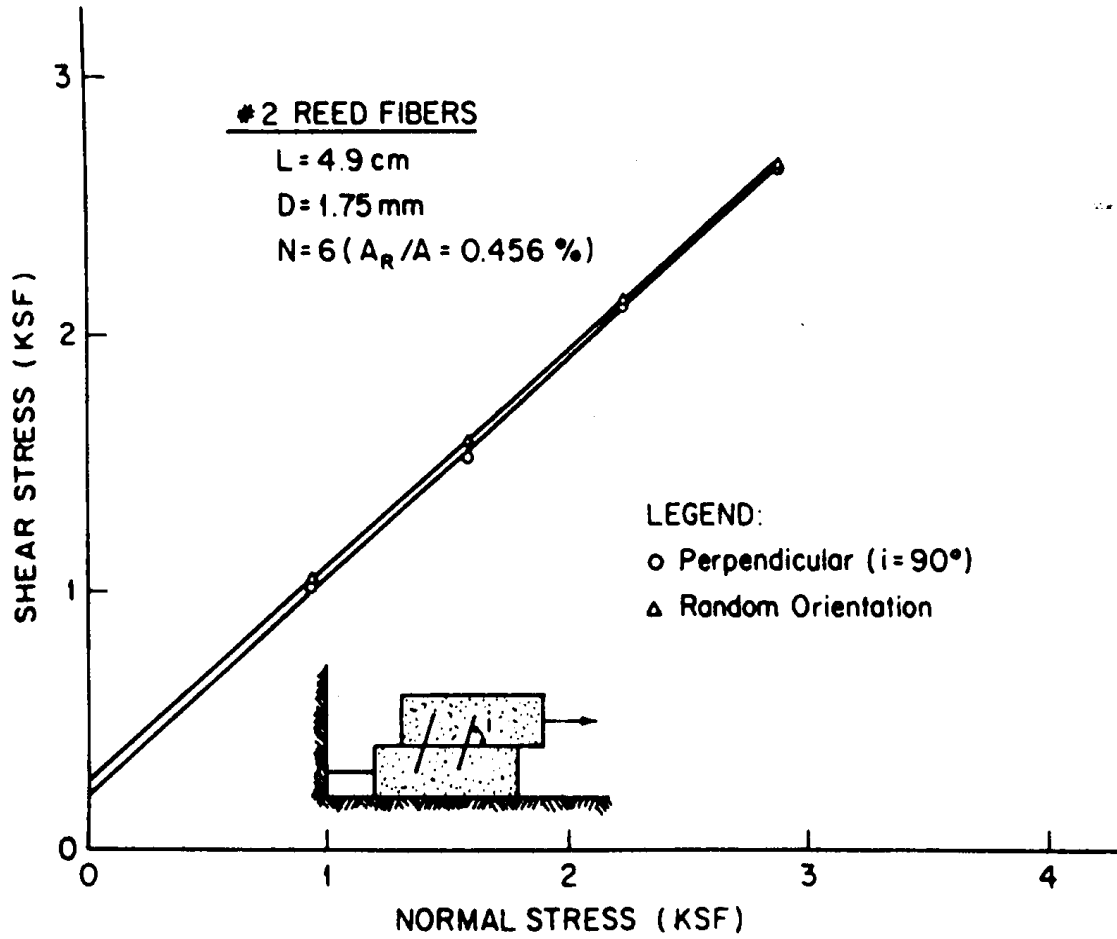
Figure 14: Comparison of Perpendicular versus 'random' orientation of fibers on shear strength envelopes (after Gray and Oneshi, 1983)
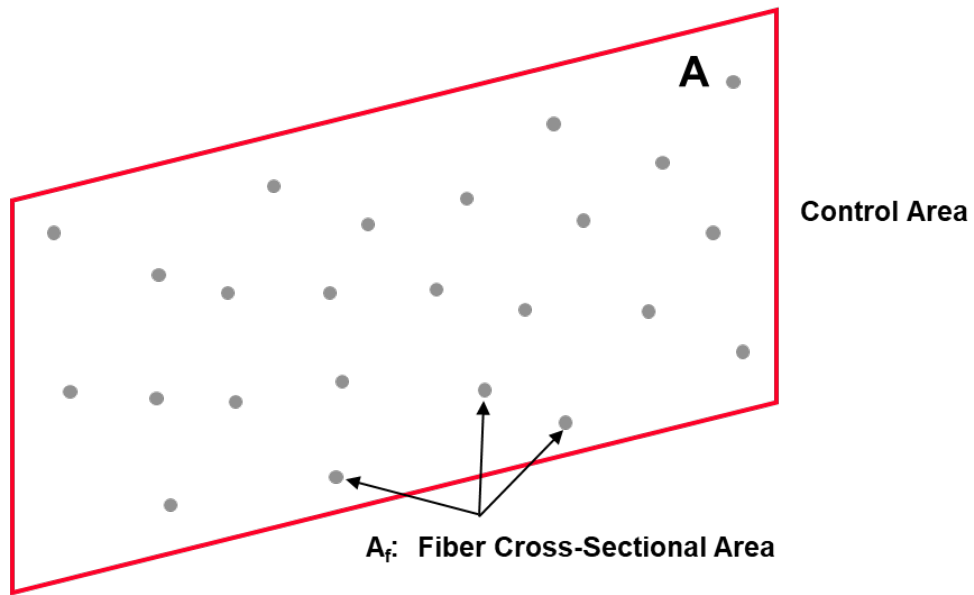
Figure 15: Cross-sectional area of all the fibers in a control section
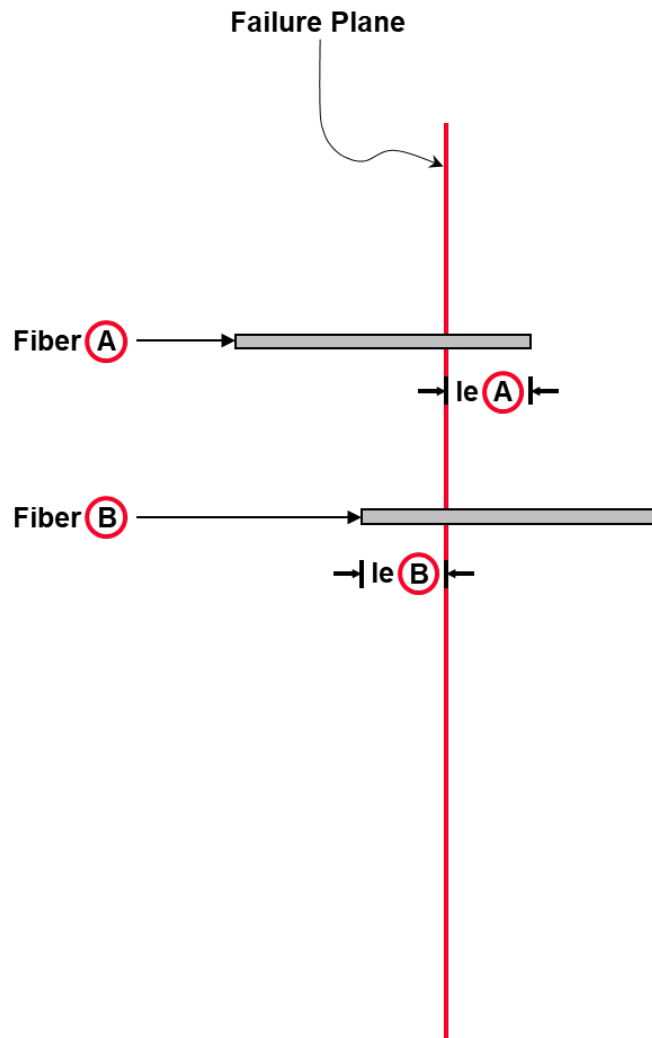
Figure 16: Fiber embedment length
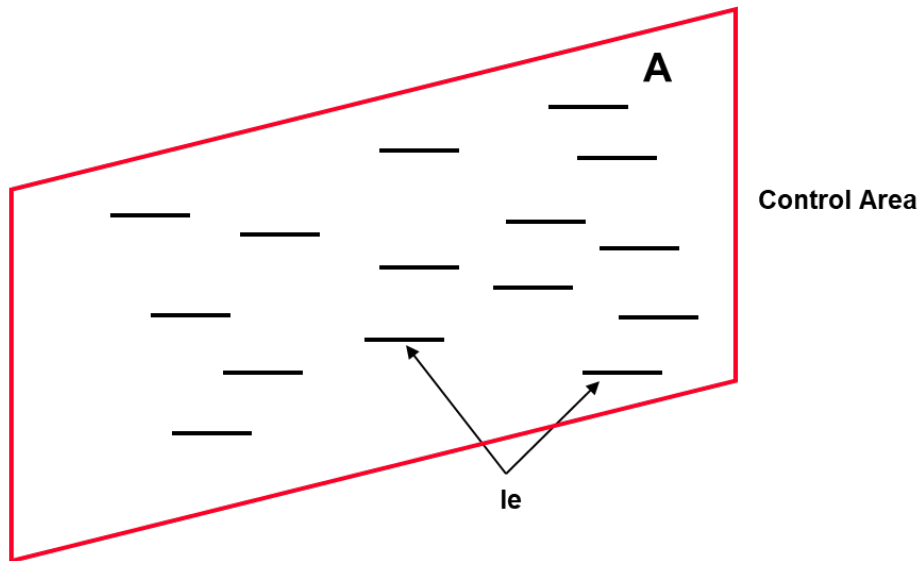
Figure 17: Fiber embedment length through a control section
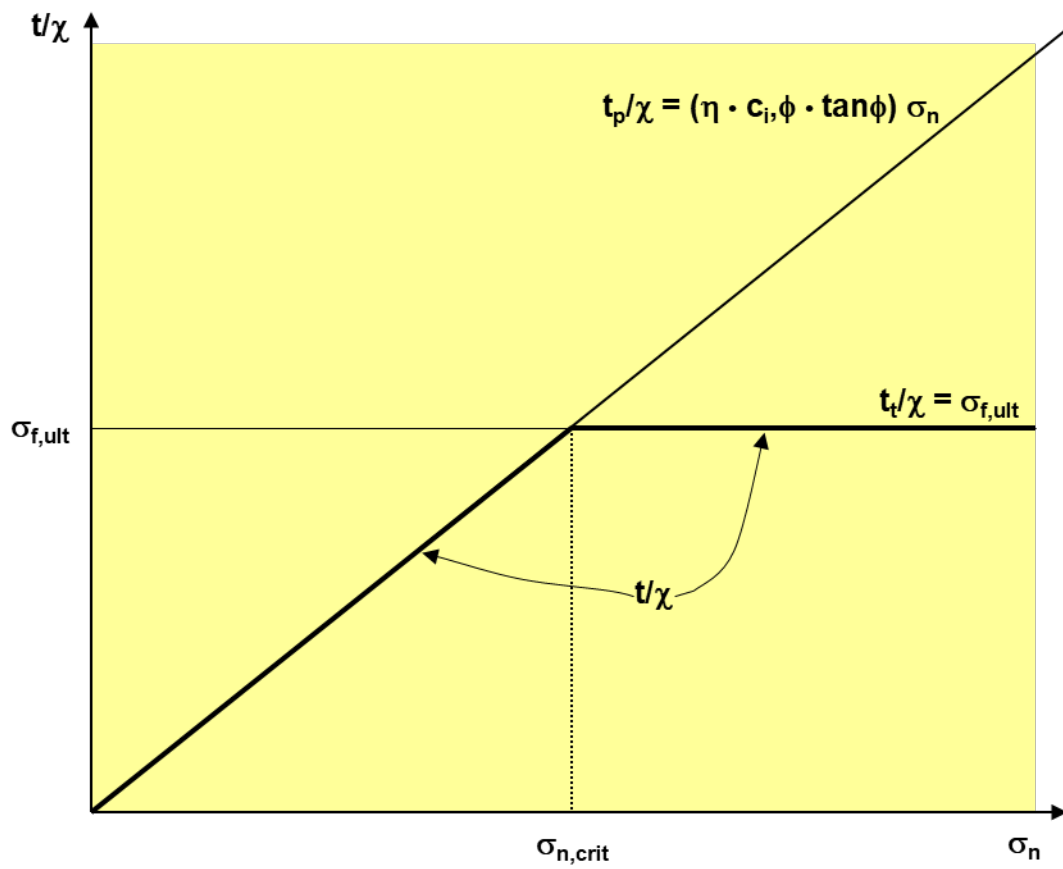
Figure 18: Normalized fiber-induced distributed tension for a cohesionless soil.
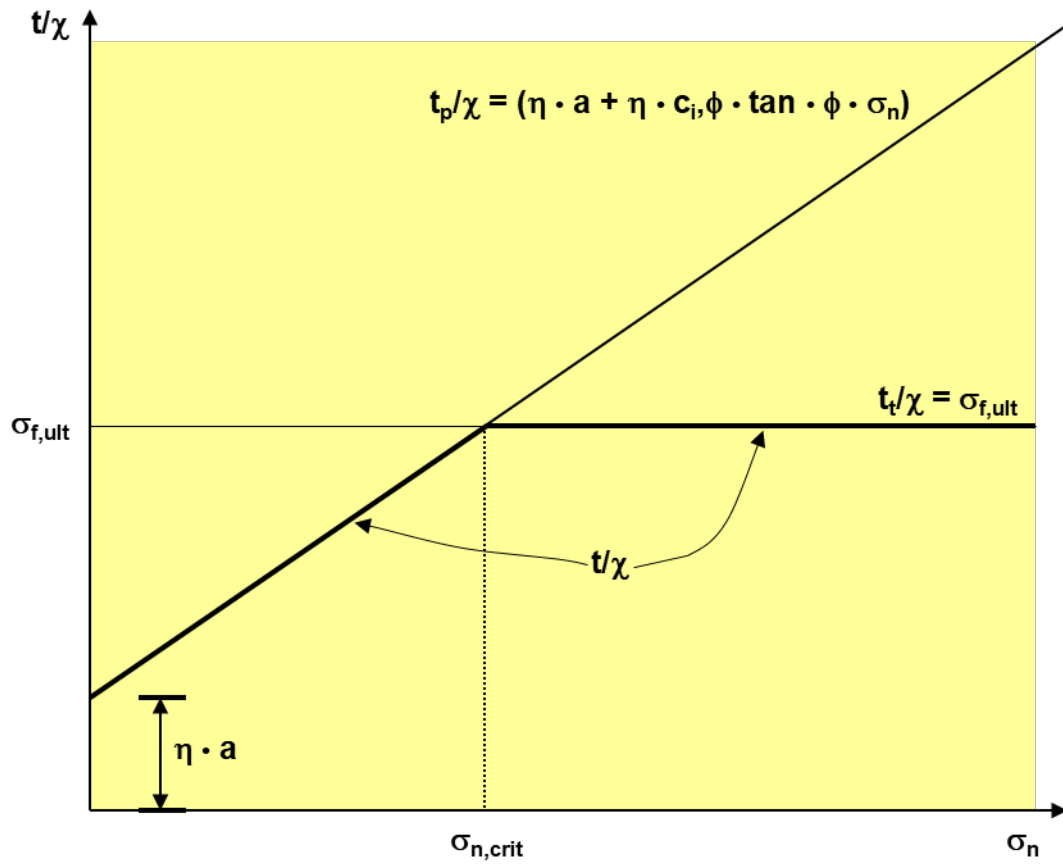
Figure 19: Normalized fiber-induced distributed tension for a cohesive soil.
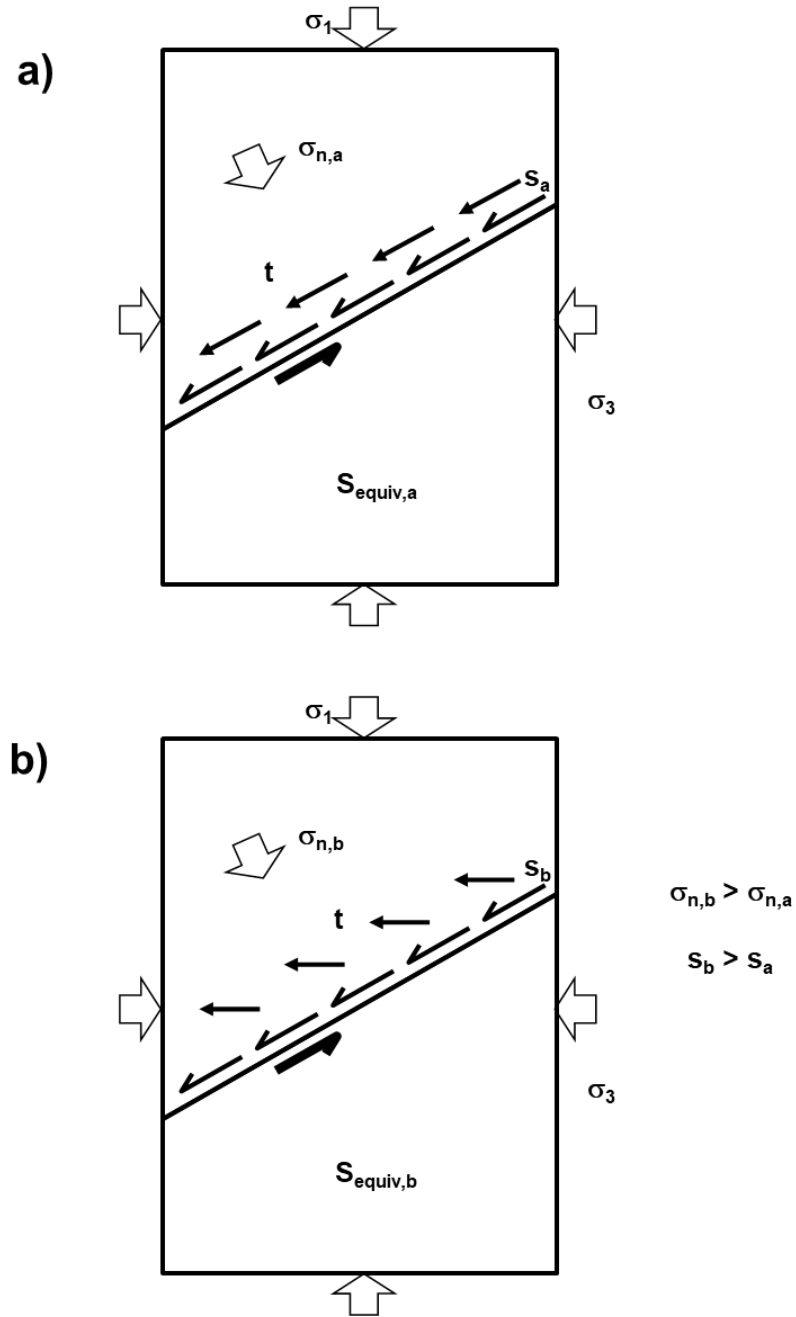
Figure 20: Possible Directions for the fiber-induced distributed tension: (a) fiber-induced distributed tension parallel to the shear plane; and (b) horizontal fiber-induced distributed tension.
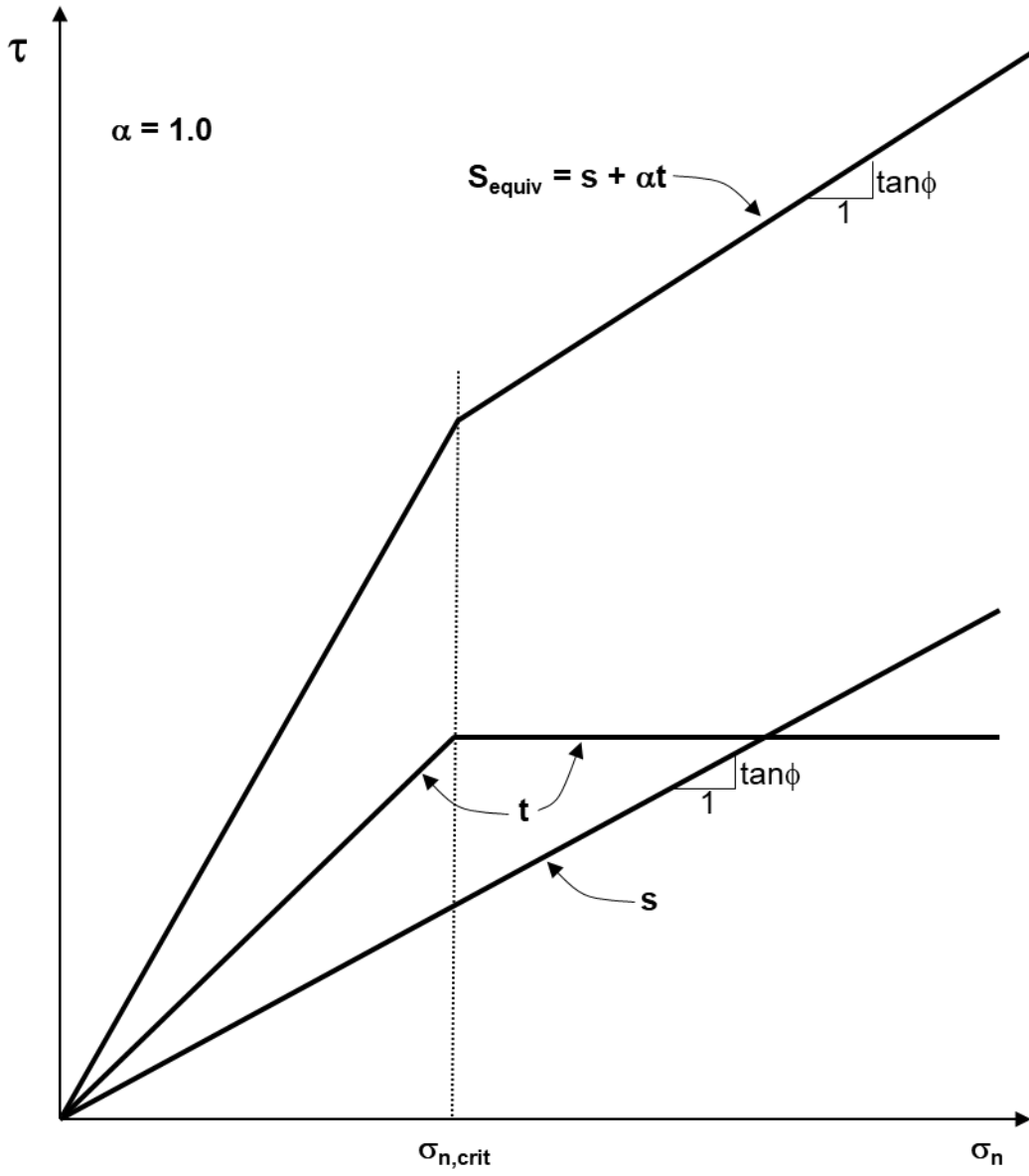
Figure 21: Equivalent shear strength for a cohesionless soil
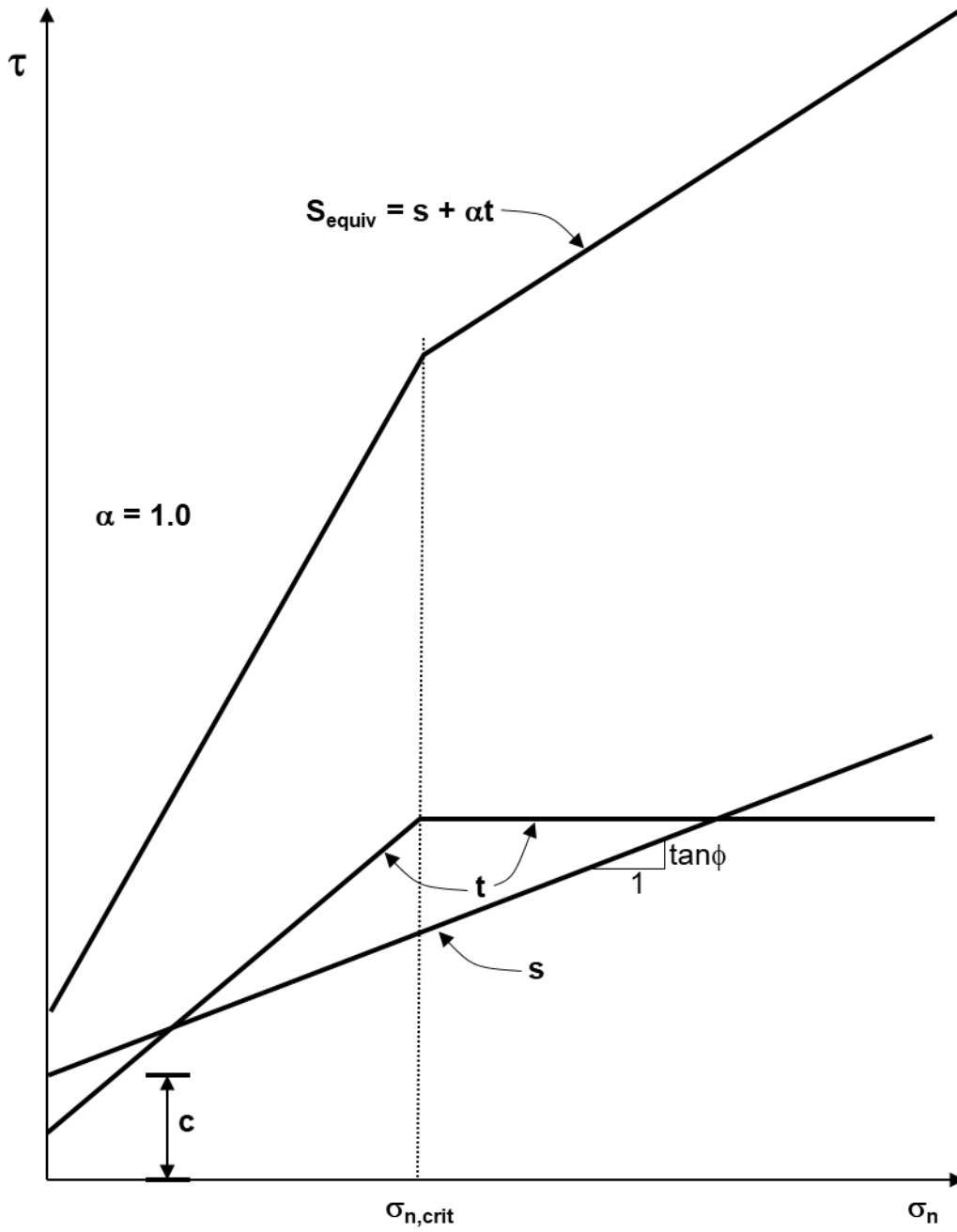
Figure 22: Equivalent shear strength for a cohesive soil
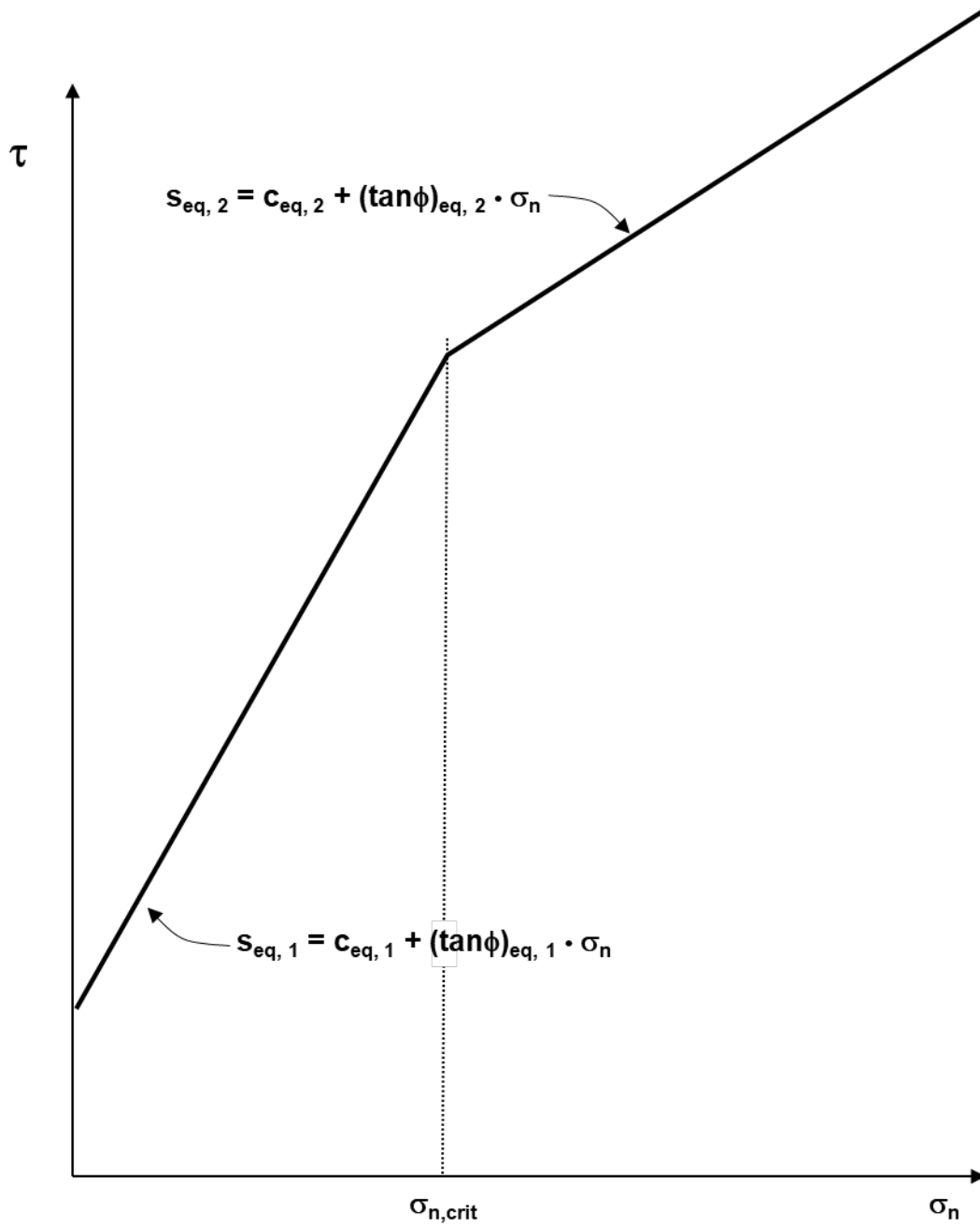
Figure 23: Generic "equivalent strength" envelope for a fiber-reinforced soil mass.
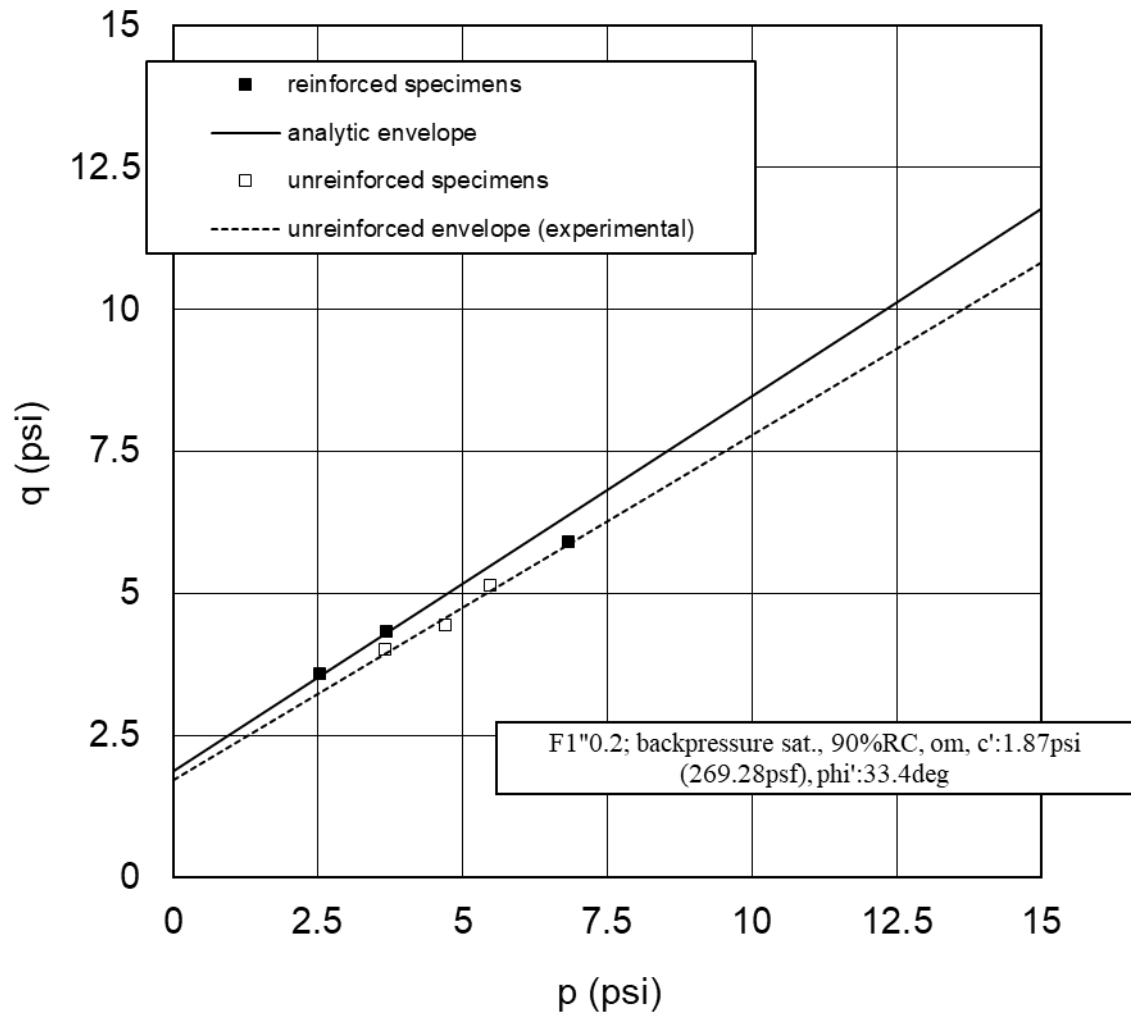
Figure 24: Comparison of experimental and predicted equivalent shear strength (1" fibers, 0.2% fiber content)
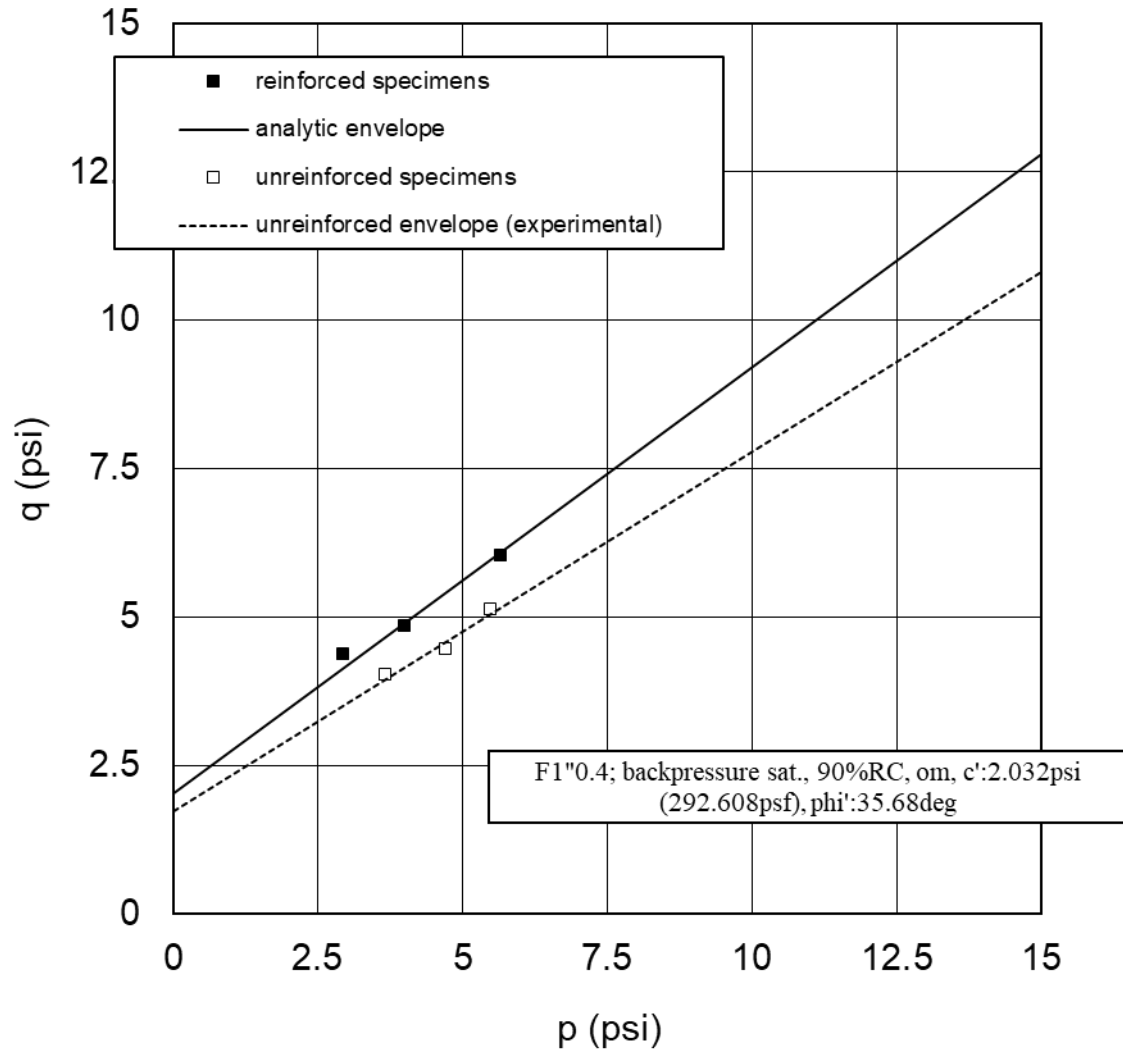
**Figure 25: Comparison of experimental and predicted equivalent shear strength (1"
fibers, 0.4% fiber content)**
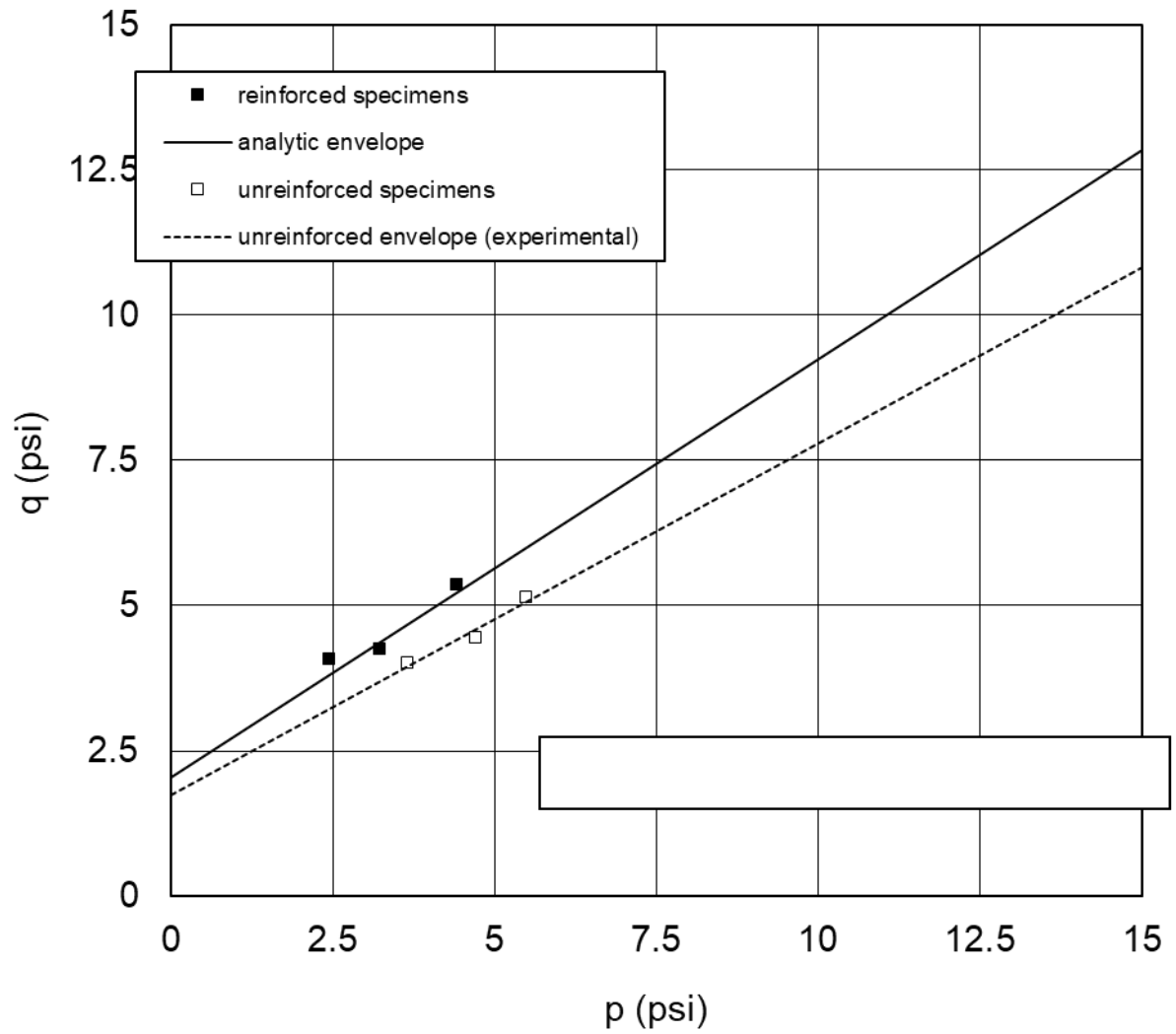
Figure 26: Comparison of experimental and predicted equivalent shear strength (2"
fibers, 0.2% fiber content)
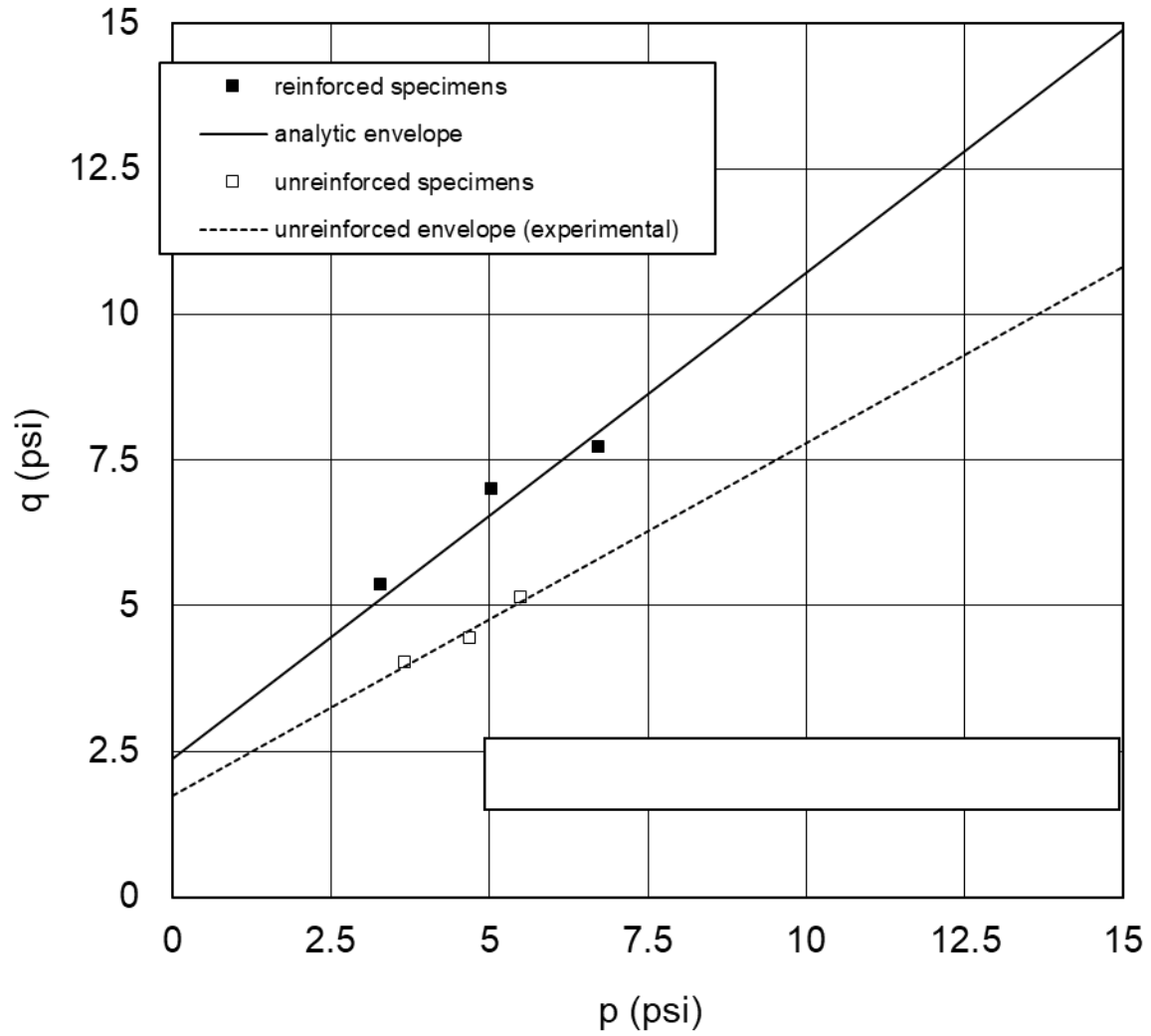
Figure 27: Comparison of experimental and predicted equivalent shear strength (2" fibers, 0.4% fiber content)
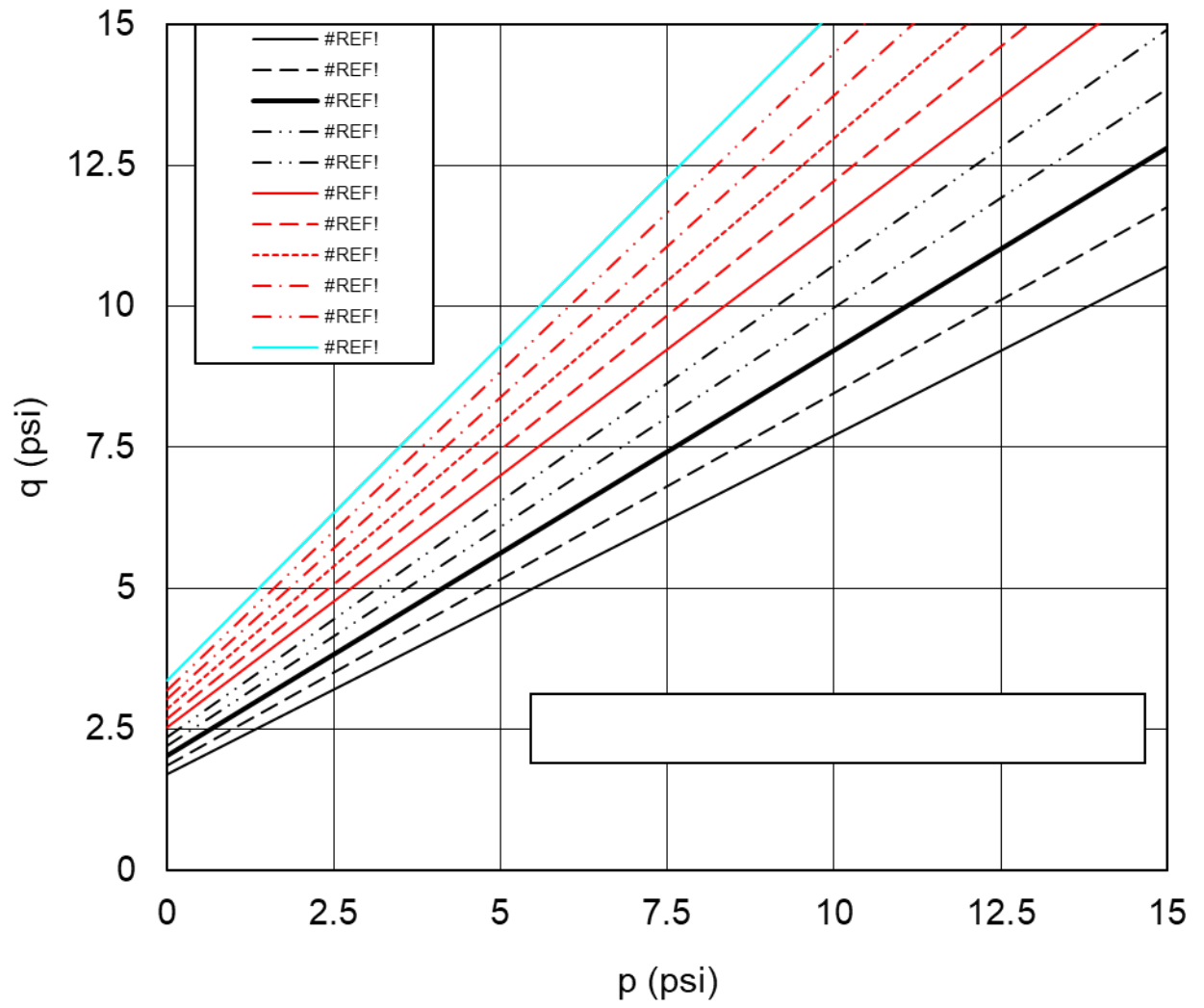
Figure 28: Sensitivity of the equivalent shear strength to the fiber aspect ratio
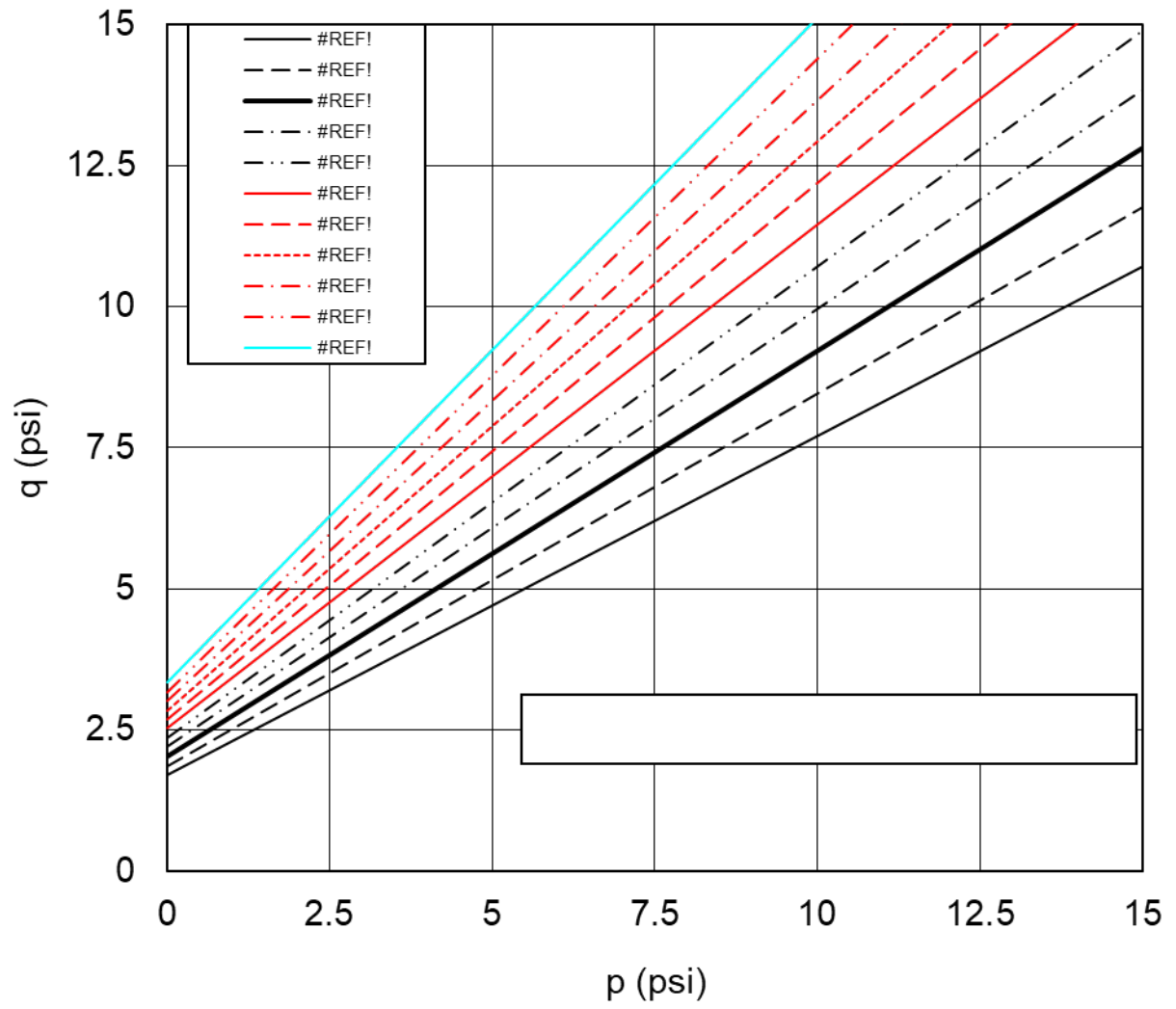
Figure 29: Sensitivity of the equivalent shear strength to the gravimetric fiber content
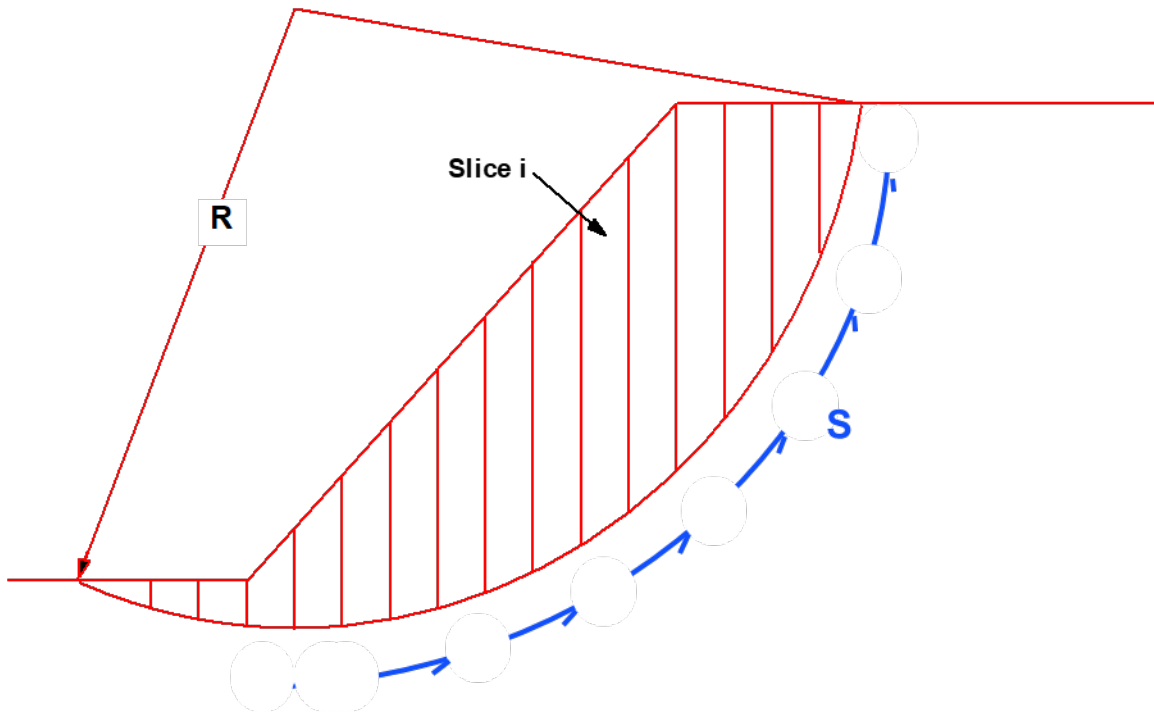
Figure 30: Conventional method of slices for limit equilibrium analysis
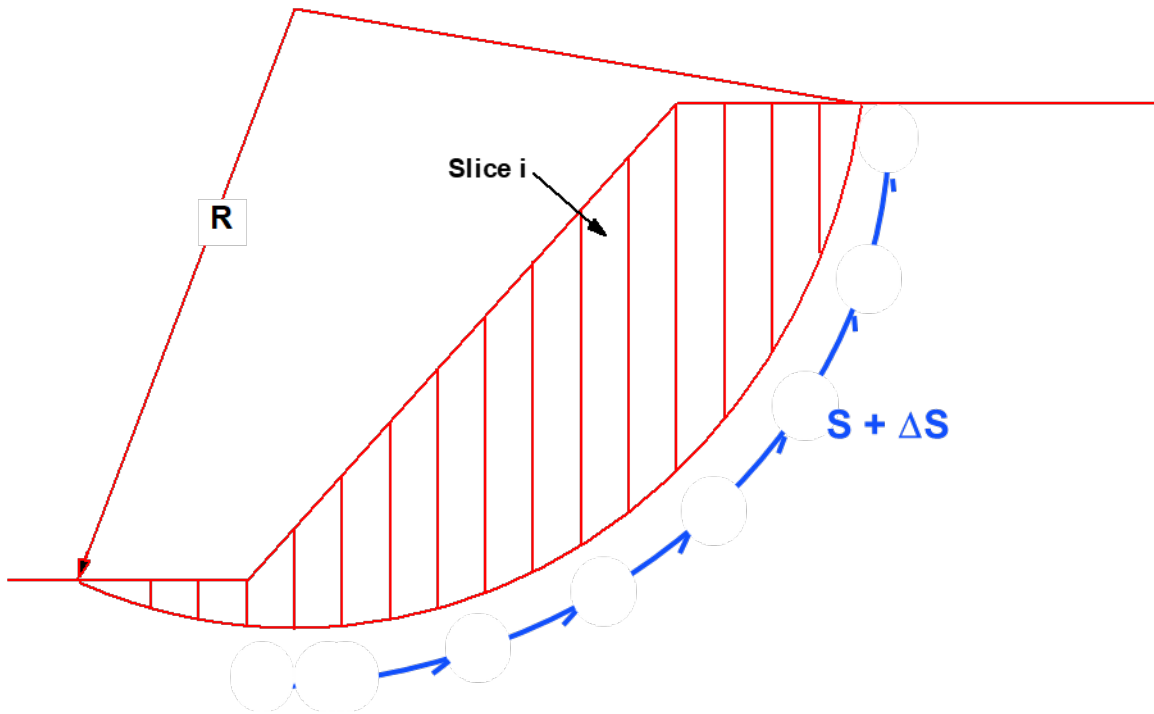
Figure 31: Conventional method of slices for limit equilibrium analysis of a fiber-reinforced soil mass (composite approach)
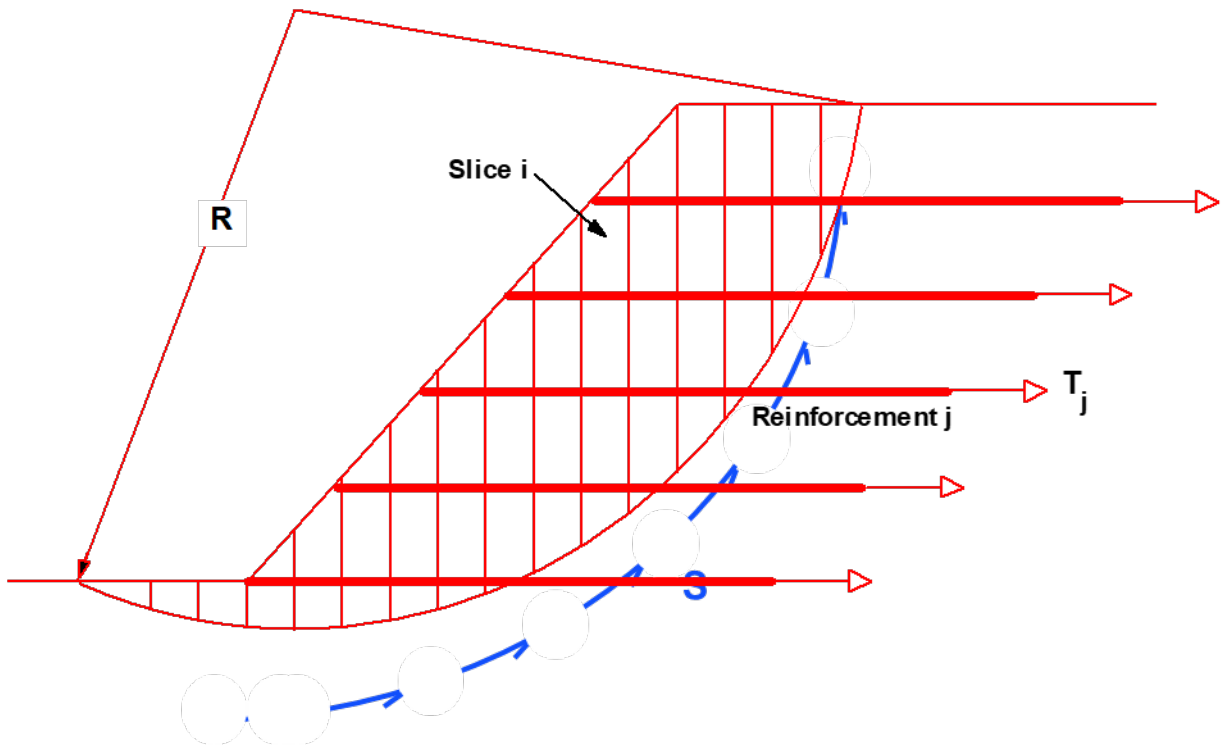
Figure 32: Conventional method of slices for limit equilibrium analysis of slope reinforced with planar reinforcement elements
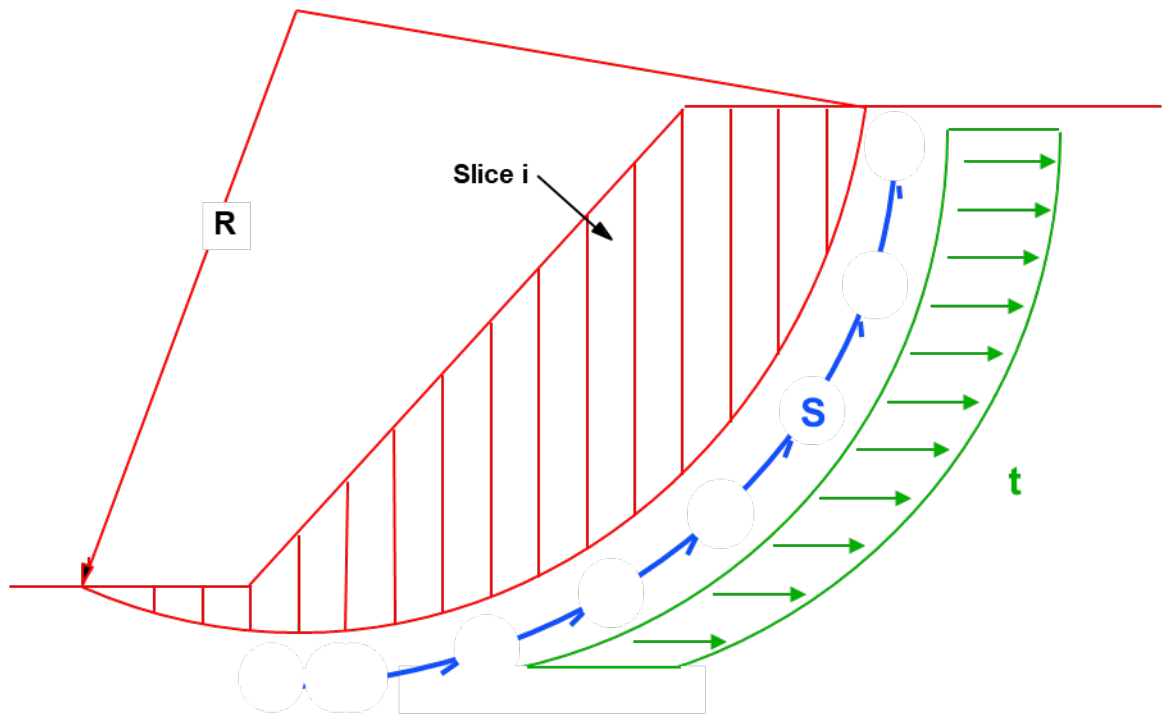
Figure 33: Method of slices for limit equilibrium analysis of fiber-reinforced slope using discrete approach (horizontal fiber-induced distributed tension)
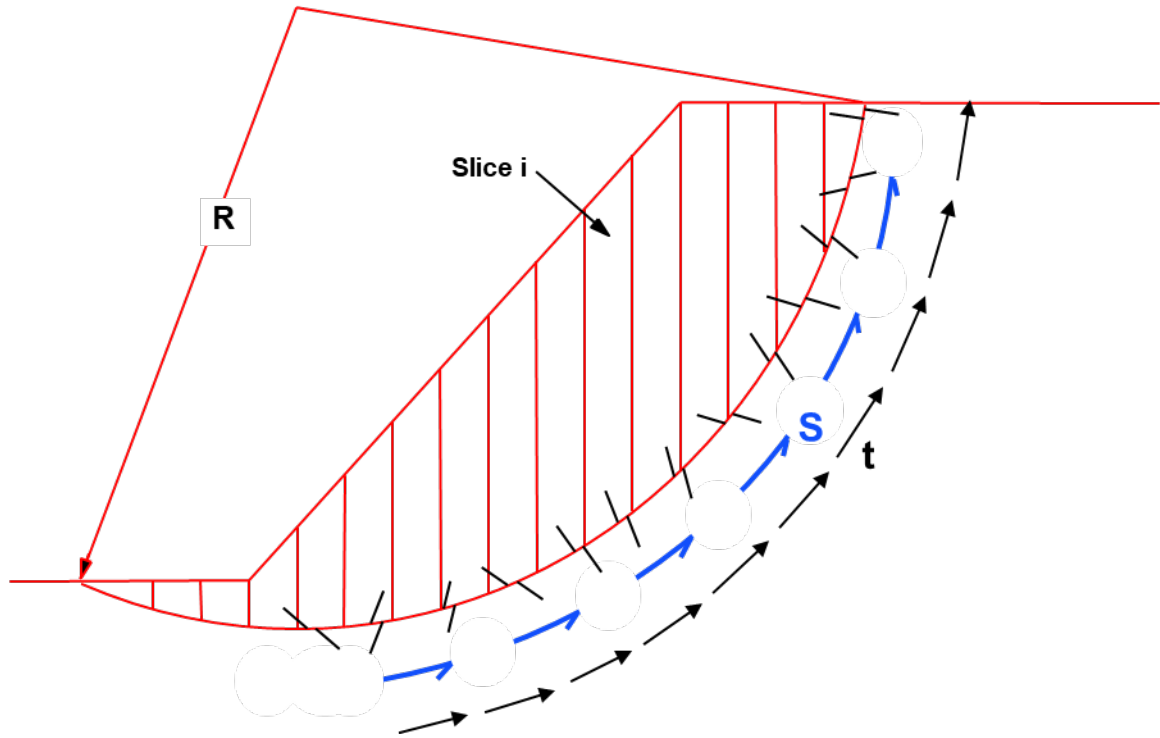
Figure 34: Method of slices for limit equilibrium analysis of fiber-reinforced slope using discrete approach (fiber-induced distributed tension parallel to failure surface)
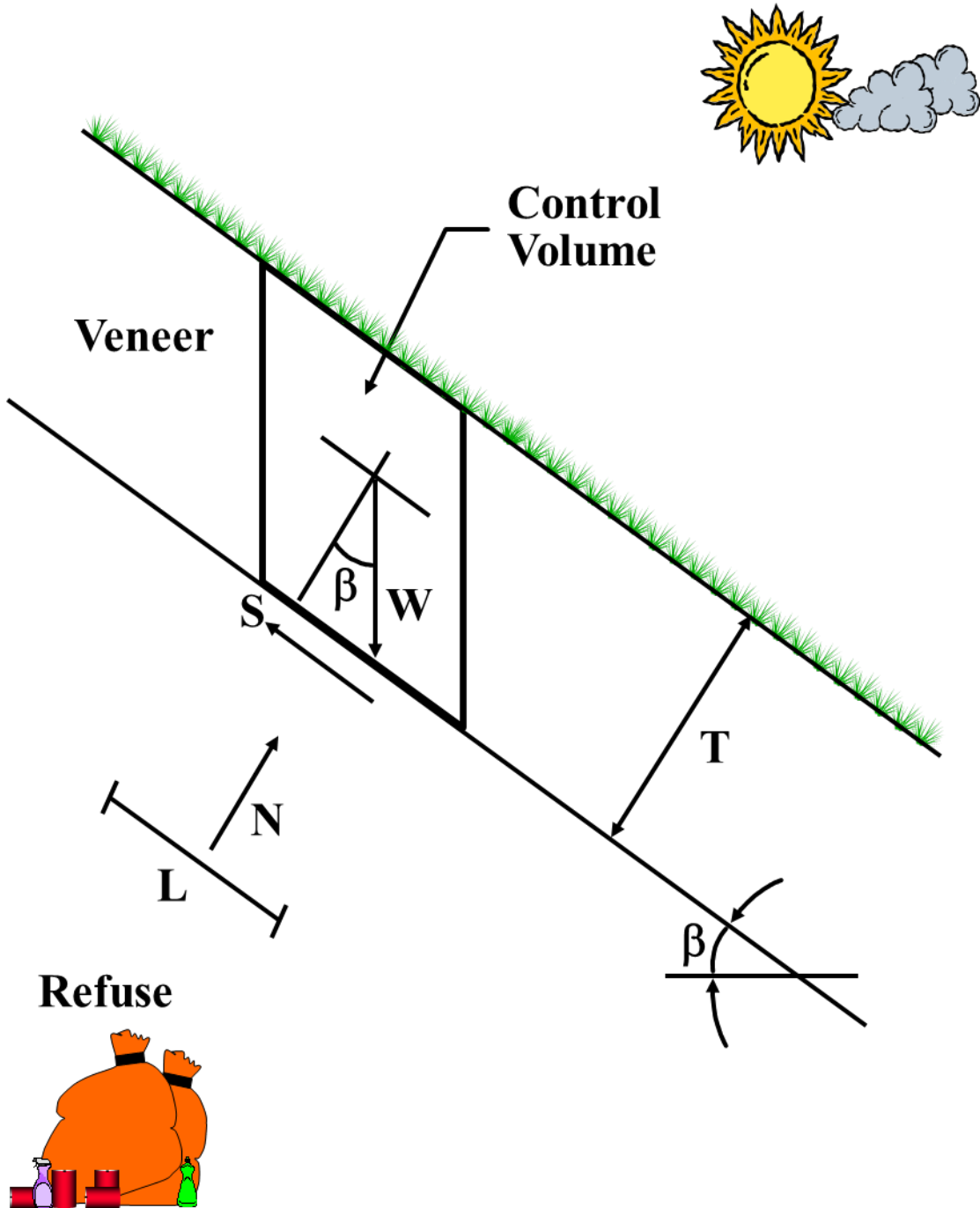
Figure 35: Infinite slope (soil veneer)

Control Volume

Veneer

β **W**

S

N **t**

L

T

β

Refuse
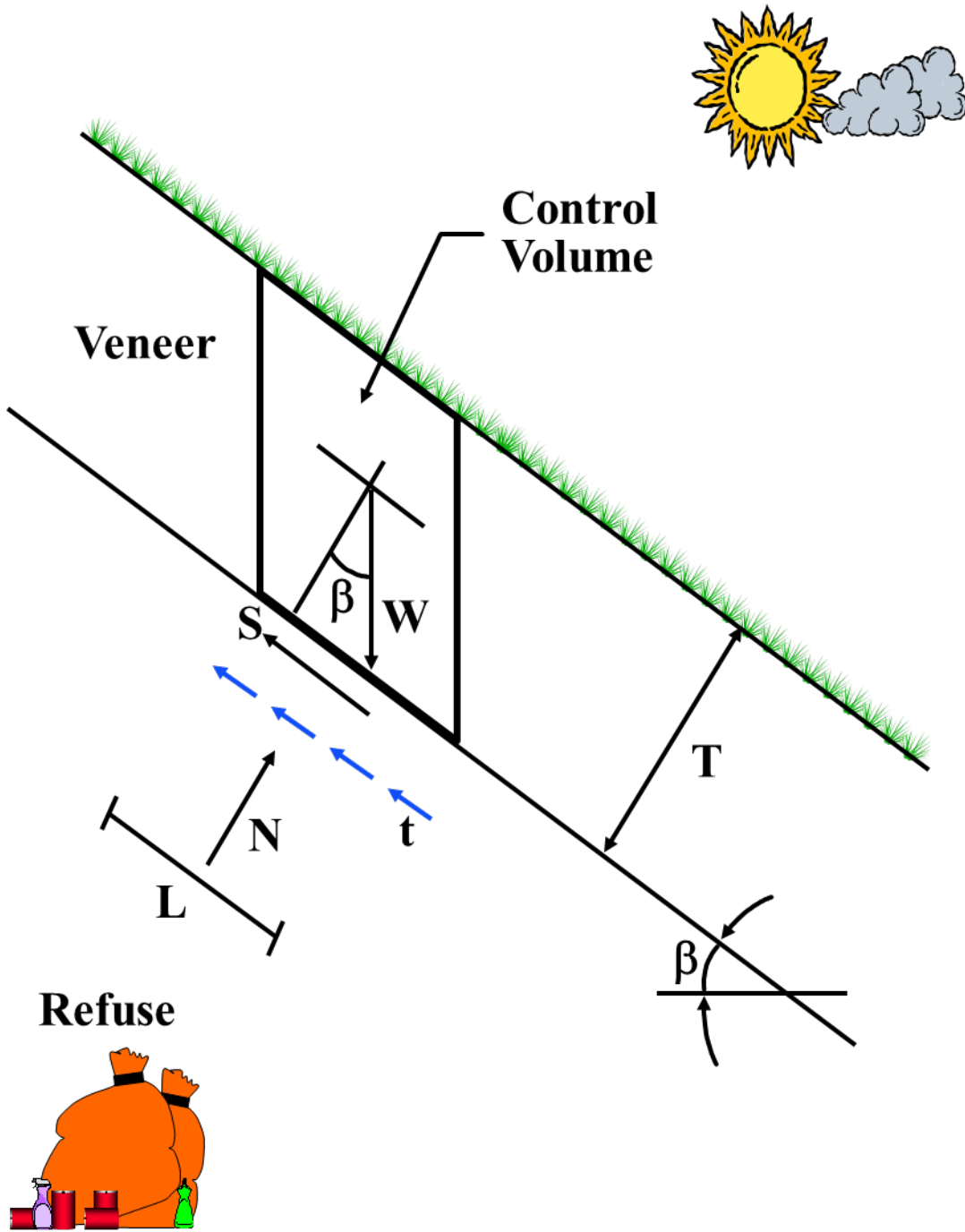
Figure 36: Fiber-reinforced infinite slope (soil veneer)
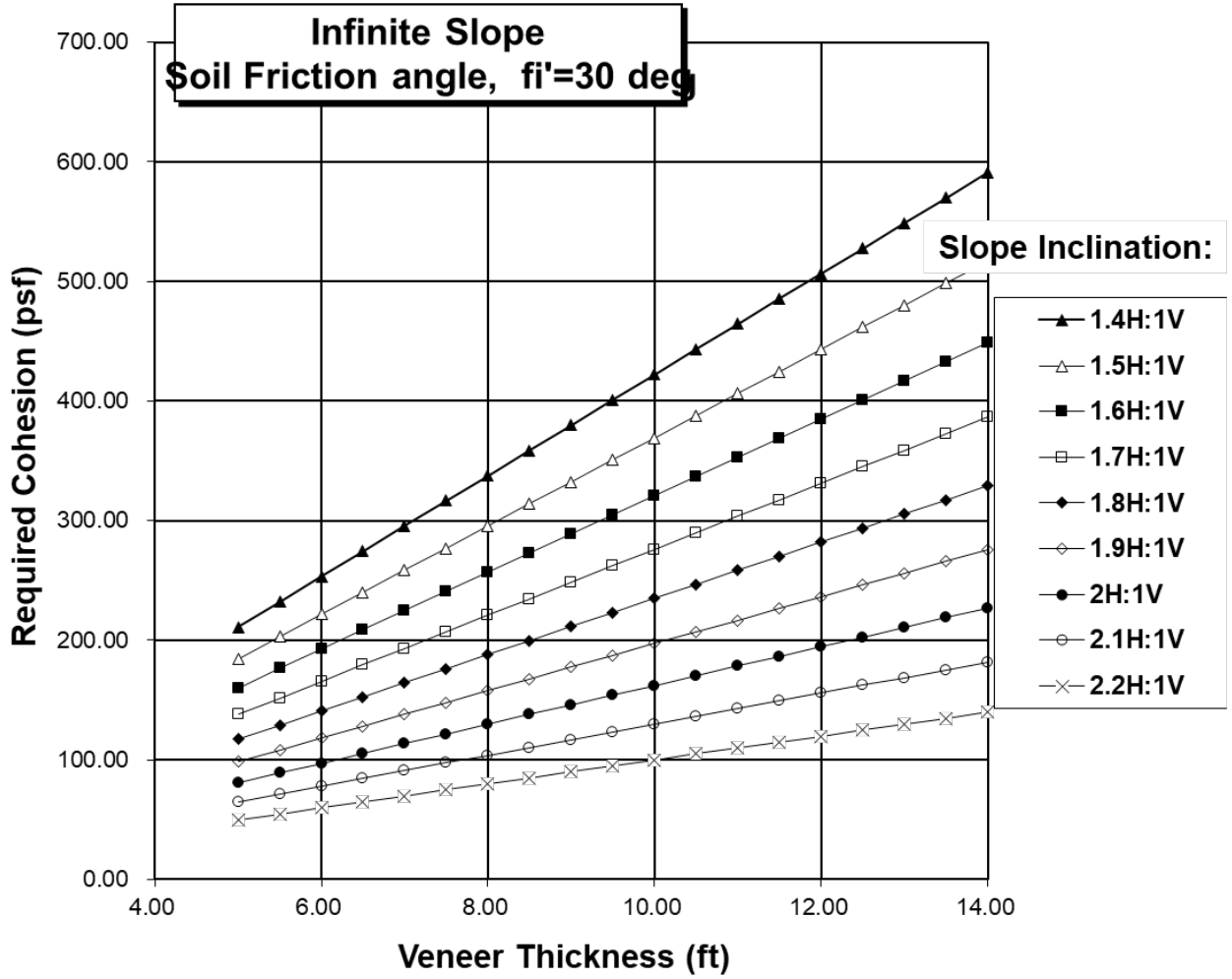
Figure 37: Required cohesion for a factor of safety of 1.5
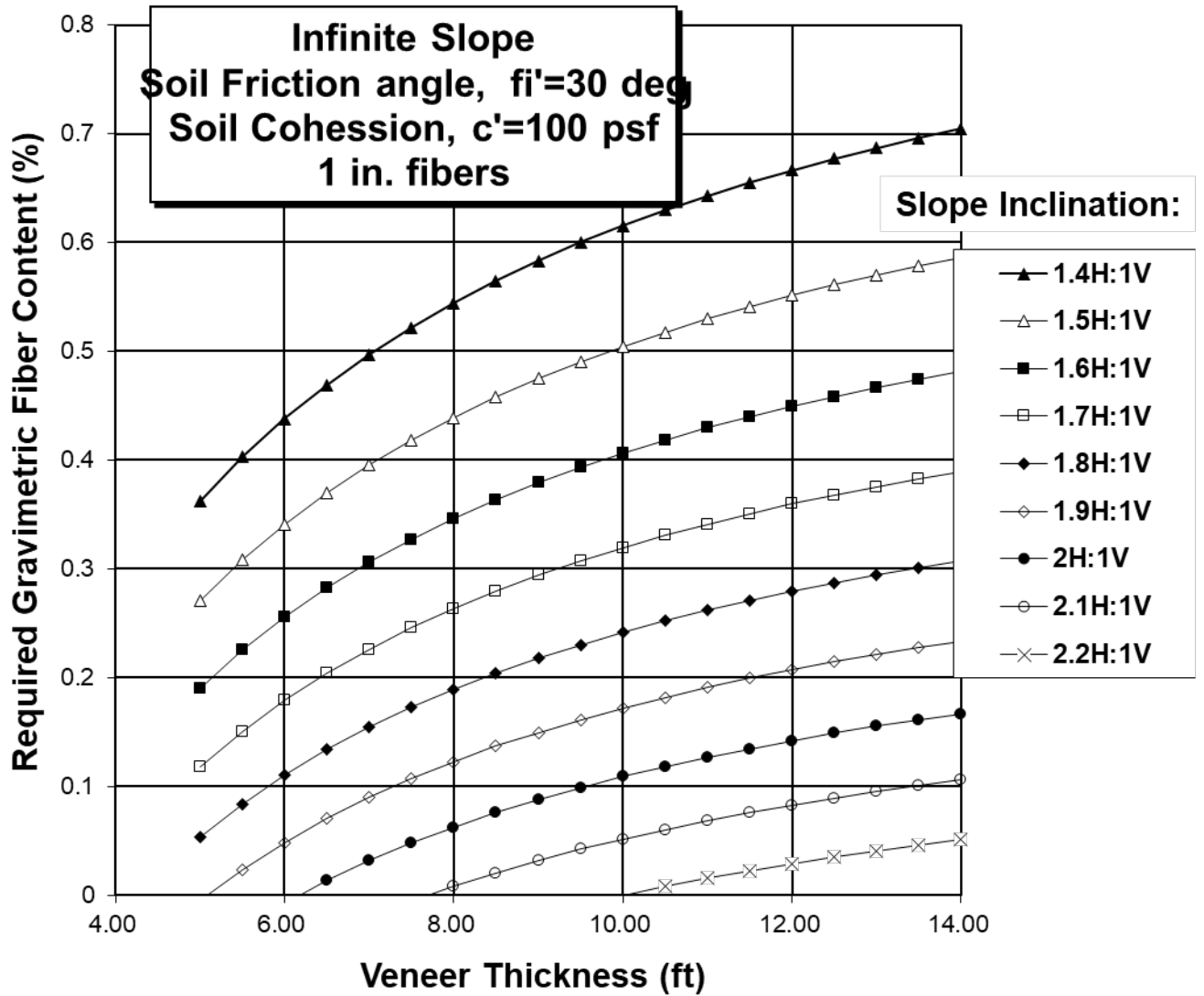
Figure 38: Required fiber content for a factor of safety of 1.5 (1" fibers)
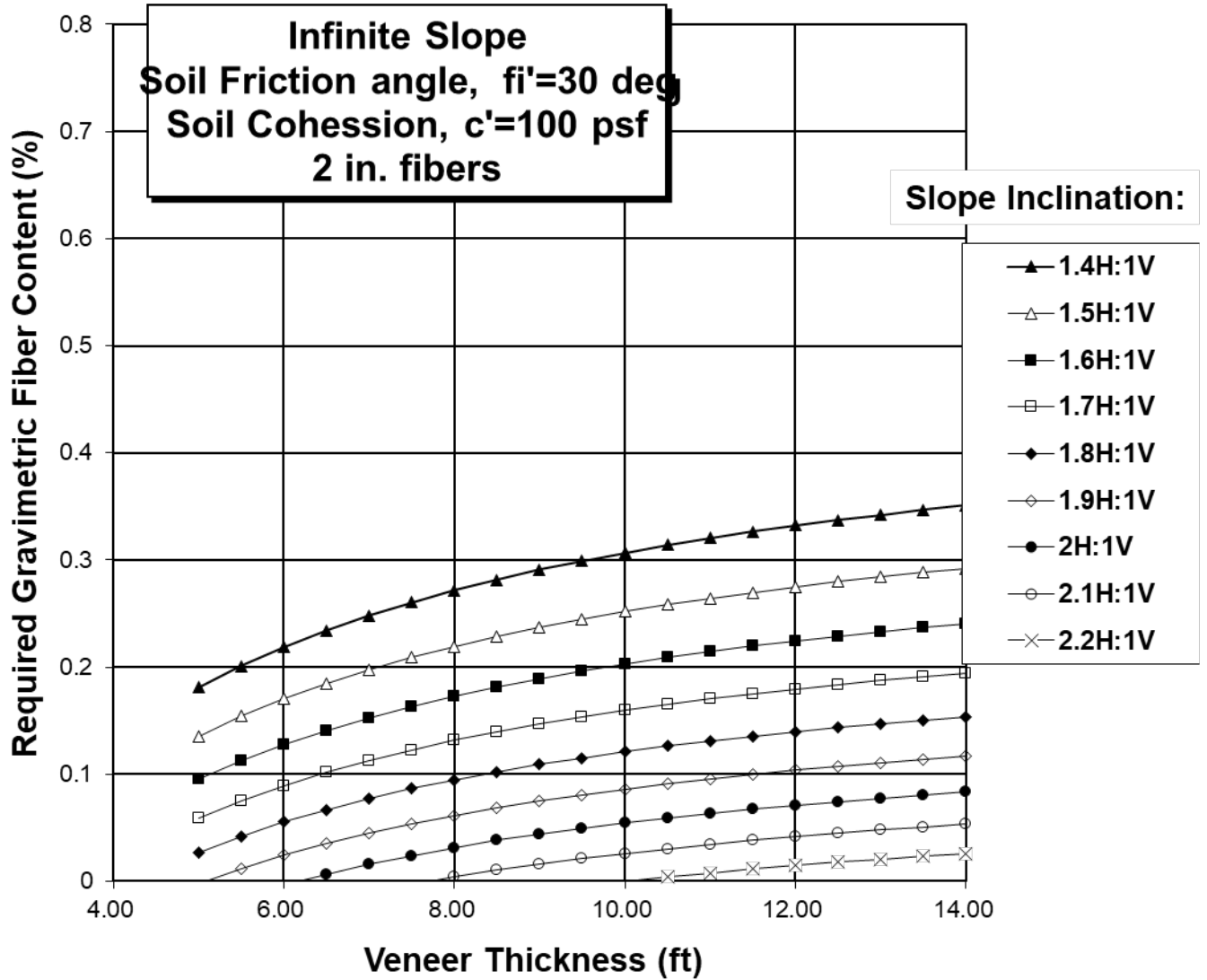
Figure 39: Required fiber content for a factor of safety of 1.5 (2" fibers)

$\gamma = 105$ pcf
$c' = 100$ psf
$\phi' = 30$ deg

a)

$\gamma = 105$ pcf
$c' = 100$ psf
$\phi' = 30$ deg
$\chi_w = ?$

H = 30 ft

W : 25 ft

b)

$\gamma = 105$ pcf
$c' = 100$ psf
$\phi' = 30$ deg
$\chi_w = 0.6\%$

H = 30 ft

W : ?
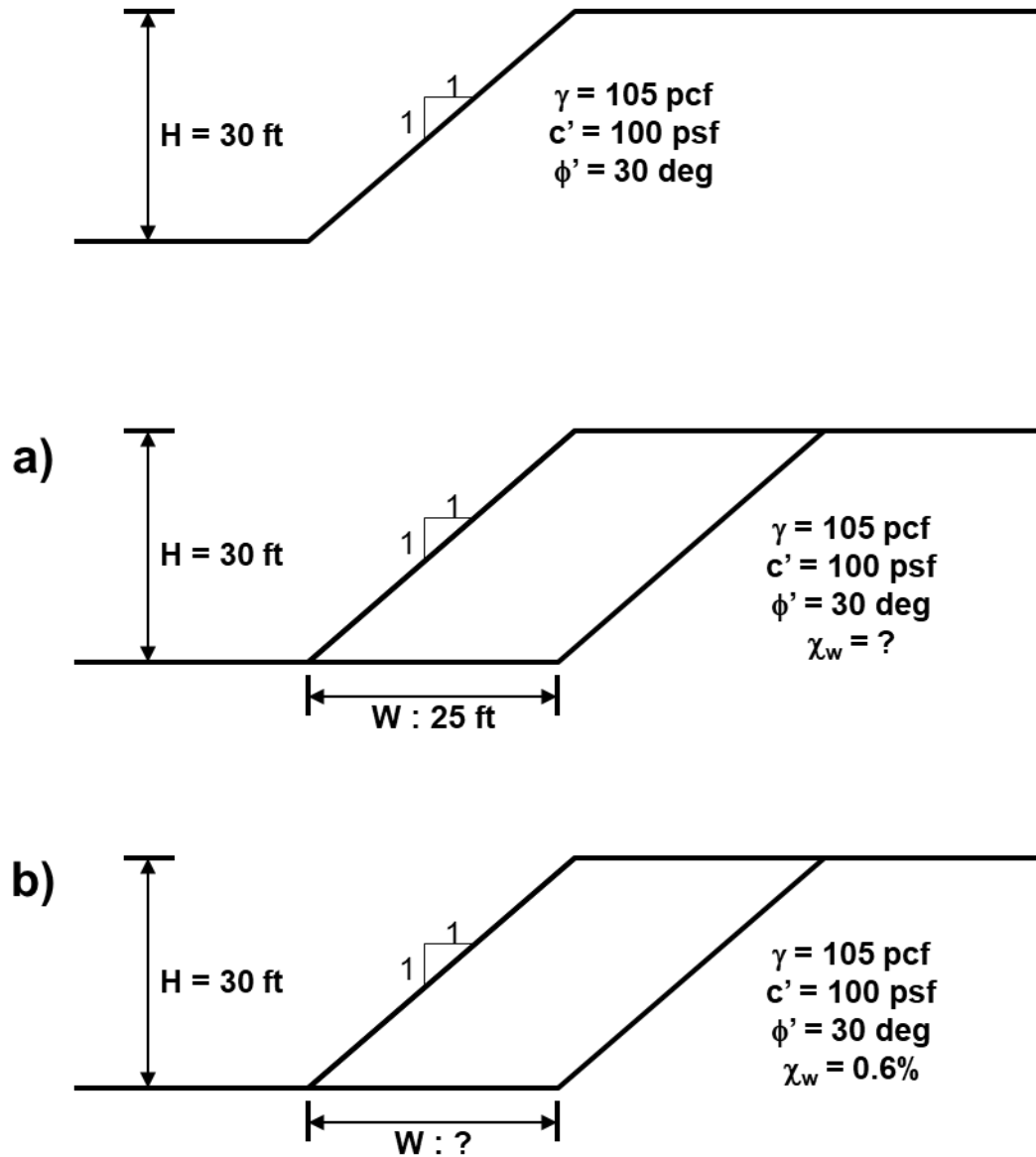
Figure 40: Schematic representation of the design example
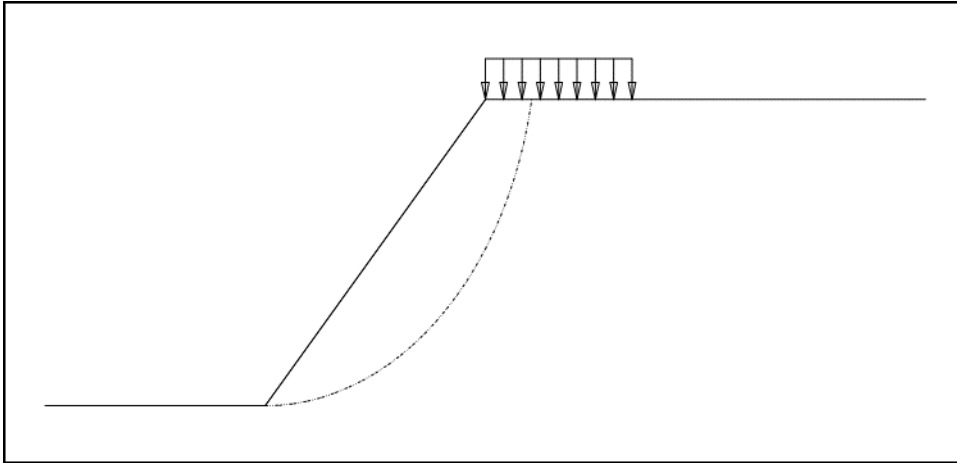
Figure 41: 2D fiber-reinforced slope analysis (unreinforced)
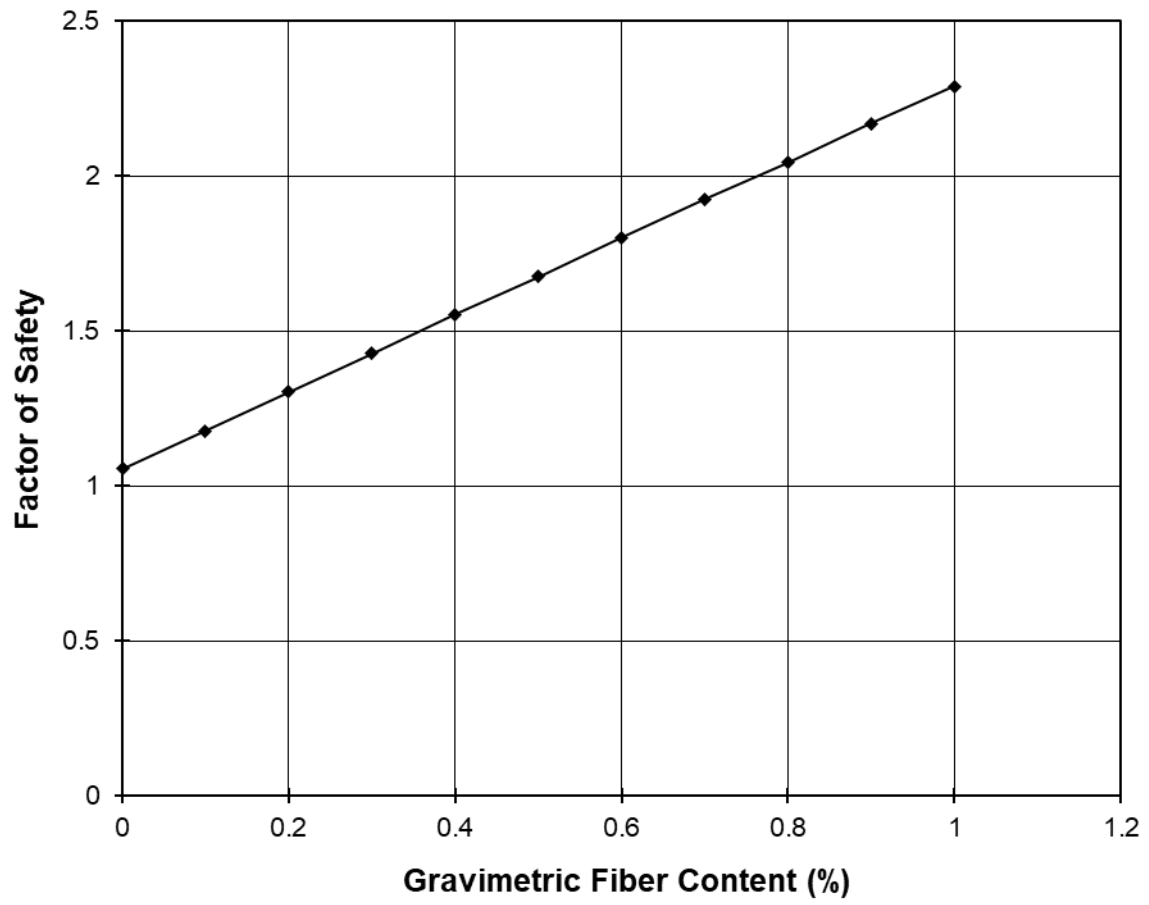
Figure 42: 2D fiber-reinforced slope analysis (a)
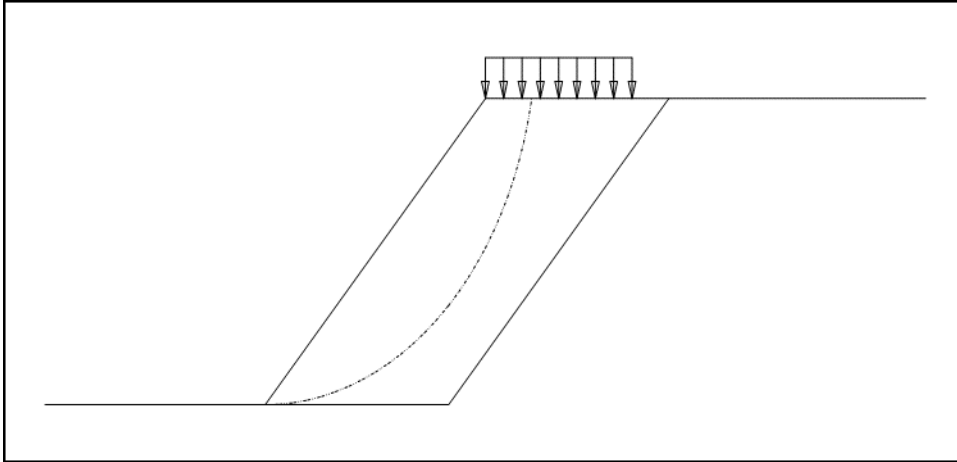
Figure 43: 2D fiber-reinforced slope analysis (a)
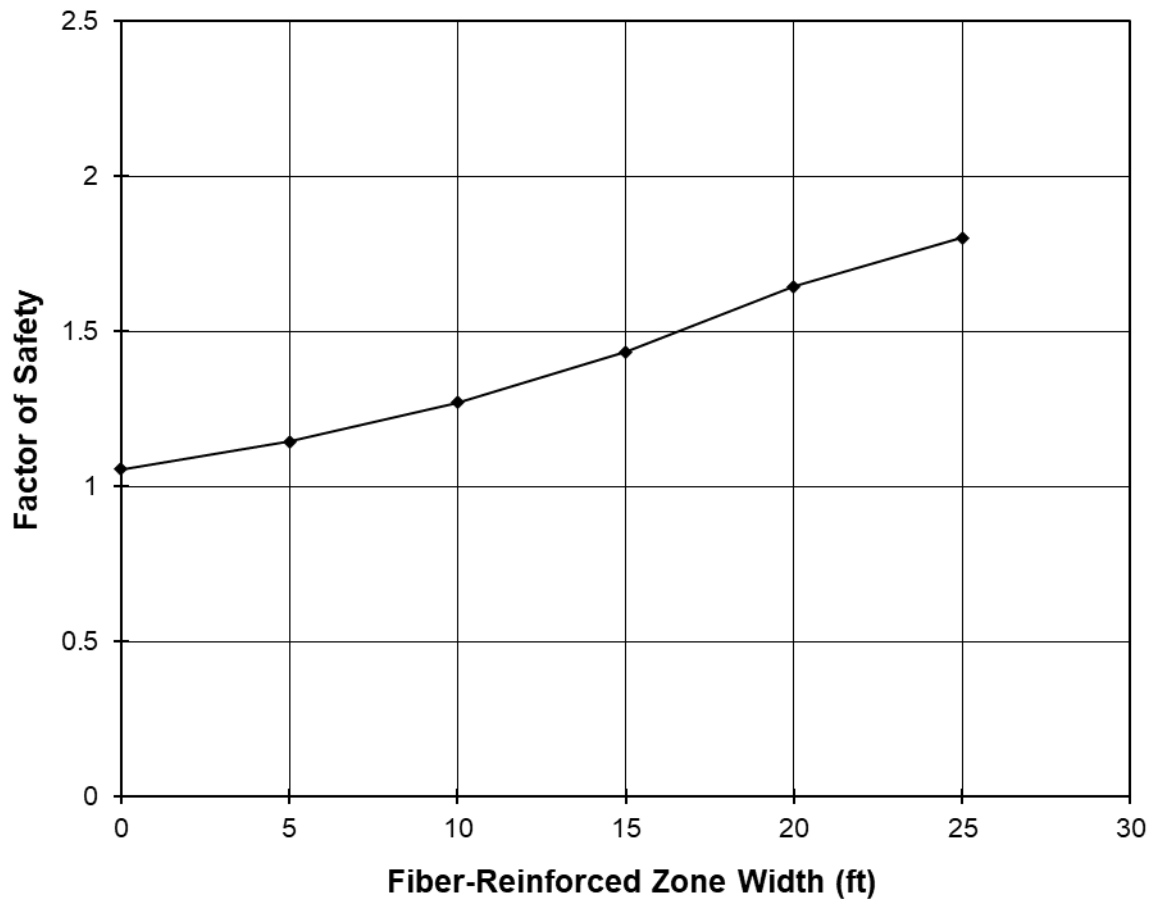
Figure 44: 2D fiber-reinforced slope analysis (b)

Figure 45: 2D fiber-reinforced slope analysis (b)

DEVELOPMENT OF A DISCRETE DESIGN METHODOLOGY FOR FIBER-REINFORCED SOIL

Jorge G. Zornberg, Ph.D., P.E.

APPENDIX A: SYMBOLS

Appendix A: Symbols

a :   Adhesive component of the interface shear strength

A :   Control surface area

A_f :   Cross-sectional area of all fibers in the control section

$A_{f,i}$:   Cross-sectional area of an individual fiber

$c_{i,c}$:   Interaction coefficient of the cohesive component of the interface shear strength

$c_{i,\phi}$:   Interaction coefficient of the frictional component of the interface shear strength

d_f :   Equivalent diameter of a single fiber

f_f :   Interface shear strength of individual fibers

G_f :   Specific weight of the fibers (dimensionless)

L :   Length of the control volume along a veneer slope

l_e :   Embedment length of a fiber

$l_{e,ave}$:   Average embedment length of the fibers

l_f :   Fiber length

n :   Number of fibers in the control section

N :   Normal force

S :   Shear force

t: Fiber-induced distributed tension

T :   Thickness of a veneer slope

t_p :   Fiber-induced distributed tension when failure is governed by the pullout of individual fibers

t_t :   Fiber-induced distributed tension when failure is governed by the tensile strength of individual fibers

V: Volume of fiber-reinforced soil

V_f :   Volume of fibers

W :   Weight of the fiber-reinforced soil control volume

W_f :   Weight of fibers

W_s :   Dry weight of soil

α :   Empirical coefficient that accounts for the effect of the direction of the fiber-induced distributed tension

β :   Slope inclination

δ :   Interface friction angle

ΔS: Increased strength of the fiber-reinforced soil in a composite approach

ϕ :   Soil friction angle

γ: Total dry unit weight of the fiber-reinforced soil

γ_w :   Unit weight of water

η :   Aspect ratio of individual fibers

ρ :   Volumetric fiber content

ρ_w :   Gravimetric fiber content

$\sigma_{f,ult}$:   Ultimate tensile strength of an individual fiber

σ_n :   Normal pressure

$\sigma_{n,crit}$:   Critical confining pressure

DEVELOPMENT OF A DISCRETE DESIGN METHODOLOGY FOR FIBER-REINFORCED SOIL

Jorge G. Zornberg, Ph.D., P.E.

APPENDIX B: BIBLIOGRAPHY ON FIBER-REINFORCEMENT

Bibliography on Fiber-reinforcement

1. Al-Moussawi, H. M. and Andersland, O. B. (1987), "Behavior of Fabric versus Fiber-reinforced Sand," *J. Geotech. Engrg.,* ASCE, Discussion, Vol. 113, pp. 383-385.

2. Al Refeai, T. (1991). "Behaviour of Granular Soils Reinforced with Discrete Randomly Oriented Inclusions," *Geotextiles and Geomembranes*, Vol.10, No.4, pp.319-333.

3. Al Wahab, R.M., and Al-Qurna, H.H. (1995), "Fiber-reinforced Cohesive Soils for Application in Compacted Earth Structures," *Proc., Geosynthetics '95 Conference*, Nashville, Tennessee, Vol. 2, pp.433-446.

4. Al Wahab, R.M., and El-Kedrah, M.M. (1995), "Using Fibers to Reduce Tension Cracks and Shrink/Swell in Compacted Clays," *Proc., Geoenvironment 2000*, New Orleans, Louisiana, Vol. 2, pp.433-446.

5. Ashmawy, A. K., and Sukumaran, B. (1997), "Probabilistic Analysis of Randomly Distributed Fiber-Reinforced Soil," *J. of Geotechnical and Geoenvironmental. Engineering.,* ASCE, Discussion, Vol. 123, No.109, pp. 986-987.

6. Foose, G.J., Benson, C.H., and Bosscher, P.J. (1996), "Sand Reinforced With Shredded Waste Tires," *J. Geotech. Engrg.,* ASCE, Vol. 122, No. 9, pp. 760-767.

7. Freitag, D.R. (1986). "Soil Randomly Reinforced with Fibers," *Journal of Geotechnical Engineering, ASCE*, Vol. 112, No.8, pp. 823-826.

8. Fugro-McClelland (Southwest), Inc. (1996), *Geotechnical Engineering Study Laboratory Testing of Nebraska Soil Samples and Hypothetical Slope Analyses, Fort Worth, Texas.* Report no. 1401-0004, prepared by Fugro McCelland to Synthetic Industries, May 2, 1997.

9. Fugro-McClelland (Southwest), Inc. (1997), *Geotechnical Engineering Study Bowie Slope - Highway 287 and Fruitland Road - Case Study, Bowie, Texas.* Report no. 1401-0014, prepared by Fugro McCelland to Synthetic Industries, May 2, 1997.

10. Goran, W.P. and Johnson, W.G. (1994). "Stabilization of high plasticity clay and silty sand by inclusion of discrete fibrillated polypropylene fibers for use in pavement subgrades." *CPAR Report GL-94-2*, Geotechnical Laboratory, U.S. Army Corps of Engineers, Vicksburg, MS.

11. Gray, D.H. and Al-Refeai, T. (1986), "Behavior of Fabric versus Fiber-reinforced Sand," *J. Geotech. Engrg.,* ASCE, Vol. 112, No. 8, pp. 804-820.

12. Gray, D.H. and Al-Refeai, T. (1987), "Behavior of Fabric versus Fiber-reinforced Sand," *J. Geotech. Engrg.,* ASCE, Closure, Vol. 113, pp. 385-387.

13. Gray, D.H. and Ohashi, H. (1983), "Mechanics of Fiber-reinforcement in Sand," *J. Geotech. Engrg.,* ASCE, Vol. 109, No. 3, pp. 335-353.

14. Gregory, G.H. (1996). *Design Guide for Fiber-Reinforced Soil Slopes*. Version 1.0, Fugro-McClelland (Southwest).

15. Gregory, G. H. and Chill, D. S. (1998), "Stabilization of Earth Slopes with Fiber-reinforcement," *Proc., Int. Conf. Geosynthetics*, Atlanta, Georgia, March 1998, pp.1073-1078.

16. Hausmann, M.R. (1987), "Behavior of Fabric versus Fiber-reinforced Sand," *J. Geotech. Engrg.,* ASCE, Discussion, Vol. 113, pp. 381-383.

17. Leflaive, E. (1985), "Soils reinforced with continuous yarns: the Texol," *Proc., Eleventh Int. Conf. on Soil Mech. and Found. Engrg.*, San Francisco, Vol.3, pp.1787-1790.

18. Maher, M.H. and Gray, D.H. (1990), "Static Response of Sand Reinforced With Randomly Distributed Fibers," *J. Geotech. Engrg.,* ASCE, Vol. 116, No. 11, pp. 1661-1677.

19. Maher, M. H. and Ho, Y. C. (1994), "Mechanical Properties of Kaolinite/Fiber Soil Composite," *J. Geotech. Engrg.,* ASCE, Vol. 120, No. 8, pp. 1381-1393.

20. Maher, M.H. and Woods, R.D. (1990), "Dynamic Response of Sand Reinforced With Randomly Distributed Fibers," *J. Geotech. Engrg.,* ASCE, Vol. 116, No. 7, pp. 1116-1131.

21. McGown, A., Andrawes, K.Z, Hytiris, N., and Mercel, F.B. (1985), "Soil strengthening using randomly distributed mesh elements," *Proc., Eleventh Int. Conf. on Soil Mech. and Found. Engrg.*, San Francisco, Vol.3, pp.1735-1738.

22. Michalowski, R.L. and Zhao, A. (1996), "Failure of Fiber-Reinforced Granular Soils," *J. Geotech. Engrg.,* ASCE, Vol. 122, No. 3, pp. 226-234.

23. Morel, J.C. and Gourc, J.P., 1997, "Mechanical Behavior of Sand Reinforced with Mesh Elements," *Geosynthetics International*, Vol.4, No.5, pp. 481-508.

24. Morel, J.C. and Gourc, J.P. (1998). "Static and Cyclic Behaviour of Sand Reinforced by Mesh Elements," *Proc., Int. Conf. Geosynthetics*, Atlanta, Georgia, March 1998, pp.1069-1072.

25. Nataraj, M.S., and McManis, K.L. (1997). "Strength and Deformation Properties of Soils Reinforced with Fibrillated Fibers," *Geosynthetics International*, Vol.4, No.1, pp. 65-79.

26. Noorany, I., and Uzdavines, M. (1989). "Dynamic Behavior of Saturated Sand Reinforced with Geosynthetic Fabrics," *Proc. Geosynthetics '89 Conf.*, Vol.2, San Diego, CA, pp. 385-396.

27. Ranjan, G., Vassan, R.M. and Charan, H.D. (1996), "Probabilistic Analysis of Randomly Distributed Fiber-Reinforced Soil," *J. Geotech. Engrg.,* ASCE, Vol. 120, No. 6, pp. 419-426.

28. Ranjan, G., Vassan, R.M. and Charan, H.D. (1997), "Probabilistic Analysis of Randomly Distributed Fiber-Reinforced Soil," *J. of Geotechnical and Geoenvironmental. Engineering.,* ASCE, Closure, Vol. 123, No.109, pp. 987-988.

29. Saunders, S.A., Brandon, T.L., and Collin, J.G. (1997), "Effects of Mesh Element Reinforcement on Surficial Slope Stability," *Proc., Second Panamerican Conference on Landslides,* Rio de Janeiro, Brazil.

30. Schaefer, V.R. (1997). *Ground Improvement, Ground Reinforcement, Ground Treatment*, Proc. of sessions in Geo-Logan'97 Conference, ASCE, Geotechnical Special Publication No.69.

31. Shewbridge, S.E. and Sitar, N. (1989). "Deformation Characteristics of Reinforced Sand in Direct Shear," *J. Geotechnical Engineering,* ASCE, vol. 115, no. 8, pp. 1134-1147.

32. Shewbridge, S.E. and Sitar, N. (1990). "Deformation Based Model for Reinforced Sand," *J. Geotechnical Engineering,* ASCE, vol. 116, no. 7, pp. 1153-1170.

33. Shewbridge, S.E. and Sitar, N. (1996). "Formation of Shear Zones in Reinforced Sand," *J. Geotechnical Engineering,* ASCE, vol. 122, no. 11, pp. 873-885.

DEVELOPMENT OF A DISCRETE DESIGN METHODOLOGY FOR FIBER-REINFORCED SOIL

Jorge G. Zornberg, Ph.D., P.E.

APPENDIX C: EXPERIMENTAL TEST RESULTS

DEVELOPMENT OF A DISCRETE DESIGN METHODOLOGY FOR FIBER-REINFORCED SOIL

Jorge G. Zornberg, Ph.D., P.E.

APPENDIX D: TENSILE PROPERTIES OF FIBERS

DEVELOPMENT OF A DISCRETE DESIGN
METHODOLOGY FOR FIBER-REINFORCED SOIL

Jorge G. Zornberg, Ph.D., P.E.

D.1 Product Specifications

DEVELOPMENT OF A DISCRETE DESIGN
METHODOLOGY FOR FIBER-REINFORCED SOIL

Jorge G. Zornberg, Ph.D., P.E.

D.2 ASTM D 2256-97

DEVELOPMENT OF A DISCRETE DESIGN
METHODOLOGY FOR FIBER-REINFORCED SOIL

Jorge G. Zornberg, Ph.D., P.E.

D.3: Tensile Strength Results

DEVELOPMENT OF A DISCRETE DESIGN METHODOLOGY FOR FIBER-REINFORCED SOIL

Jorge G. Zornberg, Ph.D., P.E.

APPENDIX E: RELATIONSHIPS

E.1 Gravimetric fiber content as a function of volumetric fiber content

Determine: Relationship defining the gravimetric fiber content, χ_w , as a function of the volumetric fiber content, χ.

Volumetric fiber content:

$$\chi = \frac{V_f}{V}$$

Gravimetric fiber content:

$$\chi_w = \frac{W_f}{W_s}$$

Dry unit weight of fiber-reinforced soil:

$$\gamma = \frac{W_f + W_s}{V}$$

From the relationships above:

$$\chi_w = \frac{\gamma_w \cdot G_f \cdot V_f}{\left(W_s + W_f\right) - W_f} = \frac{\gamma_w \cdot G_f \cdot V_f}{\left(W_s + W_f\right) - \gamma_w \cdot G_f \cdot V_f}$$

$$\chi_w = \frac{\gamma_w \cdot G_f \cdot \dfrac{V_f}{V}}{\dfrac{\left(W_s + W_f\right)}{V} - \gamma_w \cdot G_f \cdot \dfrac{V_f}{V}}$$

$$\chi_w = \frac{\chi \cdot G_f \cdot \gamma_w}{\gamma - \chi \cdot G_f \cdot \gamma_w}$$

E.2 Volumetric fiber content as a function of gravimetric fiber content

Determine: Relationship defining the volumetric fiber content, χ , as a function of the gravimetric fiber content, χ_w.

From Appendix E.1:

$$\left(\gamma - \chi \cdot G_f \cdot \gamma_w\right)\chi_w \ = \ \chi \cdot G_f \cdot \gamma_w$$

$$\gamma \cdot \chi_w - \chi \cdot G_f \cdot \gamma_w \cdot \chi_w \ = \ \chi \cdot G_f \cdot \gamma_w$$

$$\chi \ = \ \frac{\chi_w \cdot \gamma}{\left(1 + \chi_w\right) \cdot G_f \cdot \gamma_w}$$

E.3 Equivalent Shear Strength (Cohesionless Soil, Confinement below Critical)

Determine: Relationship defining S_{eq} for the case of cohesionless soils. Case $\sigma_n <$ $\sigma_{n,crit}$.

Using Equations (27) and (17):

$$S_{eq} = S + \alpha \cdot t$$
$$S_{eq} = \sigma_n \cdot \tan\phi + \alpha \cdot t$$
$$S_{eq} = \sigma_n \cdot \tan\phi + \alpha \cdot t_p \, (because \, \sigma_n < \sigma_{n,crit})$$
$$S_{eq} = \sigma_n \cdot \tan\phi + \alpha \cdot \eta \cdot \chi \cdot c_{i,\phi} \cdot \tan\phi \cdot \sigma_n$$
$$S_{eq} = \tan\phi \left(1 + \alpha \cdot \eta \cdot \chi \cdot c_{i,\phi}\right)\sigma_n$$

E.4 Equivalent Shear Strength (Cohesionless Soil, Confinement above Critical)

Determine: Relationship defining S_{eq} for the case of cohesionless soils. Case $\sigma_n >$ $\sigma_{n,crit}$.

Using Equations (27) and (7):

$$S_{eq} \; = \; S + \alpha \cdot t$$
$$S_{eq} \; = \; \sigma_n \cdot \tan\phi + \alpha \cdot t$$
$$S_{eq} \; = \; \sigma_n \cdot \tan\phi + \alpha \cdot t_t \; (because \; \sigma_n > \sigma_{n,crit})$$
$$S_{eq} \; = \; \alpha \cdot \chi \cdot \sigma_{f,ult} + \tan\phi \cdot \sigma_n$$

E.5 Equivalent Shear Strength (Cohesive Soil, Confinement below Critical)

Determine: Relationship defining S_{eq} for the case of cohesive-frictional soils. Case $\sigma_n < \sigma_{n,crit}$.

Using Equations (27) and (19):

$$S_{eq} = S + \alpha \cdot t$$
$$S_{eq} = (c + \sigma_n \cdot \tan\phi) + \alpha \cdot t$$
$$S_{eq} = (c + \sigma_n \cdot \tan\phi) + \alpha \cdot t_p \, (because \, \sigma_n < \sigma_{n,crit})$$
$$S_{eq} = (c + \sigma_n \cdot \tan\phi) + \alpha \cdot (\eta \cdot \chi \cdot c_{i,c} \cdot c + \eta \cdot \chi \cdot c_{i,\phi} \cdot \tan\phi \cdot \sigma_n)$$
$$S_{eq} = (1 + \alpha \cdot \eta \cdot \chi \cdot c_{i,c})c + (1 + \alpha \cdot \eta \cdot \chi \cdot c_{i,\phi})\tan\phi \sigma_n$$

The above relationship can be expressed by:

$$S_{eq,1} = c_{eq,1} + (\tan\phi)_{eq,1} \cdot \sigma_n$$

where:

$$c_{eq,1} = (1 + \alpha \cdot \eta \cdot \chi \cdot c_{i,c}) \cdot c$$

$$(\tan\phi)_{eq,1} = (1 + \alpha \cdot \eta \cdot \chi \cdot c_{i,\phi}) \cdot \tan\phi$$

E.6 Equivalent Shear Strength (Cohesive Soil, Confinement above Critical)

Determine: Relationship defining S_{eq} for the case of cohesive-frictional soils. Case $\sigma_n > \sigma_{n,crit}$.

Using Equations (27) and (7):

$$
\begin{aligned}
S_{eq} &= S + \alpha \cdot t \\
S_{eq} &= \left(c + \sigma_n \cdot \tan\phi\right) + \alpha \cdot t \\
S_{eq} &= \left(c + \sigma_n \cdot \tan\phi\right) + \alpha \cdot t_t \ \left(because \ \sigma_n > \sigma_{n,crit}\right) \\
S_{eq} &= \left(c + \alpha \cdot \chi \cdot \sigma_{f,ult}\right) + \tan\phi \cdot \sigma_n
\end{aligned}
$$

The above relationship can be expressed by:

$$
S_{eq,2} = c_{eq,2} + \left(\tan\phi\right)_{eq,2} \cdot \sigma_n
$$

where:

$$
c_{eq,2} = c + \alpha \cdot \chi \cdot \sigma_{f,ult}
$$

$$
\left(\tan\phi\right)_{eq,2} = \tan\phi
$$

E.7 Infinite Slope

Determine: Relationship defining t_{req} for the case of an infinite slope.

From the definition of factor of safety:

$$FS = \frac{c + \gamma\, T \cos\beta \tan\phi}{\gamma\, T \sin\beta - \alpha \cdot t_{req}}$$

$$\gamma\, T \sin\beta - \alpha \cdot t_{req} = \frac{1}{FS}\left(c + \gamma\, T \cos\beta \tan\phi\right)$$

$$\alpha \cdot t_{req} = \gamma\, T \sin\beta - \frac{1}{FS}\left(c + \gamma\, T \cos\beta \tan\phi\right)$$

$$t_{req} = \frac{\gamma\, T \sin\beta}{\alpha \cdot FS}\left(FS - \frac{c}{\gamma\, T \sin\beta} - \frac{\tan\phi}{\tan\beta}\right)$$

E.8 Infinite Slope, Required Fiber Content (Confinement below Critical)

Determine: Relationship defining the fiber content, $\chi_{req,1}$, required to satisfy a given FS criterion for the case of $\sigma_n < \sigma_{n,crit}$.

From Equations (19), (38), and (48)

$$t_p \;=\; \eta \cdot \chi \cdot c_{i,c} \cdot c + \eta \cdot \chi \cdot c_{i,\phi} \cdot \tan\phi \cdot \sigma_n \qquad\qquad (19)$$

$$\sigma_n \;=\; \gamma \cdot T \, \cos\beta \qquad\qquad \text{from Equation (38)}$$

$$t_{req} \;=\; \frac{\gamma\, T \sin\beta}{\alpha \cdot FS}\left(FS - \frac{c}{\gamma\, T \sin\beta} - \frac{\tan\phi}{\tan\beta}\right) \qquad\qquad (48)$$

Making $t_p = t_{req}$

$$\eta \cdot \chi_{req,1} \cdot \left(c_{i,c} \cdot c + c_{i,\phi} \cdot \tan\phi \cdot \gamma \cdot T \cdot \cos\beta\right) \;=\; \frac{\gamma\, T \sin\beta}{\alpha \cdot FS}\left(FS - \frac{c}{\gamma\, T \sin\beta} - \frac{\tan\phi}{\tan\beta}\right)$$

or:

$$\chi_{req,1} \;=\; \frac{FS - \left(\dfrac{c}{\gamma\, T \sin\beta} + \dfrac{\tan\phi}{\tan\beta}\right)}{\alpha \cdot FS \cdot \eta \left(c_{i,c} \dfrac{c}{\gamma\, T \sin\beta} + c_{i,\phi} \dfrac{\tan\phi}{\tan\beta}\right)}$$

E.9 Infinite Slope, Required Fiber Content (Confinement above Critical)

Determine: Relationship defining the fiber content, $\chi_{req,2}$, required to satisfy a given FS criterion for the case of $\sigma_n > \sigma_{n,crit}$.

From Equations (7), (38), and (48)

$$t_t = \sigma_{f,ult} \cdot \chi \qquad (7)$$

$$\sigma_n = \gamma \cdot T \cos \beta \qquad \text{from Equation (38)}$$

$$t_{req} = \frac{\gamma \, T \sin \beta}{\alpha \cdot FS} \left(FS - \frac{c}{\gamma \, T \sin \beta} - \frac{\tan \phi}{\tan \beta} \right) \qquad (48)$$

Making $t_t = t_{req}$

$$\chi_{req,2} \cdot \sigma_{f,ult} = \frac{\gamma \, T \sin \beta}{\alpha \cdot FS} \left(FS - \frac{c}{\gamma \, T \sin \beta} - \frac{\tan \phi}{\tan \beta} \right)$$

or:

$$\chi_{req,2} = \frac{\gamma \, T \sin \beta}{\alpha \cdot FS \cdot \sigma_{f,ult}} \left(FS - \frac{c}{\gamma \, T \sin \beta} - \frac{\tan \phi}{\tan \beta} \right) \qquad (52)$$

DEVELOPMENT OF A DISCRETE DESIGN METHODOLOGY FOR FIBER-REINFORCED SOIL

Jorge G. Zornberg, Ph.D., P.E.

APPENDIX F: LIMIT EQUILIBRIUM INPUT FILES

DEVELOPMENT OF A DISCRETE DESIGN METHODOLOGY FOR FIBER-REINFORCED SOIL

Jorge G. Zornberg, Ph.D., P.E.

APPENDIX G: EXPERIMENTAL VALIDATION OF THE DISCRETE FRAMEWORK

EXPERIMENTAL VALIDATION OF THE DISCRETE FRAMEWORK

By: Paula Pugliese, Ph.D. and Jorge G. Zornberg, Ph.D., P.E.

Geotechnical Research Report

University of Colorado at Boulder

June 2000

EXPERIMENTAL VALIDATION OF THE DISCRETE FRAMEWORK

By: Paula Pugliese, Ph.D. and Jorge G. Zornberg, Ph.D., P.E.

<u>Introduction</u>

The discrete approach was applied in four design projects with the objectives of experimentally establishing the equivalent shear strength of the soil to be reinforced. The experimental results were compared with the shear strength of fiber-reinforced soil predicted using the discrete approach. The four projects are: LA 22 slopes, Cardinal Road Slope Failures, Vanderbilt Stadium, and Las Colinas Slopes (TETCO).

Information regarding to the fiber-reinforcement material is shown in Table 1. Information on the soil characteristics for each of the 4 cases investigated is shown in Table 2.

Table 1: Fiber-reinforced material properties

Properties	Units	Values
Length	in	2
Width	in	0.289
Thickness	in	0.0017
G_f (specific gravity of the fibers)		0.91
Fiber Linear Density	deniers	2610
Fiber Tensile Strength ($\sigma_{f,ult}$)	psi	40000

Table 2: Soil and interface properties used for each of the 4 cases investigated

SOIL DATA	UNITS	LA-22	CARDINAL	VANDERBILT	TETCO
Dry unit weigh of soil (γ)	pcf	103.67	100.83	104.9	89.7
Friction angle' (ϕ')	(^{0})	26.2	24.1	35.8	11.2
Cohesion' (c')	psi	1.6	1.5	0.8	4.1
$c_{i,c}$		0.8	0.8	0.8	0.8
$c_{i,\theta}$		0.8	0.8	0.8	0.8
α		1	1	1	1
Fiber content (X_w)	%	0.2	0.2	0.2	0.2

First case study – LA 22 slopes

The following five steps [(a) through (e)] lead to the determination of the equivalent shear strength to be assumed by the designer after applying the discrete approach. The fiber-induced tension is assumed to be parallel to the failure plane. The soil and fiber reinforcement characteristics used in the calculations are those indicated in Tables 1 and 2.

(a) Determination of the volumetric fiber content, χ:

$$\chi = (\chi_w \cdot \gamma)/((1+\chi_w) \cdot G_f \cdot \gamma_w)$$

$\Rightarrow \quad \chi = 0.0036425$

(b) Determination of the equivalent diameter, d_f :

(b1) Using reported fibers geometry:

$$d_f = ((4 \cdot A_f)/ \pi)^{1/2}$$

$$A_f = 3.1709 \times 10^{-7} \, m^2 \quad or \quad 4.9149 \times 10^{-4} \, in$$

$\Rightarrow \quad d_f = 0.0006354 \, m \quad or \quad d_f = 0.0250157 \, in$

(b2) Using reported linear density of the fibers. This second calculation is one way to check the value obtained in (b1).

$$d_f = ((4 \cdot A_f)/ \pi)^{1/2}$$

$$A_f = 3.1868 \times 10^{-7} \, m^2 \quad or \quad 4.93954 \times 10^{-4} \, in$$

$\Rightarrow \quad d_f = 0.0006372 \, m \quad or \quad d_f = 0.0250866 \, in$

(c) Determination of fiber aspect ratio, η:

$$\eta = l_f /d_f$$

$$\Rightarrow \quad \eta = 79.73$$

Where:

l_f is the length of the fiber in (m),

d_f is the equivalent diameter in (m) obtained in (b2).

(d) Determination of $\sigma_{n,crit}$

$$\sigma_{n,crit} = (\sigma_{f,ult} - \eta \cdot c_{i,c} \cdot c)/(\eta \cdot c_{i,\phi} \cdot \tan\phi)$$

$$\Rightarrow \quad \sigma_{n,crit} = 7323.89 \text{ kPa} \quad \text{or} \quad 1041.69 \text{ psi}$$

The critical confining pressure is too high for practical applications. Consequently, only the first portion of the bilinear equivalent shear strength envelope of the fiber-reinforced composite is of interest.

(e) Determination of equivalent shear strength, S_{eq}

The equivalent shear strength for the range of confining pressure of interest is obtained as:

$$S_{eq,I} = c_{eq,1} + (\tan\phi)_{eq,1} \cdot \sigma_n$$

The cohesive component of the equivalent shear strength is estimated by:

$$c_{eq,1} = (1 + \alpha \cdot \eta \cdot \chi \cdot c_{i,c}) \, c$$

$$\Rightarrow \quad c_{eq,1} = 13.86 \text{ kPa} \quad \text{or 1.97 psi}$$

The frictional component of the equivalent shear strength is estimated by:

$$(\tan\phi)_{eq,1} = (1 + \alpha \cdot \eta \cdot \chi \cdot c_{i,\phi}) \, \tan\phi$$

$$\Rightarrow \quad (\phi)_{eq,1} = 31.23^0$$

Table 3 shows the results of soil parameters obtained from the application of discrete approach, the parameters of the soil without reinforcement and the results obtained in triaxial tests using reinforced soil.

Table 3: Comparison between experimental and predicted soil parameters

Results	Predicted parameters using the discrete approach	Without Fibers	Best-fit parameters defined from test results
$\phi'^{(o)}$	31.23	26.20	33.3
c' (psi)	1.97	1.60	1.4
c' (kPa)	13.86	11.25	9.84

The predicted and best-fit parameters shown in Table 3 correspond to 2 inch fibers mixed at a dosage of 0.2%. Figure 1 shows the corresponding Mohr circles and Mohr-Coulomb shear strength envelope for the unreinforced soil. Figure 2 shows the experimental results obtained from testing of fiber-reinforced specimens (actual results at three confining pressures) as well as the shear strength envelope predicted using the discrete approach. As can be observed in the figure, there is a very good agreement between analytic and experimental shear strength values.
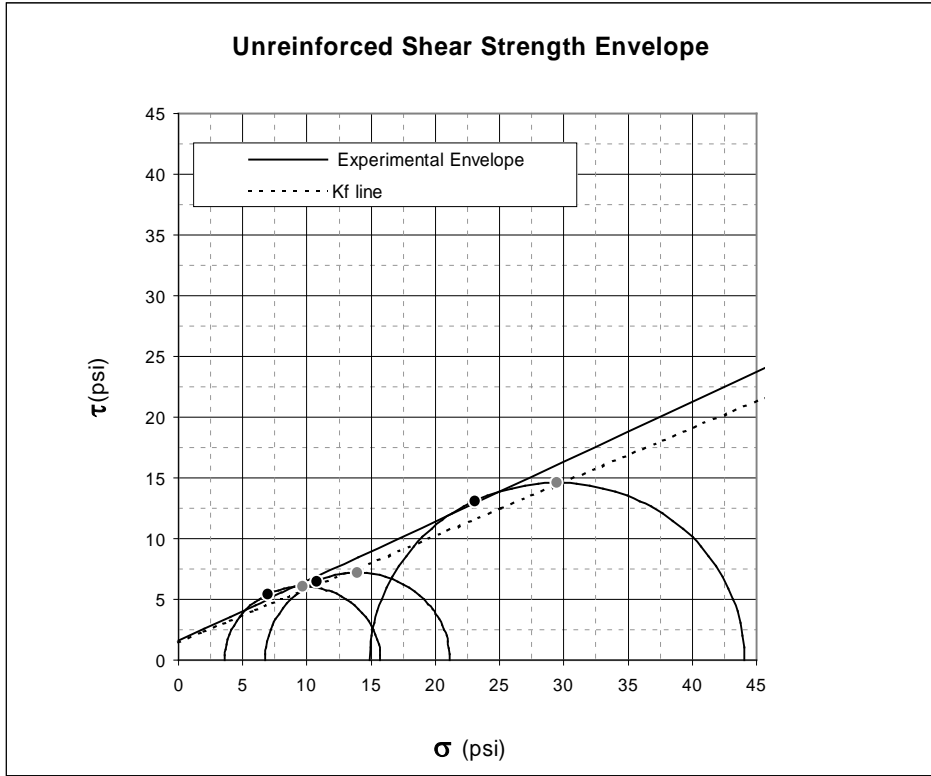
Figure 1: Shear strength results of unreinforced specimens
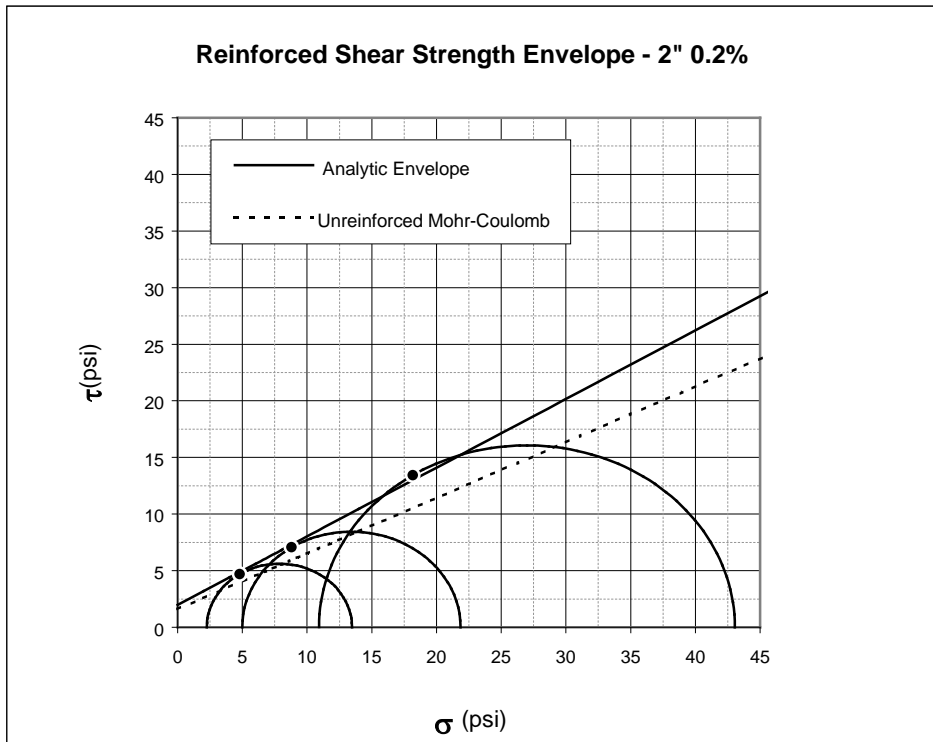
Figure 2: Shear strength results of the fiber reinforced specimens (experimental and predicting using the discrete approach). Fiber length: 2". Fiber content: 0.2%

Second case study – Cardinal Road Slope Failures

Steps (a) through (e), indicated below, lead to the determination of the equivalent shear strength to be assumed by the designer after applying the discrete approach. The fiber-induced tension is assumed parallel to the failure plane. The soil and fiber reinforcement characteristics used in the calculations are those indicated in Tables 1 and 2.

(a) Determination of the volumetric fiber content, χ:

$$\chi = (\chi_w \cdot \gamma)/((1+\chi_w) \cdot G_f \cdot \gamma_w)$$

$$\Rightarrow \quad \chi = 0.0035427$$

(b) Determination of the equivalent diameter, d_f :

(b1) Using reported fibers geometry:

$$d_f = ((4 \cdot A_f)/ \pi)^{1/2}$$

$$A_f = 3.1709 \times 10^{-7} \, m^2 \quad or \quad 4.9149 \times 10^{-4} \, in$$

$$\Rightarrow \quad d_f = 0.0006354 \, m \quad or \quad d_f = 0.0250157 \, in$$

(b2) Using reported linear density of the fibers. This second calculation is one way to check the value obtained in (b1)

$$d_f = ((4 \cdot A_f)/ \pi)^{1/2}$$

$$A_f = 3.1868 \times 10^{-7} m^2 \quad or \quad 4.93954 \times 10^{-4} in$$

$$\Rightarrow \quad d_f = 0.0006372 \, m \quad or \quad d_f = 0.0250866 \, in$$

(c) Determination of fiber aspect ratio, η:

$$\eta = l_f /d_f$$

$$\Rightarrow \quad \eta = 79.73$$

Where:

l_f is the length of the fiber in (m),
d_f is the equivalent diameter in (m) obtained in (b2).

(d) Determination of $\sigma_{n,crit}$

$$\sigma_{n,crit} = (\sigma_{f,ult} - \eta \cdot c_{i,c} \cdot c)/(\eta \cdot c_{i,\phi} \cdot \tan\phi)$$

$\Rightarrow \sigma_{n,crit} = $ 7325.06 kPa   or   1041.85 psi

The critical confining pressure is too high for practical applications. Consequently, only the first portion of the bilinear equivalent shear strength envelope of the fiber-reinforced composite is of interest.

(e) Determination of equivalent shear strength, S_{eq}

The equivalent shear strength for the range of confining pressure of interest is obtained as:

$$S_{eq,I} = c_{eq,1} + (\tan\phi)_{eq,1} \cdot \sigma_n$$

The cohesive component of the equivalent shear strength is estimated by:

$$c_{eq,1} = (1 + \alpha \cdot \eta \cdot \chi \cdot c_{i,c})\, c$$

$\Rightarrow c_{eq,1} = $ 12.93 kPa   or   1.84 psi

The frictional component of the equivalent shear strength is estimated by:

$$(\tan\phi)_{eq,1} = (1 + \alpha \cdot \eta \cdot \chi \cdot c_{i,\phi})\, \tan\phi$$

$\Rightarrow (\phi)_{eq,1} = $ 28.74^0

Table 4 shows the results of soil parameters obtained from the application of discrete approach, the parameters of the soil without reinforcement and the results obtained in triaxial tests using reinforced soil.

Table 4: Comparison between experimental and predicted soil parameters

Results	Predicted parameters using the discrete approach	Without Fibers	Best-fit parameters defined from test results
$\phi'^{(o)}$	28.74	24.10	29.2
C' (psi)	1.84	1.50	1.4
C' (kPa)	12.93	10.54	9.84

The predicted and best-fit parameters shown in Table 4 correspond to 2 inch fibers mixed at a dosage of 0.2%. Figure 3 shows the corresponding Mohr circles and Mohr-Coulomb shear strength envelope for the unreinforced soil. Figure 4 shows the experimental results obtained from testing of fiber-reinforced specimens (actual results at three confining pressures) as well as the shear strength envelope predicted using the discrete approach. As can be observed in the figure, there is a very good agreement between analytic and experimental shear strength values.
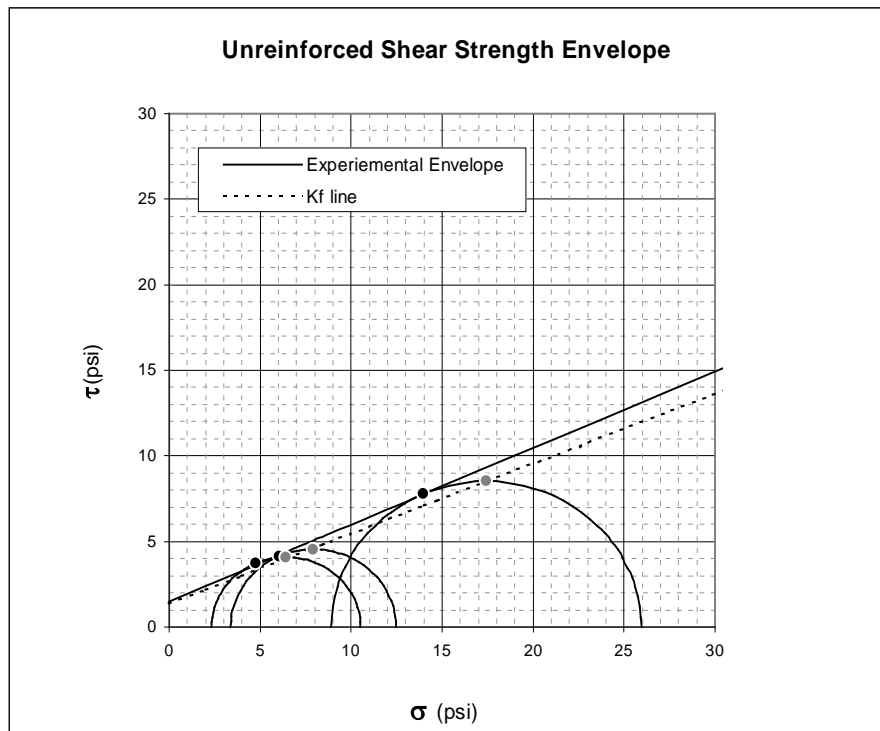
Figure 3: Shear strength results of unreinforced specimens
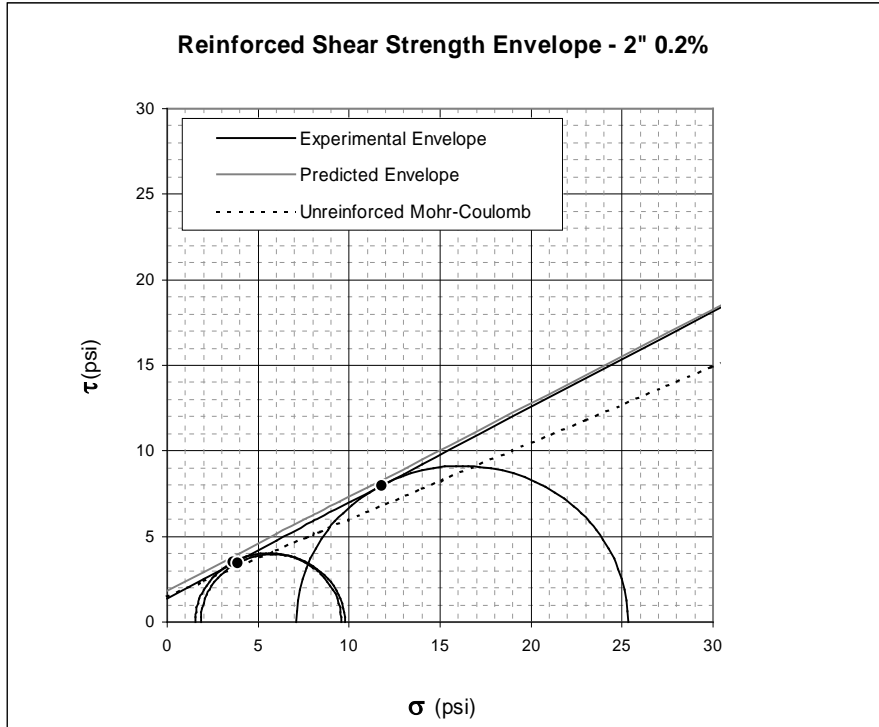
Figure 4: Shear strength results of the fiber reinforced specimens (experimental and predicting using the discrete approach). Fiber length: 2". Fiber content: 0.2%

Third case study – Vanderbilt Stadium

Steps (a) through (e), indicated below, lead to the determination of the equivalent shear strength to be assumed by the designer after applying the discrete approach. The fiber-induced tension is assumed parallel to the failure plane. The soil and fiber reinforcement characteristics used in the calculations are those indicated in Tables 1 and 2.

(a) Determination of the volumetric fiber content, χ:

$$\chi = (\chi_w \cdot \gamma)/((1+\chi_w) \cdot G_f \cdot \gamma_w)$$

$$\Rightarrow \quad \chi = 0.0036857$$

(b) Determination of the equivalent diameter, d_f :

(b1) Using reported fibers geometry:

$$d_f = ((4 \cdot A_f)/ \pi)^{1/2}$$

$$A_f = 3.1709 \times 10^{-7} m^2 \quad or \quad 4.9149 \times 10^{-4} in$$

$$\Rightarrow \quad d_f = 0.0006354 \ m \quad or \quad d_f = 0.0250157 \ in$$

(b2) Using reported linear density of the fibers. This second calculation is one way to check the value obtained in (b1)

$$d_f = ((4 \cdot A_f)/ \pi)^{1/2}$$

$$A_f = 3.1868 \times 10^{-7} m^2 \quad or \quad 4.93954 \times 10^{-4} in$$

$$\Rightarrow \quad d_f = 0.0006372 \ m \quad or \quad d_f = 0.0250866 \ in$$

(c) Determination of fiber aspect ratio, η:

$$\eta = l_f / d_f$$

$$\Rightarrow \quad \eta = 79.73$$

Where:

l_f is the length of the fiber in (m),

d_f is the equivalent diameter in (m) obtained in (b2).

(d) Determination of $\sigma_{n,crit}$

$$\sigma_{n,crit} = (\sigma_{f,ult} - \eta \cdot c_{i,c} \cdot c)/(\eta \cdot c_{i,\phi} \cdot \tan\phi)$$

$$\Rightarrow \quad \sigma_{n,crit} = 7333.26 \text{ kPa} \quad \text{or} \quad 1043.02 \text{ psi}$$

The critical confining pressure is too high for practical applications. Consequently, only the first portion of the bilinear equivalent shear strength envelope of the fiber-reinforced composite is of interest.

(e) Determination of equivalent shear strength, S_{eq}

The equivalent shear strength for the range of confining pressure of interest is obtained as:

$$S_{eq,l} = c_{eq,1} + (\tan\phi)_{eq,1} \cdot \sigma_n$$

The cohesive component of the equivalent shear strength is estimated by:

$$c_{eq,1} = (1 + \alpha \cdot \eta \cdot \chi \cdot c_{i,c}) \, c$$

$$\Rightarrow \quad c_{eq,1} = 6.95 \text{ kPa} \quad \text{or} \quad 0.99 \text{ psi}$$

The frictional component of the equivalent shear strength is estimated by:

$$(\tan\phi)_{eq,1} = (1 + \alpha \cdot \eta \cdot \chi \cdot c_{i,\phi}) \tan\phi$$

$$\Rightarrow \quad (\phi)_{eq,1} = 41.7^0$$

The predicted and best-fit parameters shown in Table 5 correspond to 2 inch fibers mixed at a dosage of 0.2%. Figure 5 shows the corresponding Mohr circles and Mohr-Coulomb shear strength envelope for the unreinforced soil. Figure 6 shows the experimental results obtained from testing of fiber-reinforced specimens (actual results at three confining pressures) as well as the shear strength envelope predicted using the discrete approach. As can be observed in the figure, there is a very good agreement between analytic and experimental shear strength values.

Table 5: Comparison between experimental and predicted soil parameters

Results	Predicted parameters using the discrete approach	Without Fibers	Best-fit parameters defined from test results
$\phi'^{(o)}$	41.7	35.8	42.7
C' (psi)	0.99	0.8	1.4
C' (kPa)	6.96	5.62	9.84

In the following figures, Figure 5 and 6, it can be seen the Mohr circles, the Mohr-Coulomb Envelop of the soil with and without reinforcement while making a comparison with the results obtained with the discrete approach.
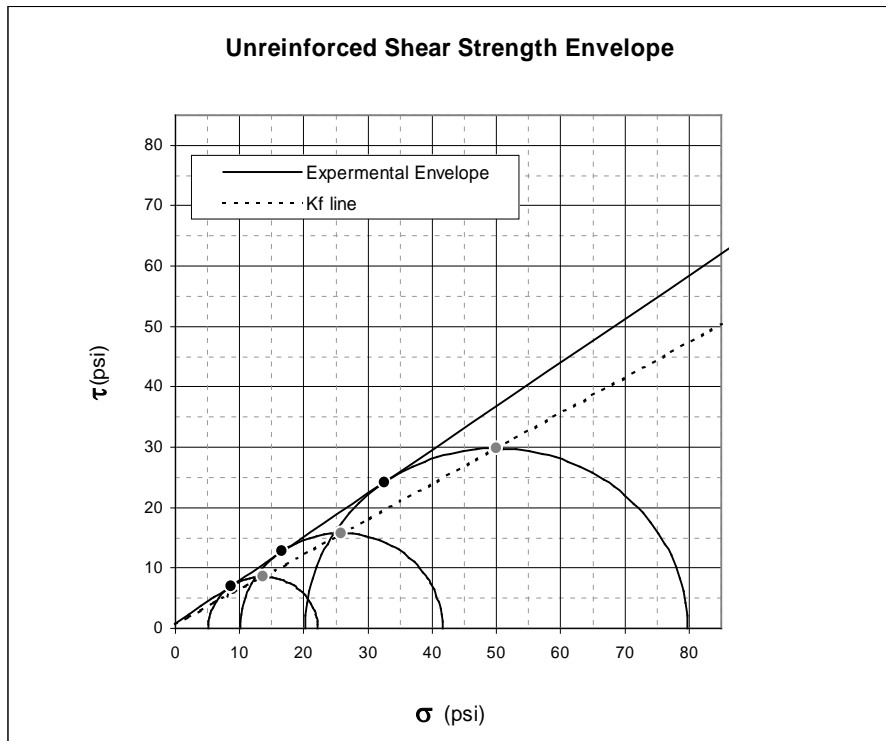
Figure 5: Shear strength results of unreinforced specimens
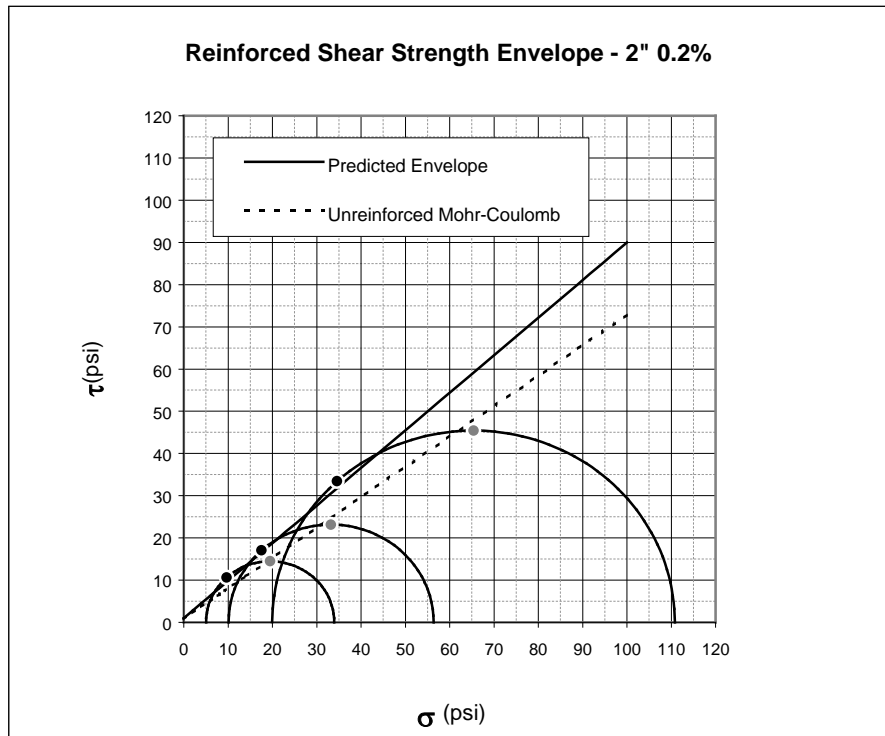
Figure 6: Shear strength results of the fiber reinforced specimens (experimental and predicting using the discrete approach). Fiber length: 2". Fiber content: 0.2%

Fourth case study – Las Colinas Slopes (TETCO)

Steps (a) through (e), indicated below, lead to the determination of the equivalent shear strength to be assumed by the designer after applying the discrete approach. The fiber-induced tension is assumed parallel to the failure plane. The soil and fiber reinforcement characteristics used in the calculations are those indicated in Tables 1 and 2.

(a) Determination of the volumetric fiber content, χ:

$$\chi = (\chi_w \cdot \gamma)/((1+\chi_w) \cdot G_f \cdot \gamma_w)$$

$$\Rightarrow \quad \chi = 0.0031366$$

(b) Determination of the equivalent diameter, d_f :

(b1) Using reported fibers geometry:

$$d_f = ((4 . A_f)/ \pi)^{1/2}$$

$$A_f = 3.1709 \times 10^{-7} \, m^2 \quad or \quad 4.9149 \times 10^{-4} \, in$$

$$\Rightarrow \quad d_f = 0.0006354 \, m \quad or \quad d_f = 0.0250157 \, in$$

(b2) Using reported linear density of the fibers. This second calculation is one way to check the value obtained in (b1)

$$d_f = ((4 . A_f)/ \pi)^{1/2}$$

$$A_f = 3.1868 \times 10^{-7} m^2 \quad or \quad 4.93954 \times 10^{-4} in$$

$$\Rightarrow \quad d_f = 0.0006372 \, m \quad or \quad d_f = 0.0250866 \, in$$

(c) Determination of fiber aspect ratio, η:

$$\eta = l_f / d_f$$

$$\Rightarrow \quad \eta = 79.73$$

Where:
l_f is the length of the fiber in (m),
d_f is the equivalent diameter in (m) obtained in (b2).

(d) Determination of $\sigma_{n,crit}$

$$\sigma_{n,crit} = (\sigma_{f,ult} - \eta . c_{i,c} . c)/(\eta . c_{i,\phi} . \tan\phi)$$

$$\Rightarrow \quad \sigma_{n,crit} = 7294.62 \text{ kPa} \quad \text{or} \quad 1037.52 \text{ psi}$$

The critical confining pressure is too high for practical applications. Consequently, only the first portion of the bilinear equivalent shear strength envelope of the fiber-reinforced composite is of interest.

(e) Determination of equivalent shear strength, S_{eq}

The equivalent shear strength for the range of confining pressure of interest is obtained from:

$$S_{eq,I} = c_{eq,1} + (\tan\phi)_{eq,1} \cdot \sigma_n$$

The cohesive component of the equivalent shear strength is estimated by:

$$c_{eq,1} = (1 + \alpha \cdot \eta \cdot \chi \cdot c_{i,c}) \, c$$

$$\Rightarrow \quad c_{eq,1} = 34.59 \text{ kPa} \quad \text{or} \quad 4.92 \text{ psi}$$

The frictional component of the equivalent shear strength is estimated by:

$$(\tan\phi)_{eq,1} = (1 + \alpha \cdot \eta \cdot \chi \cdot c_{i,\phi}) \tan\phi$$

$$\Rightarrow \quad (\phi)_{eq,1} = 13.37^0$$

The predicted and best-fit parameters shown in Table 6 correspond to 2 inch fibers mixed at a dosage of 0.2%. Figure 7 shows the corresponding Mohr circles and Mohr-Coulomb shear strength envelope for the unreinforced soil. Figure 8 shows the experimental results obtained from testing of fiber-reinforced specimens (actual results at three confining pressures) as well as the shear strength envelope predicted using the discrete approach. As can be observed in the figure, there is a very good agreement between analytic and experimental shear strength values.

Table 6: Comparison between experimental and predicted soil parameters

Results	Predicted parameters using the discrete approach	Without Fibers	Best-fit parameters defined from test results
$\phi'^{(o)}$	13.37	11.20	15.5
C' (psi)	4.92	4.1	4.1
C' (kPa)	34.54	28.82	28.82

In the following figures, Figure 7 and 8, it can be seen the Mohr circles, the Mohr-Coulomb Envelop of the soil with and without reinforcement while making a comparison with the results obtained with the discrete approach.

Unreinforced Shear Strength Envelope
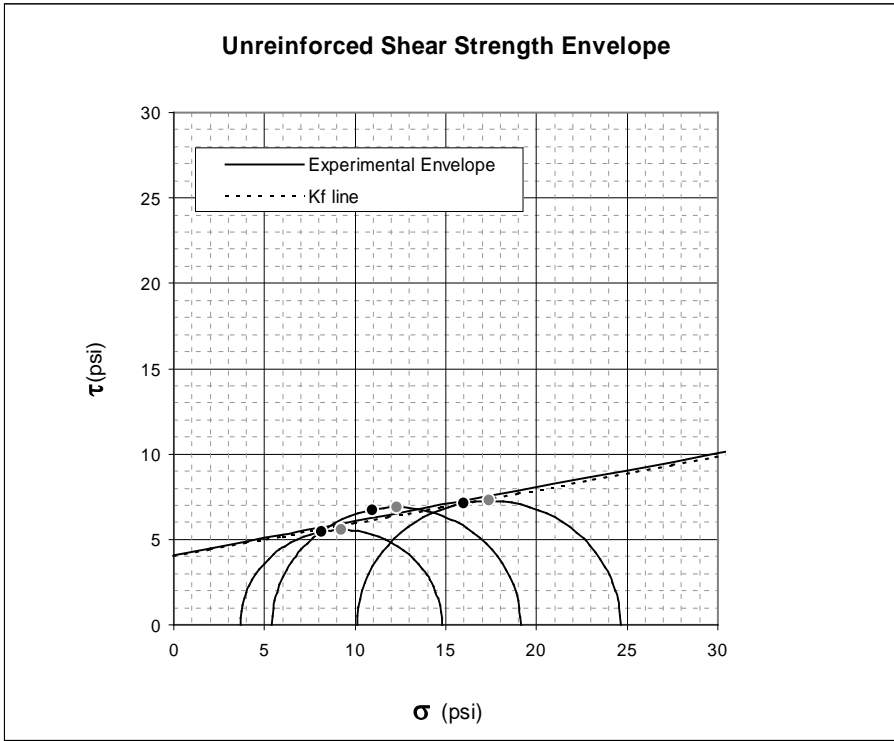
Figure 7: Shear strength results of unreinforced specimens
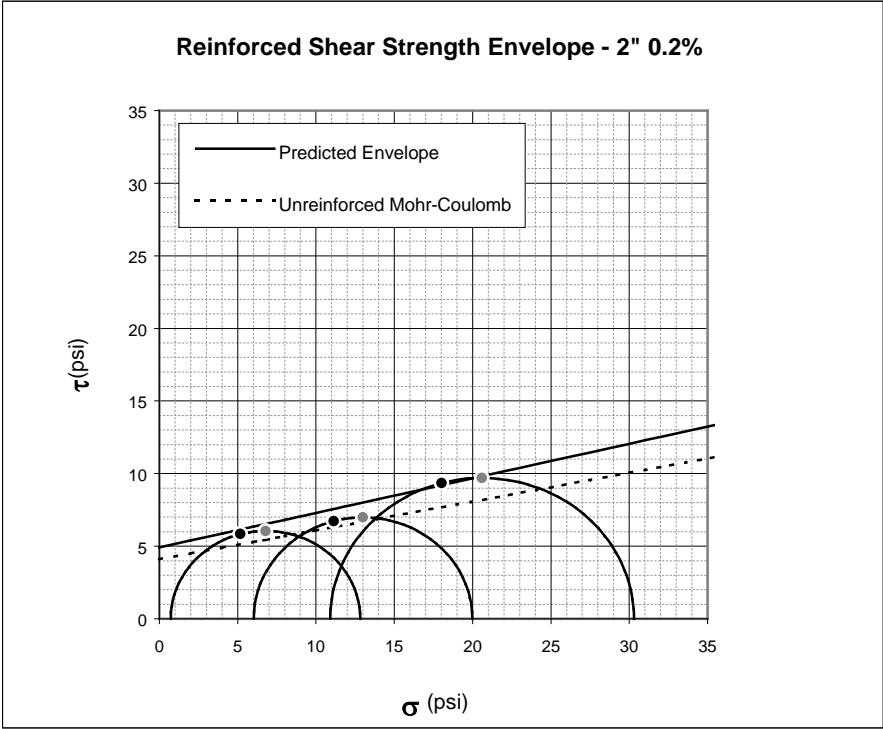
Figure 8: Shear strength results of the fiber reinforced specimens (experimental and predicting using the discrete approach). Fiber length: 2". Fiber content: 0.2%

Final Remarks

Very good agreement was obtained for the case of four additional soils between experimental shear strength values obtained on fiber-reinforced soil specimens and the analytical shear strength envelopes obtained using the discrete approach. This provides significant additional evidence on the suitability of the discrete method proposed in this investigation.